

March 2020

## Investigating Mechanisms of Immune Suppression Secondary to an Inflammatory Microenvironment

Wendy Michelle Kandell  
*University of South Florida*

Follow this and additional works at: <https://digitalcommons.usf.edu/etd>

 Part of the [Biology Commons](#), and the [Immunology and Infectious Disease Commons](#)

---

### Scholar Commons Citation

Kandell, Wendy Michelle, "Investigating Mechanisms of Immune Suppression Secondary to an Inflammatory Microenvironment" (2020). *Graduate Theses and Dissertations*.  
<https://digitalcommons.usf.edu/etd/8955>

This Dissertation is brought to you for free and open access by the Graduate School at Digital Commons @ University of South Florida. It has been accepted for inclusion in Graduate Theses and Dissertations by an authorized administrator of Digital Commons @ University of South Florida. For more information, please contact [scholarcommons@usf.edu](mailto:scholarcommons@usf.edu).

Investigating Mechanisms of Immune Subversion  
Secondary to an Inflammatory Microenvironment

by

Wendy Michelle Kandell

A dissertation submitted in partial fulfillment  
of the requirements for the degree of  
Doctor of Philosophy  
Department of Cell Biology, Microbiology and Molecular Biology  
College of Arts and Sciences  
University of South Florida

Major Professor: Kenneth L. Wright, Ph.D.  
James J. Mulé, I-Ph.D.  
Javier Pinilla-Ibarz, M.D., Ph.D.  
Dennis Adeegbe, Ph.D.  
Wasif Noor Khan, Ph.D.  
Tomar Ghansah, Ph.D.

Date of Approval:  
04/03/2020

Keywords: antitumor immunity, T cell, NK cell, DAMPs

Copyright © 2020, Wendy Michelle Kandell

## DEDICATION

I dedicate this thesis to two of the most important people in my life who I lost during this process within two months of one another: **Arthur Lewis and Sandra Joy**. I didn't think I could survive a single day without either of you. Grandma, I will continue to fight so that not a single other person ever has to suffer like you did from metastatic disease. I will never stop loving you, and there will not be a day that goes by that I don't think about you.

To my grandparents, **Lynn and Phil**: You two have been supportive of every single decision I have made from the day I was born. My education in all of its facets would not have been possible without you two, regardless of how much it took me to get through undergrad dealing with all of my health issues. We get closer and closer every year, and I have no idea how I got so lucky. You two know me better than anyone and know exactly how to cheer me up no matter what I'm going through.

To my parents, **Cathie and David**. Your endless support, and more than anything else, love, have gotten me through every single day of this crazy experience. I think you both are probably surprised that I was able to become even crazier than I already was prior to this Ph.D. program, but I succeeded!

To my stepmom and dad, **Sherri and Sol**: Thank you both for being outstanding sounding boards for me, and always being supportive. Sol, thanks for convincing me to apply to USF, even when I said I didn't want to live in Tampa!

**Adam William**: The man of my dreams. As I put on facebook when we got engaged, "Thanks for letting me pick you up by pretending to not know where the IL-2 was". A partnership built from a shared love of immunology is a funny one, built on 2AM conversations debating T cell dynamics and complaining about phosflow. But really, I wouldn't have it any other way. Thank you for not letting me quit. Thank you for picking me up off of the floor (or more often, the cytometry core floor) when I wouldn't stop crying about not being cut out for this when my T cells wouldn't cooperate. Thank you for teaching me to challenge paradigm every second of every day. I love you madly.

P.S. I'm still a better cytometrist than you are.

**Erika and SW**: I literally couldn't have done any of this without you guys. Erika, thank you for taking a chance on me, and convincing SW to take on another student even after he said he was done. You guys inspired me day in and day out, let me fly, and gave me all I ever wanted. You both created the most beautiful lab family, full of support and nonstop care for all. You two taught me how to fight – to never take no for an answer and to be the Queen of certain things. I love you both, and there will never be appropriate words to describe how grateful I am for you two.

**Wasif:** You instilled a love for immunology in me from day one before I even knew what a T cell was. We bonded over the microbiome and all of its complexities before it was in vogue. For some strange reason, you believe in me, and keep fighting for me. I don't know what I did to deserve mentorship like this, but I am finally putting my thank you in writing instead of my incessant "thanks, you're amazing" text messages. You taught me how fun science is supposed to be, and to never, ever take myself or my work too seriously. However, I promise you to always be team T cell and will never try to understand your B cell world. My mom reminded recently that at my undergraduate graduation you said "see you next at your dissertation". It's such a beautiful thing that you are coming to be my outside chair! Things really do come full circle. So much love to you.

My siblings, **Lauren, Sarah, Rena, Ashley, David and Ryan** (and basically surrogate sibling **Daniel**). Thank you for being endlessly supportive, sending me nonstop memes and providing me with a daily dose of reality when I get stuck in science land. Sometimes its hard to realize there is a world outside of cancer immunology, and this group was always there to bring me back to reality.

## ACKNOWLEDGMENTS

**The Djeu/Wei/Wright Lab** in all of its many permutations, but in particular Le, Nhan and Danni: You are the only group of people who could listen to the way I talk about science and still want to be my friend. Thank you for actually making this time fun, talking me down from my crazy emotions, and teaching me to stop being so serious. Xianghong and Pingyan, thank you for pushing me, challenging me, and picking me up when I've totally convinced myself that I can't do it.

**My committee:** Thank you for coming through for me, especially in the craziest of circumstances. Jim Mule, Dennis Adeegbe, and Javier Pinilla-Ibarz: I am so grateful for the three of you, and wish I could have gotten to know you all better through the years.

**My past mentors:** Allison Bayer, Anannya Banga, and Daniel Abate-Daga: Thank you for the foundation, the support, and the constant reminders that there is more to this world than science. Thank you for teaching me that it isn't just OK to fail, but normal. Allison and Anannya, thank you for inspiring me as two strong women in science. Daniel, thank you for providing me with a home for my first two years, nurturing my love for T cells, and helping me through all of the bumps in the road as I grew up as a scientist.

**Jodi Kroeger:** Thank you for teaching me to love flow even more than I already did. You are an inspiration and have been one of the most fun people to talk to at Moffitt.

**Ken Wright:** Another person whom I couldn't have gotten through even day one without. I don't know how you do it – you balance more on your plate than anyone I have ever seen in my life and yet still have a smile on your face. The number of times over the past four years I have been in your office crying about one thing or another and you help me through it is honestly too numerous to count. I am so grateful for your mentorship, help, assistance, literally all synonyms for that word. Thank you through during this most recent tough time taking me in as one of your own. I am so, so incredibly grateful.

## Table of Contents:

List of Figures .....	iv
Abstract .....	vi
Chapter One: Introduction .....	1
Introduction to NK Cells .....	1
NK Cells and Cancer .....	2
microRNAs and Cancer .....	3
Myelodysplastic Syndromes .....	5
DAMPS and S100A9 .....	8
S100A9 and Myelodysplastic Syndromes .....	10
T Cells .....	12
Bone Marrow T cells + T cells in Myelodysplastic Syndromes .....	14
Pattern Recognition Receptors and T cells .....	15
Chapter Two: Immune Evasion by TGF $\beta$ -induced miR-183 Repression of MICA/B Expression in Human Lung Tumor Cells .....	18
Introduction .....	18
Results .....	20
MiR-183 is overexpressed and MICA/B is underexpressed in human Lung Cancer .....	20
MiR-183 targets MICA in lung tumor cells .....	25
TGF $\beta$ drives miR183 expression to downregulate MICA/B .....	27
miR-183 expression blocks NKG2D-mediated lysis of tumor cells .....	29
Discussion .....	32
Materials and Methods .....	36
Cell Culture and Reagents .....	36
Flow Cytometry .....	37
Type I interferon neutralization .....	37
Chromium release assay .....	38
Quantitative RT-PCR .....	38
Immunohistochemical staining of lung TMAs .....	39
Bioinformatics analysis of miR binding .....	39
Cloning, transfection and luciferase assay .....	39
Lentiviral transfection of cell lines .....	40
Analysis of published lung cancer datasets .....	41



Chapter Three: MicroRNA-155 governs SHIP-1 expression and localization in NK cells and regulates subsequent infiltration into murine AT3 Mammary Carcinoma .....	42
Introduction .....	42
Results .....	44
NK cells in bic/miR-155 <sup>-/-</sup> mice retain normal cytotoxic function .....	44
miR-155 is linked to SHIP1 and influences chemotaxis .....	46
miR-155 deficiency confers impaired NK cell tumor tropism in vivo .....	52
Discussion .....	55
Materials and Methods .....	59
Mice, Cells, and Tumor Challenge .....	59
NK Cell Isolation .....	60
Flow Cytometry .....	60
Chromium Release Assay .....	61
Migration assay .....	62
Western blot analysis .....	62
Immunohistochemistry .....	63
Confocal Microscopy .....	64
Statistics .....	65
Chapter Four: S100A9 Contributes To T Cell Dysfunction Through Its Interaction with RAGE in Myelodysplastic Syndromes .....	66
Introduction .....	66
Results .....	67
T cells from MDS Patients are antigen experienced and functionally normal .....	67
S100A9 is a major source of inflammation in the MDS Bone Marrow Microenvironment and suppresses T cell proliferation .....	72
The Receptor for Advanced Glycation Endproducts (RAGE) is expressed on T cells and is activation responsive .....	80
Discussion .....	85
Materials and Methods .....	88
Cell culture and reagents .....	88
T cell activation and culture .....	88
Flow cytometry analysis .....	89
Interferon Gamma Enzyme Linked Immunosorbent Assay .....	90
Cytometric Bead Array .....	90
Western Blot .....	90
Virus Production and Transduction .....	91
Statistical Analysis .....	91
Chapter Five: Implications and Future Perspectives .....	92
References .....	100
Appendix A: Copyright Clearances .....	124

Appendix B: Institutional Animal Care & Use Committee Approvals .....	125
Appendix C: Institutional Review Board Approval .....	126

## LIST OF FIGURES

Figure 1: Overview of the Dissertation .....	ix
Figure 2: Human lung tumor cells express high levels of miR-183 but low levels of MICA/B .....	22
Figure 3: MICA/B surface expression on non-lung human cell lines is higher than that of lung cancers .....	23
Figure 4: Immunohistochemical analysis of MICA/B expression in human lung tumor tissues .....	24
Figure 5: miR-183 targets the 3'UTR of MICA/B mRNA.....	26
Figure 6: TGF $\beta$ suppresses MICA/B expression via miR 183.....	28
Figure 7: TGF $\beta$ suppresses MICA/B expression via miR-183 in the absence of Type I interferon .....	33
Figure 8: MHC Class I expression on Tumor Cell lines.....	31
Figure 9: Depletion of miR-183 in tumor cells enhances sensitivity to lysis by activated T cells .....	31
Figure 10: Characterization of miR-155 <sup>-/-</sup> NK cells .....	46
Figure 11: miR-155 <sup>-/-</sup> NK cells overexpress SHIP-1 and do not polymerize actin .....	47
Figure 12: miR-155 <sup>-/-</sup> NK cells exhibit an altered response to CCL2.....	50
Figure 13: Time Course Characterization of C57BL/6 (Wildtype) Derived Splenic NK cells .....	51
Figure 14: Time Course Characterization of B6.Cg-MiR-155 <sup>tm1.1Rsky/J</sup> ( <i>bic</i> /miR-155 <sup>-/-</sup> ) derived splenic NK cells .....	51
Figure 15: Time Course Characterization of C57BL/6 (Wildtype) and B6.Cg-MiR-155 <sup>tm1.1Rsky/J</sup> ( <i>bic</i> /miR-155 <sup>-/-</sup> ) derived Splenic NK cells.....	52

Figure 16: AT3 tumor burden is higher in miR-155 <sup>-/-</sup> hosts .....	54
Figure 17: NK cells fail to traffic to AT3 tumors in miR-155 <sup>-/-</sup> hosts .....	55
Figure 18: The Role of S100A9 in Myelodysplastic Syndromes .....	67
Figure 19: Phenotypic Characterization of Healthy and MDS PBMC.....	70
Figure 20: Phenotypic Characterization of Healthy and MDS PBMC.....	71
Figure 21: Phenotypic Characterization of Healthy and MDS BMMNC .....	71
Figure 22: Phenotypic Characterization of Healthy and MDS BMMNC .....	72
Figure 23: PBMC and BMMNC proliferation are inhibited by S100A9 .....	74
Figure 24: S100A9 does not induce cell death or apoptosis of PBMC but may induce cell cycle arrest.....	75
Figure 25: Interferon Gamma production is decreased with S100A9 treatment .....	76
Figure 26: S100A9 pretreatment sensitizes the T cell to degranulate.....	78
Figure 27: Schematic of T cell gating for degranulation .....	79
Figure 28: S100A9 decreases NF-κB phosphorylation through the TCR.....	80
Figure 29: RAGE is expressed in PBMC and T cells and decreases after T cell activation .....	81
Figure 30: RAGE is expressed in MDS Patients .....	82
Figure 31: RAGE is restricted to the CD4 T Cell compartment .....	82
Figure 32: RAGE+ T Cells are Th2 polarized.....	83
Figure 33: RAGE+ T cells are more proliferative and susceptible to S100A9 induced proliferative suppression.....	84
Figure 34: Schematic for RAGE (AGER) knockdown in T cells .....	85

## ABSTRACT

The immune system plays a dynamic role in cancer progression. The theory of immunoediting suggests that the relationship between the tumor cell and the immune cell is one that is in flux: initially highly active and responsive to tumor antigen to one that has escaped immune responsiveness. Once the tumor has formed and effectively “escaped”, there are multiple mechanisms that work against a conventional immune response. The tumor cell clones that have escaped the elimination phase are those that are less immunogenic. These clones downregulate MHC, have increased apoptosis through DAMP-driven mechanisms, and suppressive cell phenotypes are driven through cytokine-driven cues and innate feed-forward mechanisms. This project aims to understand three different mechanisms of tumor-induced immune suppression: the first, a model of lung adenocarcinoma, exploring innate NK subversion by repression of the NKG2D-MICA/B axis; the second, a model of mammary carcinoma used as a basis to explore differences in NK trafficking and exclusion from the tumor microenvironment due to upregulation of inhibitory signaling mediators; the third, a mechanism of T cell suppression induced by excessive production of danger associated molecular pattern (DAMP) S100A9 in Myelodysplastic Syndromes (MDS).

Lung Cancers of all subtypes are the leading cancer death in both men and women in the United States. While progress has been made in developing immunotherapies, we chose to focus on basic mechanisms of immunosuppression in order to identify ways to

reinvigorate tumor-immune responsiveness. Micro-RNAs (miRs) function via RNA interference and are implicated in cancer development and progression due to their effects on genes involving the cell cycle, apoptosis, and metabolism. Our group has previously shown that Transforming Growth Factor-beta (TGF $\beta$ ) inhibits NK cell function by means of inducing miR-183 and subsequent repression of DAP12, thus halting NK cell signaling. Here, we found that NKG2 ligand MICA/B which is normally upregulated in situations of stress or damage is suppressed in the presence of high levels of miR-183. This miR, employed by the suppressive TGF $\beta$ , renders NK cells dysfunctional by depleting MICA/B from the tumor cell itself so that the NK cell cannot recognize it through activating receptor NKG2D. This is a profound mechanism that hits at one of the earliest effector mechanisms in the tumor microenvironment.

Micro-RNA 155 is another oncomir that is expressed in NK cells and other leukocytes, where it is upregulated by inflammatory stimuli in the tumor microenvironment. SH2-containing inositol polyphosphate 5-phosphatase (SHIP-1) negatively regulates interferon gamma production in NK cells and regulates the actin cytoskeleton, having diverse effects on NK cell motility. SHIP-1 is a defined target of miR-155, and thus SHIP-1 is decreased in the context of excessive miR-155 expression. This miR is thus important to NK cell function, as we showed in our work that in the absence of this miR, there exists a dysfunctional NK cell that cannot traffic or produce proper amounts of cytokine in response to normal stimuli. Here, we found that miR-155 regulates chemotaxis and NK tumor infiltration downstream of SHIP-1 using a mouse model of mammary carcinoma. This is a basic science mechanism that teases apart the complexity of the relationship between this miR and leukocyte trafficking into the tumor bed,

identifying another mechanism of immune subversion in this case mediated by a lack of trafficking present in the inflammatory tumor microenvironment, and thus has applicability to many tumor types.

MDS are a disease driven by excessive inflammation secondary to peripheral blood cytopenias and hypercellular bone marrow. This disease is predominately driven by an excess of myeloid derived suppressor cells (MDSC) and suppressive cytokines that dampen conventional mechanisms of immunity. The role of T cells in the disease is incompletely understood. Here, we report on a newly identified mechanism of T cell suppression in the disease mediated by DAMP S100A9 through the Pattern Recognition Receptor (PRR) Receptor for Advanced Glycation Endproducts (RAGE). Rather than inducing a potent immune response as DAMP/PRR signaling should, we uniquely found that T cells are inhibited in their function when exposed to exogenous DAMP signaling. T cell proliferation is almost completely shut down, and interferon gamma production is halted.

While many PRRs are present on adaptive cells, RAGE was found to be exclusive to CD4<sup>hi</sup> T cells, whereby S100A9 signals through. These T cells did not express any lineage specificity, and produced normal amounts of cytokine when activated with anti-CD3/28. Treatment with S100A9 was able to induce RAGE expression on these T cells, indicating a positive feed forward loop. This RAGE expression was dynamic and decreased rapidly after T cell receptor (TCR) engagement, indicating that this RAGE/S100A9 signaling response may act as a pre-activation checkpoint for the T cell prior to responding to antigen. We found that RAGE<sup>+</sup> T cells are significantly increased

in the bone marrow of patients with MDS, and thus this may represent a way to capitalize on a lack of T cell responsiveness in a disease with typically limited treatment options.

The work presented here furthers our understanding of tumor-immune biology from both a basic science approach and more translational approaches. The questions asked throughout this work attempt to unpack the complexity of the relationship between the immune cell and the cancer cell in a push-pull that, given future efforts for translation, can improve outcomes and in the case of the RAGE/S100A9 axis, be translated into new therapies (Fig. 1).

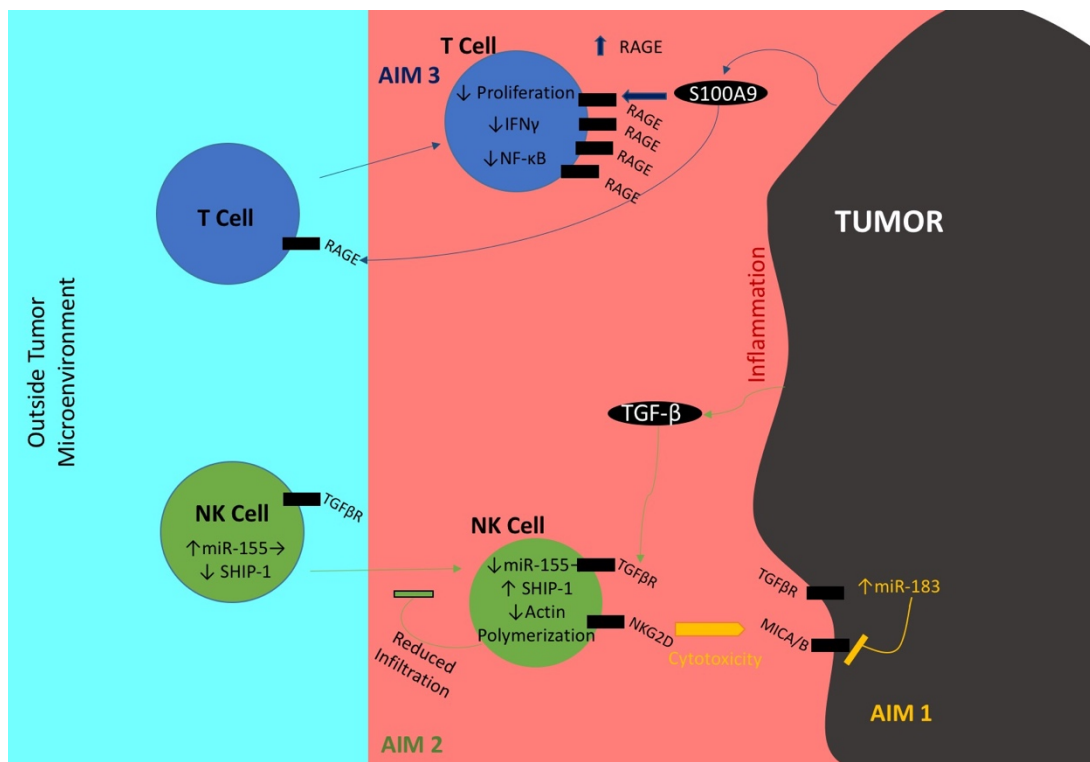


Figure 1: Overview of the Dissertation: Integration of the three projects presented within the dissertation.



## CHAPTER ONE:

### INTRODUCTION

#### *Introduction to NK cells*

Natural Killer (NK) cells are an innate effector lymphocyte cell subtype that kill and produce cytokine in a non-MHC restricted fashion (1). NK killing is dependent on a balance of positive and negative inhibitory signals or by the loss of major histocompatibility complex (MHC) class I (2). A conventional NK cell phenotype in humans is defined as CD3-CD56+, though NKT cell subsets that are double positive (CD3+CD56+) exist and are outside the scope of this dissertation (3). Murine analogs for these two subsets are CD3-NK1.1+ (or in the case of NKT CD3+NK1.1+) (4). Human NK cells can be further stratified based on their CD56 expression into CD56<sup>dim</sup>(CD16+) vs CD56<sup>bright</sup> (CD16-/dim) subpopulations. The CD56<sup>dim</sup> population is typically peripheral blood resident and the more cytotoxic NK subpopulation, and the CD56<sup>bright</sup> more secondary lymphoid organ resident and heavy producer of cytokine, typically Interferon Gamma (IFN $\gamma$ ), Tumor Necrosis Factor Alpha (TNF $\alpha$ ), and Interleukins-2,12,15, and 18 (5, 6).

NK cells display a wide variety of activating and inhibitory receptors that function to maintain a balance against effector function against healthy tissue. Situations of cell stress such as transformation induce expression of NK activating ligands such as MHC Class I and Chain-Related Protein A and B (MICA/B) on the tumor cell, leading to lysis of

the tumor or stressed cell (7-9). This is relevant in all contexts of health and disease including autoimmunity, viral infection, and cancer. Mechanisms of NK cell cytotoxicity can either be through release of lytic granules on lipid rafts such as perforin and granzyme B or through engagement of receptor/ligand pairs such as Fas/FasL which induce apoptosis secondary to caspase activation (10, 11). NK cell activation itself leads to production of numerous cytokines that can shape the immune milieu. This informs the subsequent immune response through T cell polarization (discussed further under **T cell** header below) and reinforces antigen presentation through IFN $\gamma$  production through MHC upregulation (12-15).

### ***NK cells and Cancer***

While a lack of MHC should be enough for the NK cell to recognize and lyse a given cell based on the missing-self hypothesis, tumor cells have evolved potent mechanisms to subvert NK cells through upregulation of ligands for inhibitory receptors. In addition to the NK activating/inhibitory receptor pairs, much like T cells, NK cells express checkpoint receptors such as PD-1 and TIM3, which engage with PD-L1/2 or Gal9 on the tumor cell. Sustained engagement and signaling with these receptor/ligand pairs leads to NK cell exhaustion and dysfunction (16-18). PD-1 blocking antibodies have been found to reinvigorate the suppressed NK cell similar to that of T cells (19). NK cells, like their adaptive cytotoxic counterparts, can be uniquely used as platforms for adoptive cell transfer. In earlier years, IL-2 activated lymphokine activated killer (LAK) cells were used as a platform for immunotherapy (20, 21), and in more recent years, these NK cells

have been endowed with chimeric antigen receptors (CARs) to direct these cells to recognize and kill tumor directly through specific antigen recognition (22, 23).

NK cells are found amongst tumor infiltrating lymphocytes (TIL) in melanoma, breast, colorectal carcinomas as well as other malignancies, and while their presence may be a positive prognostic indicator, the functional phenotype inside the tumor varies in terms of active functional output (24).

Identifying basic mechanisms of NK cell suppression can lead to reinvigoration of the suppressed NK cell phenotype. Studying tumor cell induced factors that may affect NK cell function is the basis for **Chapter 2**.

### ***microRNAs and Cancer***

MicroRNA's (miR) are small (19-24 nucleotide) noncoding RNAs that regulate gene expression through posttranscriptional interference by RNA repression. To function, they bind to a region at the 3' UTR of their target mRNA. They were originally thought to be noise in the genome but were later discovered to be tightly regulated and important in all aspects of development and normal hematopoiesis (25). MiRs have been found to be dysregulated in multiple diseases and have been extensively linked to cancer. In particular, they have been shown to be involved in the regulation of oncogenes, tumor suppressor genes and genes associated with metastasis (26). The phrase "oncomir" was coined to describe oncogenic miR's which themselves have been shown to drive cancers. Many of these miRNA expression patterns have been linked to negative outcomes across various cancer subtypes, and specific miR expression patterns have been tightly tied to specific cancer subtypes (27). These expression patterns have been proposed for use as

cancer biomarkers for stratification and prognosis. Over 2000 miRs have been identified at this time, and many have sequence homology with each other and are referred to as clusters (28). Our past work focuses on the cluster miR-183-96-182, which despite playing normal roles in organogenesis, has been associated with the prognosis of liver, breast and lung cancers when overexpressed (29-32). MiR-183 has been found to be inducible in tumors through cytokine TGF $\beta$  expression which dominates in many suppressive tumor microenvironments (33, 34). Our group has shown that it suppresses NK cell function against tumor through the suppression of NK adaptor molecule DAP12 (35). Thus miR-183 can directly suppress anti-tumor immunity. This older work and more our recent follow-up work will be extensively discussed in **Chapter 2**.

Additional work discussed in this thesis focuses on miR-155. miR-155, like miR-183 is expressed in leukocytes and is upregulated by inflammatory stimuli such as TNF $\alpha$  and IFN $\gamma$  (36, 37). It is overexpressed in various cancers including leukemias and lymphomas as well as many solid tumors (38-42). SH2-containing inositol polyphosphate 5-phosphatase (SHIP-1) is expressed in NK cells, where it negatively regulates IFN $\gamma$  production, and is a target of miR-155 (43, 44). SHIP-1 is absolutely critical for NK cell development and function, and overexpression of miR-155 decreases SHIP-1 expression (45). This oncomir has been studied extensively in T cells, where it has been found to promote effector T cell responses, and in knockout experiments, the T cells are rendered dysfunctional (46, 47). In both NK cells and T cells, miR-155 is cytokine and activation responsive (48-50). These past reports have demonstrated the importance of this miR in NK cell functionality, but we were intrigued by the fact that excessive miR-155 leads to an increase in SHIP-1, and chose to interrogate this further utilizing a miR-155 knockout

mouse. In this work we identified a physiologic role of miR-155 in NK cell chemotaxis that leads to reduced tumor infiltrating NK cells and thus reduced tumor clearance in a mouse model of mammary carcinoma. This work will be discussed in **Chapter 3**.

### ***Myelodysplastic Syndromes***

Myelodysplastic syndromes are a group of diseases of aging, affecting between 5.3 and 13.1 cases per 100,000 people (51-53). Central to the disease is ineffective hematopoiesis driven by mutational burden and inflammatory aging (inflammaging) associated increases in suppressive populations such as MDSC and Treg as well as an increased rate of apoptosis (54-64). This increased apoptosis leads to cytopenias noted in the peripheral blood, and a hypercellular bone marrow with increased blasts (immature myeloid progenitor accumulation)(63-70). MDS affects those >65 years of age and has a grim prognosis of six months once it approaches high risk disease staging. Up to one-third of patients with MDS will transform to acute myeloid leukemia (AML), thus this disease deserves much focus in research to determine mechanisms contributing to issues with immunosurveillance and ways in which we can halt disease progression(71).

MDS is staged using the International Prognostic Scoring System (Revised) (IPSS-R). Patients are staged from 0-6 (ranging from very low risk to very high risk) based on cytogenetics (mutational status), blast percentage, hemoglobin, platelets and absolute neutrophil count (ANC) (72, 73). Patients with lower risk disease can live for many years prior to transformation occurring, and with these patients the focus is more about symptom management with less intense therapies (74). With the higher risk patients, the risk of transformation is very high, and the survival time drops to months. In these patients,

oftentimes stronger cocktails of chemotherapeutics are utilized or allogeneic bone marrow transplant (BMT) (75).

Mutational burden of MDS is often a driver of disease, affecting myeloid progenitors and thus impacting those cells originating from this hematopoietic lineage. Patients that progress to AML have been found to have a higher somatic mutational burden than those who do not. The most common somatic mutations in MDS include the following genes: DNA Methyltransferase 3A (DNMT3A), Serine and Arginine Rich Splicing Factor 2 (SRSF2) Janus Kinase 2 (JAK2) and TP53. Additional sets of germline mutations have been identified as associated with MDS including DEAD-Box Helicase 41 (DDX41), Runt Related Transcription Factor 1 (RUNX1) and GATA-Binding Protein 2 (GATA2). A common mutation seen in the disease is deletion of chromosome 5q (Del 5q), which is a more indolent subset of MDS that predominately affects women (54).

MDS treatment is variable and specific to disease staging. Many patients are asymptomatic when diagnosed and evidence of disease was determined through anemia noticed on a complete blood count (CBC) during a routine physical. Other symptoms include easy bruising, fatigue, weakness and bone pain. Watchful waiting is an approach taken often given that MDS is an incurable disease and not enough evidence for treatment at earlier asymptomatic stages exist. When the decision is made to treat, it is often focused on symptom control.

Typically, the first treatments decided on are hypomethylating agents such as azacytidine and decitabine, growth factors such as epoetin to stimulate erythropoiesis, GM-CSF to stimulate neutrophils, immunosuppressive therapies, and in the case of Del 5q cases, lenalidomide (74).

The hypomethylating agents inhibit DNA methyltransferases and have been shown to improve overall survival due to their response rate to treatment of 40-60% often leading to a decrease in dependence on blood transfusion. Unfortunately, some patients become resistance to the hypomethylating agents currently used in the clinic (76-78).

Immunosuppressive therapies are useful in lower risk disease. The two most common therapies in this classes are Anti-Thymocyte Immunoglobulin (ATG) and Cyclosporine. ATG is reactive against T cells, and this drug is used to suppress the smoldering inflammation present in MDS that increases apoptosis and leads to cytopenias. Cyclosporine functions similarly in that it blocks T cell activation. Oftentimes ATG and cyclosporine are used in combination as a two-hit punch against T cell mediated inflammation (79). This also helps as many MDS patients have comorbidities with T cell mediated autoimmune disease that leads to a worse prognosis, and so immunosuppression is indicated due to both diseases (80, 81).

Immunomodulatory (IMiD) drugs are thalidomide analogues. These drugs have an unknown mechanism but is anti-inflammatory and pro-erythropoetic. Unlike the immunosuppressive therapies, IMiDs increase the function of T cells but with the production of less aggressive inflammatory cytokines such as IL-10. While it is typically used in Del 5q patients with great success, it is under investigation in non-Del 5q patients and has shown some success, though it is limited in comparison to the high response rate seen in Del 5q MDS. These drugs lead to decreased transfusion dependence due to a strong erythropoetic response (79, 82).

Cellular therapies are currently under investigation for MDS. The oldest cellular therapy currently in use is allogeneic bone marrow transplant. This is the only real curative

therapy and is typically only used for those patients with later stage disease. Despite being curative, those patients with TP53 mutations still have a worse prognosis (83-86).

Newer cellular therapy options include Chimeric Antigen Receptor T cell immunotherapy (CAR-T), which are a promising treatment for many hematologic malignancies. CAR-T utilize a T cell engineered to express the scFv of an antibody targeting a given tumor associated antigen (TAA) fused to CD3 $\zeta$  via a linker. This reengineers the T cell with a new directed specificity, and upon reinfusion, these T cells specifically target their new antigen leading to tumor cytolysis and ideally, tumor control (87). They have been approved to treat acute lymphoblastic leukemia (ALL) and diffuse large B cell lymphoma (DLBCL), and these approved therapies both target CD19 (88-90). For MDS, CAR-T have been developed against the IL-3 receptor (CD123) and NKG2D ligands and both are currently in clinical trials (91, 92).

### ***DAMPS and S100A9***

S100A9 is a Danger Associated Molecular Pattern (DAMP) also known as an alarmin. DAMPs initiate an inflammatory response at its earliest stages. The S100 family consists of multiple members that exhibit homology to one another. S100A8 (Calgranulin A) / S100A9 (Calgranulin B) is often found as a heterodimeric complex known as Calprotectin, however both proteins can be found as homodimers. Neutrophils are the primary producer of S100A8 and S100A9 to initiate inflammation in many pathogenic states, but they are also produced by various other cells of myeloid origin (93, 94). In inflammatory bowel diseases such as ulcerative colitis and Crohn's disease, the presence of S100A8/S100A9 complex is a biomarker of disease activity due to leukocyte shedding



and increased neutrophil presence in the bowel (95, 96). S100A8 and S100A9 are calcium and zinc binding proteins. Calcium or Zinc are necessary for binding of S100A8/S100A9 and its ligands (97). Our group has extensively focused on S100A9 biology for the past 10 years, thus **Chapter 4** will focus on furthering our knowledge of the complex molecule that is S100A9.

S100A9 is involved in the migration of myeloid cells and is secreted from these cells. These myeloid cells are recruited to inflammatory sites and are often found within the tumor microenvironment (98, 99). Some tumor cell lines themselves produce S100A9 which promotes more inflammation inside the tumor, such as pancreatic, prostate and colorectal adenocarcinomas (98, 100). The localization of this protein varies between cell subtypes, in some situations cytoplasmic and secreted, some membrane-bound, but it is widely expressed, and outside of its overexpression in the context of disease, is a normal innate immune molecule (101, 102).

S100A9 binds multiple different elements ranging from keratin to Toll-Like Receptor 4 (TLR4), CD33, and the Receptor for Advanced Glycation Endproducts (RAGE) which will additionally be the focus of **Chapter 4** (60, 98). These multiple receptors allow S100A9 to signal through different pathways. S100A9 activates Nuclear Factor Kappa B (NF- $\kappa$ B) signaling which is a pleiotropic signal involved in myriad biological processes, as well as MAP Kinase (MAPK) signaling (103-105). S100A9 also leads to the production of multiple cytokines such as IL-6 and IL-1B (106, 107).

S100A9 is involved in a positive feedback loop and acts as a driver of immature myeloid cells in addition to its function on neutrophils. Many groups have previously shown that tumors with higher S100A9 have more Myeloid Derived Suppressor Cells

(MDSC) in inflammatory environments (108-110). Our group uniquely showed that CD33, a marker for myeloid cells, is a receptor for S100A9 (60).

### ***S100A9 and Myelodysplastic Syndromes***

Our group and now others have shown that S100A9 drives the MDS phenotype through the expansion of MDSC, promotion of pyroptosis, and PD-1 expression in hematopoietic stem and progenitor cells (HSPC) (60, 70, 111). We have shown that S100A9 is highly expressed in MDS patient plasma, in particular low risk disease plasma, compared to healthy donors, as well as the fact that S100A9 is correlated to the expression of somatic gene mutations (70).

As mentioned above, MDSC are a cell subtype prevalent in many tumor microenvironments that are the quintessential example of an immature myeloid cell. They inhibit T cell function and effector immune responses and lead to worse responses in various cancer subtypes (112, 113). MDS, being a disease of the myeloid compartment, is often one that has a high percentage of MDSC in the bone marrow microenvironment when compared to healthy patients (59). These MDSC are Lineage<sup>-</sup> HLA-DR<sup>-</sup> CD33<sup>+</sup>, and through engagement of CD33 with S100A9, TGF $\beta$  and IL-10 are produced, leading to a suppressed microenvironment. S100A9, as an alarmin, should be a more acute signal that is rapidly shut off, leading to a break in the inflammatory cascade; However, in this disease, more S100A9 is present due to more inflammation and leads to more CD33<sup>+</sup> cells, which in turn produce more S100A9 (60). This is one mechanism for a lack of restrained inflammation in the disease.

Additional work with our collaborators showed that treatment with S100A9 triggered pyroptosis, a form of inflammatory cell death, by inducing active Caspase 1 and NLR family pyrin domain containing 3 (NLRP3) via a Reactive Oxygen Species (ROS) dependent mechanism. This was found in both primary MDS samples as well as a mouse model phenocopying the disease through overexpression of S100A9 (70).

Programmed Death 1 (PD-1) and its ligand Programmed Death Ligand 1 (PD-L1) is an immune checkpoint that acts a safety switch for T cells during activation. PD-1 is sharply upregulated after activation, after which point it will come down unless it engages PD-L1, which can then induce apoptosis. In T cells that have been chronically exposed to antigen and cytokine, PD-1 may be upregulated and stay at a high expression level. In the field of tumor immunology, it is often used as a marker of an exhausted T cell (114-117). Our group has found that there are less CD4+ and CD8+ T cells in MDS, and that in both compartments, the percentage of PD-1 is markedly increased compared to healthy controls. Beyond T cell biology, our group investigated the role of this axis on HSPC and MDSCs. In MDS patients, we found that PD-1 and PD-L1 are increased on CD71+ erythroid progenitors and CD34+ HSPC, and PD-L1 is increased on MDSC. In vitro assays with recombinant human S100A9 (rhS100A9) treated healthy bone marrow mononuclear cells increased PD-L1 on MDSC and PD-1 on HSPC and erythroid progenitors. Treatment with MDS plasma instead of the recombinant protein showed a similar effect. Mechanistically, this led to active Caspase 3 and hematopoietic cell death. Blocking the PD-1/PD-L1 pathway via anti-PD-1 or PD-L1 improved hematopoiesis in a mouse model overexpressing S100A9, and those cells had increased colony forming capacity in *ex vivo* colony formation assays. This signaling is associated with abnormal

c-Myc activation, as S100A9 treatment was unable to induce PD-1 or PD-L1 in Myc+/- mice. Thus, S100A9 leads to c-Myc induction and dysregulation of the PD-1/PD-L1 axis (111). **Overall, S100A9 contributes to ineffective hematopoiesis and pathology in MDS and other diseases of inflammation, but the adaptive immune compartment is still not well studied or understood in the disease.**

## **T cells**

T lymphocytes are a white blood cell that are an essential component of the adaptive immune system. They are identified through expression of surface antigen CD3, but beyond that exist in multiple subtypes (118). Conventional T cells express an Alpha/Beta (a/b) T Cell Receptor (TCR). T cell development produces a T cell that either expresses CD4 or CD8 and should have undergone VDJ recombination and have passed through both central and peripheral tolerance to become a T cell that has unique antigen specificity and is not autoreactive (119). T cells undergo VDJ recombination when they are developing in order to gain one single functional unique antigen specificity for which they recognize. Conventionally speaking, a CD4 T cell is the dominant cytokine producer and comes in multiple polarizations that depend on the cytokines produced in its given microenvironment that it is exposed to as a naïve T cell (120). These polarizations are conventionally termed Th1, Th2, Th17 and Treg. The CD4 subset provides help to other cells in the immune system through production of cytokines that either drive or suppress an immune response. Cytotoxic CD4 T cells exist in small percentages and have been shown to produce Granzyme B, but not Granzyme A (121). The CD8 subset is the conventional cytotoxic T cell, though they also produce cytokine. T cell effector function

is similar to that of an NK cell whereby granzyme B and perforin are produced to kill other cells. These two subsets are typically found at a ratio of 2:1 CD4:CD8 in healthy patients, and abnormal skewing of this ratio can be indicative of disease (122).

More unique and rare T cell subsets include those T cells with a Gamma/Delta (g/d) TCR, which range from 1-5% of the peripheral blood and are enriched in certain tumor microenvironments and epithelial surfaces such as the gut (123, 124). They are unique in that they kill in a non-MHC restricted manner, but do have a defined TCR specificity unlike an NK cell (125, 126).

T cell activation is dependent on the T cell's TCR seeing its cognate antigen presented to it on an antigen presenting cell (APC) such as a dendritic cell (DC), macrophage or B cell via MHC. CD4 T cells see MHC Class II, and CD8's see MHC Class I. Once this T cell has received a signal through the TCR, costimulation and cytokine are the other two activation requirements (127). If costimulation is not provided, activation induced cell death (AICD) can occur mechanistically through a Fas-FasL interaction (128). Such costimulation is provided to the T cell via the APC cell surface molecules such as B7.1, B7.1, 4-1BBL, OX40L or CD70, to the cognate T cell surface proteins CD28, 4-1BB, OX40 or CD27 (129, 130). T cells require gamma-chain cytokines such as IL-2, -7, -15 or -21 to function and survive (131). This activation signaling cascade leads to a chain of intracellular events leading to more cytokine production, proliferation, and differentiation. When a T cell becomes activated for the first time, the naïve T cell clonally expands, and at the end of the immune response, the clone contracts into long-lived memory cells (132, 133).

The T cell memory phenotype is defined based on chemokines and other receptors that are dynamic in response to a T cell's life and localization (131, 133, 134). T cells are traditionally divided into two categories: effector memory and central memory. The former of which responds quicker to secondary stimulation, and the latter of which is a longer lived, but slower responding cell. These can be defined by expression of CD45RA, CD45RO, CCR7, CD62L, CD27 and others (120, 134, 135). TEMRA T cells are those memory cells which re-express CD45RA, a marker typically lost upon activation (136). These cells can either be currently activated or express a more exhausted phenotype, which can be further discriminated based on expression of CD69 and checkpoint receptor expression.

### ***Bone Marrow T cells and T cells in Myelodysplastic Syndromes***

The bone marrow (as well as the thymus) is a primary lymphoid organ. B cells and T cells are born here in a process called lymphopoiesis, and the T cells travel to the thymus to mature. Conventional (a/b) T cells constitute 3-8% of nucleated cells in the human bone marrow (137, 138). Through signals elicited by chemokines, T cells traffic to the bone marrow and become resident there, and it is thus known as a home for long-term resident memory cells (138, 139). Egress of T cells from the bone marrow is governed by G-protein coupled receptor sphingosine-1-phosphate (S1P) and sphingosine-1-phosphate-1 (S1P1). Gradients of S1P expression allow the T cell to traffic, but CD69, an activation marker of T cells, suppresses S1P1, preventing T cell egress (140-143). Bone marrow T cells have been shown to have a higher rate of proliferation, perhaps attributable to homeostatic proliferation (144).

T cells in MDS have not been investigated much in terms of their mechanistic defects. While T cells play an essential role in immunosurveillance in many diseases, given that MDS is a disease of the myeloid compartment, not much focus is given to the lymphoid compartment. Typically, the T cells in MDS are not derived from the malignant clone, but it has been shown in rare cases (145). In MDS BM, a lower CD4 to CD8 ratio has been found compared to that in healthy BM. Less naïve T cells and more TEM/TEMRA T cells have also been shown (146). Granzyme and perforin expression between MDS and healthy bone marrow T cells was not shown to differ (147). T cell clonality has been shown to be increased in MDS bone marrow, but activation markers have not been shown to be increased (148). So interestingly, effector memory cells seem to preside but they do not seem to be activated. In terms of the T regulatory cell compartment which is of focus due to the frequent comorbidities seen with autoimmune disease in MDS, low risk MDS patients were found to have more TEM Treg cells, and they were found to be more suppressive than TCM Treg cells in vitro (61, 62).

### ***Pattern Recognition Receptors and T cells***

Pattern Recognition Receptors (PRR) are proteins capable of recognizing structurally similar motifs or molecules on pathogens or stressed cells in order to initiate an immune response. PRR's typically recognize pathogen associated molecular patterns (PAMPs) or danger associated molecular patterns (DAMPs). Typically, PRR's are present on innate cells and the goal is to initiate further inflammatory cues mediated through PAMPs/DAMPs (149-151). PRR/PAMP/DAMP signaling can induce an immune response through the APC responding to the threat and subsequently activating the T cell.

Uniquely, though, some adaptive cells also express PRRs which allow them to directly respond to stress and create their own inflammatory cascade (152). The most well-investigated PRR family on T cells is the Toll-like Receptor (TLR) family. TLR signaling activates NF- $\kappa$ B and its target genes when LPS or heat shock proteins are sensed. TLR4 signaling in particular has been investigated in T cells, where it was found to enhance T cell proliferation and survival *in vitro* particularly within CD4 T cells (153-156). Another PRR found to be present on T cells is the Receptor For Advanced Glycation Endproducts (RAGE) (157-160).

RAGE is an immunoglobulin superfamily member PRR that recognizes structural motifs such as Beta-sheets, amyloid-beta peptides, proteins or lipids that become glycosylated (nonenzymatic mediated bonding of a sugar to a protein or lipid) known as Advanced Glycation Endproducts (AGEs), S100 family proteins, and HMGB1 (161, 162). It exists in multiple isoforms including a soluble version that acts as a scavenger, though most isoforms are typically membrane-bound. RAGE expression has been found on dendritic cells, granulocytes, monocytes/macrophage, neurons, microglia, muscle cells and endothelial cells (163). Thus, it is widely expressed and has multiple roles in immunobiology and otherwise, where it signals through ERK and NF- $\kappa$ B. This PRR has been implicated in cellular stress, inflammation, and diseases, typically those of aging (164, 165). To that end, RAGE has been extensively studied in the fields of skeletal and neurobiology. It has been found to be a target for therapeutics for Alzheimer's disease due to its binding of amyloid-beta, and many compounds have been developed for clinical trial (FPS-ZM1, TTP448) (166). RAGE ligands have also been shown to signal through



RAGE in the bone and cause osteoblast apoptosis (167, 168). Importantly, RAGE has been studied in T cells, but in a limited manner with a focus on diabetes (159).

In terms of basic immunobiology, RAGE has been found to be involved with Th1 T cell polarization. Th1 polarization is governed by the transcription factor T-Bet, and Th1 polarized T cells are known to produce cytokines IFN $\gamma$ , TNF $\alpha$  and IL-2. RAGE $^{-/-}$  T cells were shown to produce more IL-10, IL-5 and TNF $\alpha$  in response to TCR engagement and costimulation (158). RAGE $^{-/-}$  T cells produced less TNF $\alpha$  and IL-2 compared to wild type T cells (160). RAGE expression was found to be higher on T cells of patients with diabetes, likely due to the chronic AGE exposure which is higher in patients with diabetes (157, 159). Expression of RAGE is shown to increase in these patients after T cell activation in the CD4 compartment, but is shown to decrease in healthy donors after T cell activation (157). The RAGE $^{+}$  T cells in these patients produced more IL-17, degranulation marker CD107a and IL-5. Transcriptomics showed that the T cells from these patients that were RAGE $^{+}$  had higher expression of inflammatory markers and activation markers(157). Since S100A9 is a ligand for RAGE and is understudied in both T cells, and unstudied in MDS, **this serves the basis for Chapter 4.**

## CHAPTER TWO:

### IMMUNE EVASION BY TGF $\beta$ -INDUCED miR-183 REPRESSION OF MICA/B EXPRESSION IN HUMAN LUNG TUMOR CELLS

**A note to the reader:** this chapter has been previously published in a research article in *Oncoimmunology*, Trinh/Kandell et. al. 2018 (169).

#### *Introduction*

Lung cancer remains a deadly disease worldwide, due in part to lack of reliable means for early diagnosis as well as lack of detailed understanding of immune escape mechanisms developed by the advancing tumor cells (170, 171). Emerging evidence indicates that microRNAs (miRs) may play a critical role in cancer and could serve as biomarkers, depending on the tumor type (26). These non-coding small RNAs function via RNA interference-mediated post-transcriptional gene regulation, and their dysregulation is of particular importance in cancer development and progression due to their potency to control genes involved in tumorigenesis, cell cycle control, metabolism, apoptosis and tumor progression (172). Recently, miR-183 has garnered considerable attention because of its overexpression in numerous human cancers, including lung cancer (32, 173, 174). It is part of the highly-conserved miR-183-96-182 cluster, located on human chromosome 7. In addition to lung cancer, upregulation of miR-183 has been associated with poor prognosis in carcinomas of the breast (175), colon (176, 177), liver (178), esophagus (179), prostate (180), and pancreas (181) and is driven by the presence of a number of promoter elements specific for  $\beta$ -catenin/TCF/LEF-1 in its 5' UTR (182)

and thus is associated with cancer development (183). Moreover, tumor-associated factors such as Transforming Growth Factor-beta (TGF $\beta$ ) (35) and AKT (184) have been identified as additional upstream regulators of miR-183 transcription. Additional effects of miR-183 include the induction of HIF-1 $\alpha$ , which has been reported to protect against hypoxia and starvation (185). Also, miR-183 inhibits apoptosis and promotes proliferation and invasion by downregulation of Programmed Cell Death 4 (PDCD4) in tumor cells (178, 179) and is reported to target protein phosphatase 2A (186), EGR1 (187), PTEN (187) and FoxO1 (188), all of which are involved in tumor cell survival and proliferation. Although a clear role of miR-183 is emerging as a tumor promoter, it is not known whether it plays a role in immune escape by the tumor.

In order for a tumor to flourish, it must dampen the immune system and avoid detection by immune cells, including natural killer (NK) cells. NK cells are poised to kill aberrant cells, including tumor cells, by virtue of high expression of activating receptors, such as NKG2D (189, 190). NKG2D is a C-type, lectin-like, type II transmembrane glycoprotein expressed on activated NK, CD8 T and  $\gamma\delta$ T cells that can recognize ligands on target cells induced by stress, DNA damage, or cell transformation (191). It utilizes a specific adaptor protein, DAP10, to signal downstream for mobilization of lytic granules towards target cells (192). NKG2D recognizes a number of ligands, which include two members of the major histocompatibility complex class I chain-related (MIC) proteins, MICA and MICB, as well as 6 members of UL16-binding proteins, ULBPs 1-6 (193-195). MICA/B constitutes a separate family of highly-glycosylated membrane-anchored MHC class I-like molecules that share structural homology to the MHC-I heavy chain but does not bind  $\beta$ -2 microglobulin or transporter-associated with antigen processing (TAP) (193).

However, this phenomenon is relevant for human NK cells only, as MICA/B are not conserved in the mouse, unlike Rae1 and ULBP1 (196) (197), so it has not been investigated in depth in this context. Unlike classical MHC-I molecules, MICA/B proteins are rarely displayed on normal cells and are only induced upon viral infection, DNA damage or transformation to serve as danger signals for clearance by NK cells. In fact, MICA/B has been reported on numerous human cancer types, including lung cancer, and its level of expression can be prognostic (198-200). Thus, a potent means for transformed tumor cells to escape immune detection is to downregulate the surface expression of NKG2D ligands. Despite the ability of NK cells to penetrate the tumor bed, the absence of NKG2D ligands could blind the NK effector cells to the surrounding tumor cells. To test this concept, we analyzed whether miR-183 could target NKG2D ligands on tumor cells, and uncovered a seminal pathway for miR-183 specific suppression of MICA/B ligands on human lung tumor cells. Therefore, in addition to promoting tumor cell survival and proliferation, miR-183 has an immunoregulatory property that disarms NK cells by depleting MICA/B from the tumor cell surface.

## **Results**

### **MiR-183 is overexpressed and MICA/B is under-expressed in human lung cancer**

Expression of MICA/B can be heterogeneous among tumor types and tumor cell lines (193, 198). In analysis of MICA/B expression in human non-small cell lung carcinoma (NSCLC) cell lines, we found low or absent levels of expression on H1155, H1355 and H2170, H1299, A549 and Wi-38. (**Fig. 2A**). This was in sharp contrast to human bronchiolar

epithelial cells, HBE4, transformed by Epstein-Barr E6/7, as well as K562 chronic myelogenous leukemia cells, both of which express high levels of MICA/B. This data initially suggested to us that this may be simply a solid tumor phenomenon, however we additionally analyzed Panc-1 and MiaPaCa and found high levels of MICA/B, similar to that seen on HBE4, K562, and HeLa (**Fig. 3A, 3B**). This indicated to us that this is perhaps a novel, lung-exclusive phenomenon. Reports have shown that tumor cells can downregulate NKG2D ligands, including MICA/B, to evade NK and effector CD8<sup>+</sup> T cell responses (201-204). Although MICA/B reportedly can be shed from tumor cell surfaces, downregulation of these genes is another important mechanism to disrupt MICA/B expression. Emerging data indicates that miRs are aberrantly expressed by tumors and can control critical genes associated with proliferation and metastasis. To understand if miRs might also control immune escape in tumor cells, we focused our efforts on miR-183 which is known to be overexpressed by tumors of diverse origin, but may be of particular interest in the solid tumor realm, particularly that of lung cancer, as shown in our previous work (35). Bioinformatics analysis of the MICA and MICB 3' UTRs by miRANDA and TargetScan revealed high affinity miR-183 binding sites in both genes (**Fig. 2B**), suggesting that both MICA and MICB could be repressed by miR-183. Of particular interest, no predicted miR-183 binding sites were present in the 3'UTR of the six ULBPs that are also ligands for the common receptor, NKG2D, indicating that they are under a separate regulatory machinery than that which controls MICA/B. We then sought to address whether there was an inverse correlation between miR-183 and MICA/B expression in the human lung cell lines. Analysis of miR-183 expression among the cell lines revealed that, in contrast to virally-transformed HBE4 cells, and leukemic K562 cells, which expressed little miR-183, all of the lung lines expressed

heightened endogenous levels of miR-183 and the level of miR183 expression occurred in reverse direction of that of MICA/B. (Fig. 2C). Further, analysis of The Cancer Genome Atlas (TCGA) human lung dataset revealed a striking increase in miR-183 expression in tumors as compared to normal tissue (Fig. 2D). In contrast, let-7c, a microRNA known to suppress expression of oncogenes thus leading to cellular proliferation (205), was sharply downregulated from normal levels in the same lung tissues, as reported by others (206). The inverse relationship between miR-183 and MICA/B, in combination with the miR-183 binding sites on MICA/B and elevated miR183 expression in the TCGA lung tumor database, suggested potential MICA/B dysregulation by miR-183 in lung cancer.

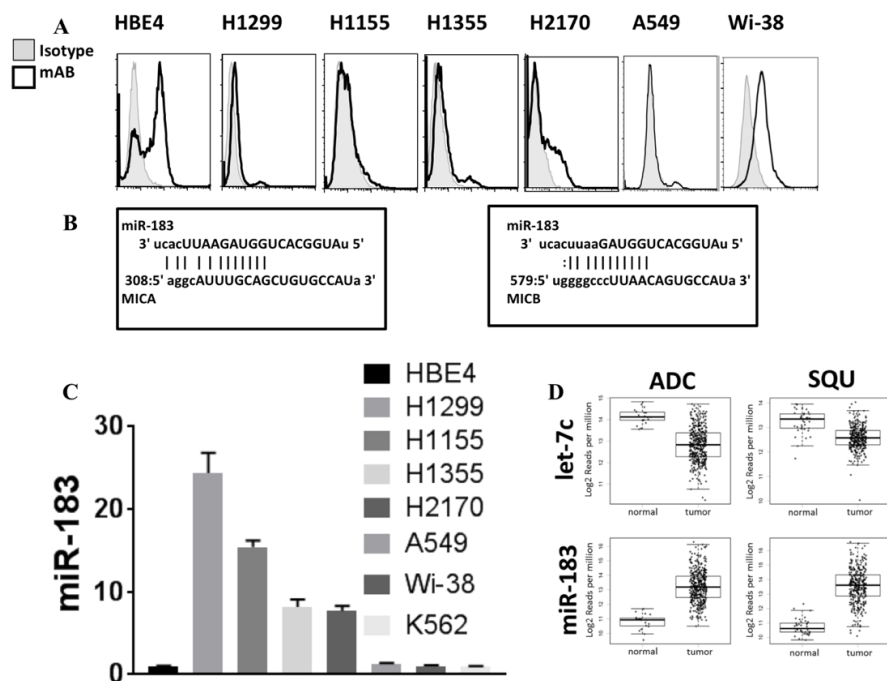


**Figure 2.** Human lung tumor cells express high levels of miR-183 but low levels of MICA/B. (a) Flow cytometric analysis of MICA/B in human lung tumor cell lines, H1299, H1155, H1355, H2170, A549, and Wi-38, in comparison to Epstein-Barr virus E6/7-transformed HBE4 lung epithelial cells. (b) Alignment of human MICA and MICB 3'UTR mRNA and miR-183 as depicted by the miRanda algorithm (microRNA.org). The number labeling the 5' end of the MICA/B mRNA represents the nucleotide position downstream of the translation termination codon. Capital letters constitute the miR seed sequences and vertical lines depict miR binding to mRNA. (c) qPCR analysis of miR-183 in the same lung cell lines as (A) showed a reverse correlation with MICA/B expression. (d) Using the TCGA database, meta-analysis was conducted for miR-183 expression in 422 human lung adenocarcinoma (ADC) samples as compared to 46 normal adjacent tissues, and 332 squamous (SQU) cell carcinoma samples as compared to 45 normal adjacent tissues. Unlike let-7 miR, which is known to be downregulated in lung cancer, miR-183 was elevated.

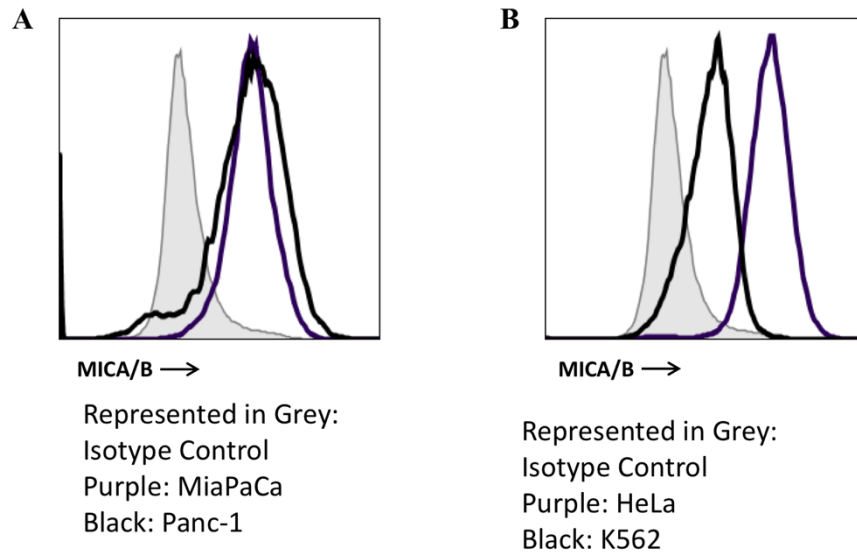


**Figure 3.** MICA/B surface expression on non-lung human cell lines is higher than that of lung cancers. (A) Human pancreatic adenocarcinoma tumor cell lines MiaPaCa and PANC-1 express high levels of MICA/B compared to isotype control. (B) HeLa cervical epithelial and K562 chronic myelogenous leukemia cells express moderate-to-high levels of MICA/B.

To confirm clinically that elevated miR-183 in the TCGA database correlated with low to absent expression of MICA/B in lung cancer, we next evaluated surface expression of MICA/B in paraffin-embedded lung tumor tissues containing adenocarcinoma and squamous NSCLC. The Allred scoring system was used and a representative figure of Scores 0-3 is shown in **Fig. 4A**, as well as non-neoplastic lung parenchyma in **Fig. 4B**. (207). Using this representative data, we see that immunohistochemical analysis demonstrates that the intensity of MICA/B staining in Grade 1, Grade 2 and Grade 3 squamous cell carcinoma specimens is no different from that seen in normal adjacent tissue. All tumor grades have approximately the same staining intensity for both squamous cell and adenocarcinomas. (**Fig. 4C**). In addition, the percentage of MICA-positive tumor cells was not higher than that of adjacent normal tissues, using the Allred scoring system of 1 = 1/100, 2= 1/10, 3 = 1/3, 4 = 2/3, 5 = >2/3 (**Fig. 4D**). In adenocarcinoma specimens, again the intensity of MICA/B staining in all the grades was

minor (Score 2) similar to that of adjacent normal tissues. Despite this, there exists a higher percentage of tumor cells expressing MICA/B (**Fig. 4E, 4F**), which correlates with earlier Grades 1-2, but not Grade 3. Thus, MICA/B expression is minor, and is not overexpressed beyond normal levels in lung cancer tissues. We earlier conducted meta-analysis of MICA and MICB mRNA gene expression in patient lung adenocarcinoma and normal tissues taken from data in a published report (208) and also found little MICA/B gene expression in the tumors, equivalent to the levels seen in normal tissues (35). Thus, similar to the low levels of MICA/B seen in lung cell lines, primary patient lung cancer tissues do not express MICA/B transcripts or proteins beyond the levels seen in adjacent normal tissues.

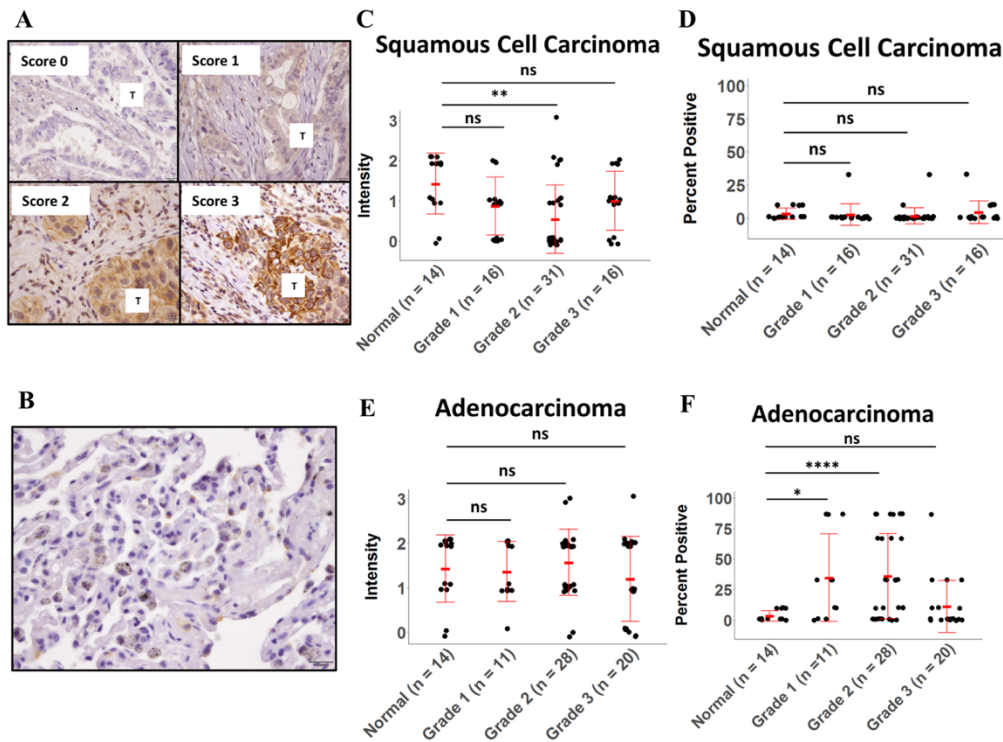


**Figure 4.** Immunohistochemical analysis of MICA/B expression in human lung tumor tissues. (a, b) Paraffin-embedded adenocarcinoma and squamous cell carcinoma tissues were stained with anti-MICA/B and scored 0–3 using the Allred Intensity scoring system. In figure 2A, tumor with different IHC scores are represented. In figure 2B, the adjacent non neoplastic lung parenchyma is represented with macrophages containing carbon deposits. (c, d) Staining Intensity and percentage of MICA/B<sup>+</sup> positive tumor cells in squamous cell carcinoma, using the Allred Percentage scoring system of 1 = 1/100, 2 = 1/10, 3 = 1/3, 4 = 2/3, 5 = >2/3. (e, f) Staining Intensity and percentage of MICA/B<sup>+</sup> positive tumor cells in adenocarcinoma. ns: not significant, \*p < 0.05, \*\*p < 0.001, \*\*\*\*p < 0.0001.



### miR-183 targets MICA in lung tumor cells

To validate the putative miR-183 binding sites on wildtype (WT) MICA/B, we generated luciferase reporter constructs containing either the MICA 3'UTR or the MICB 3'UTR. We also mutated the 6-8 nucleotide seed sequence in the 3'UTR of MICA complementary to miR183, which is required for effective transcriptional repression (**Fig. 5A**). Co-transduction of 293 cells with MICA-WT and miR-183 markedly reduced luciferase expression, as compared to MICA-WT together with scrambled control transduction, while mutant MICA-MT, when co-expressed with miR183, resisted luciferase repression, suggesting that miR183 binding is critical for MICA gene regulation (**Fig. 5B**). Similar experiments using MICB were conducted and, while miR-183 could repress luciferase activity in MICB-WT transfected cells, it could not interfere with luciferase activity in MICB-mut transfected cells. Thus, both MICA and MICB are subject to the same control by miR183.

We next verified that miR-183 directly controls MICA/B in lung tumor cells. To accomplish this, we transfected antisense miR183 into H1355 lung tumor cells to analyze if loss of miR183 expression could increase MICA/B levels on the transfected tumor cells. We first confirmed that antisense miR-183 transfection was successful in suppressing miR-183 expression by qPCR analysis (**Fig. 5C**). Next, we examined the level of MICA and MICB expression in these transfected cells by flow cytometry using a monoclonal antibody that recognizes both MICA/B. MICA/B were significantly upregulated in antisense miR-183-transfected tumor cells (mean fluorescence intensity (MFI) of 4660) as compared to scramble control (MFI of 1958) (**Fig. 5D, 5E**). To ensure that miR-183 is a common regulator of MICA/B, we also tested another lung cell line, H1299, in a similar

manner. Expression of antisense miR-183 in H1299 cells markedly increased MICA/B levels (MFI of 8263) in comparison to scramble (MFI of 3997) and upregulated MICA mRNA (Fig. 5F, 5G, 5H). Thus, blockade of miR-183 expression was sufficient to enhance MICA/B expression in lung tumor cells. Together, the results of the luciferase reporter constructs in HeLa cells together with the anti-sense miR-183 overexpression in lung tumor cells indicate that it is a direct effect of miR183 binding to the MICA/B 3'UTR that regulates its expression.

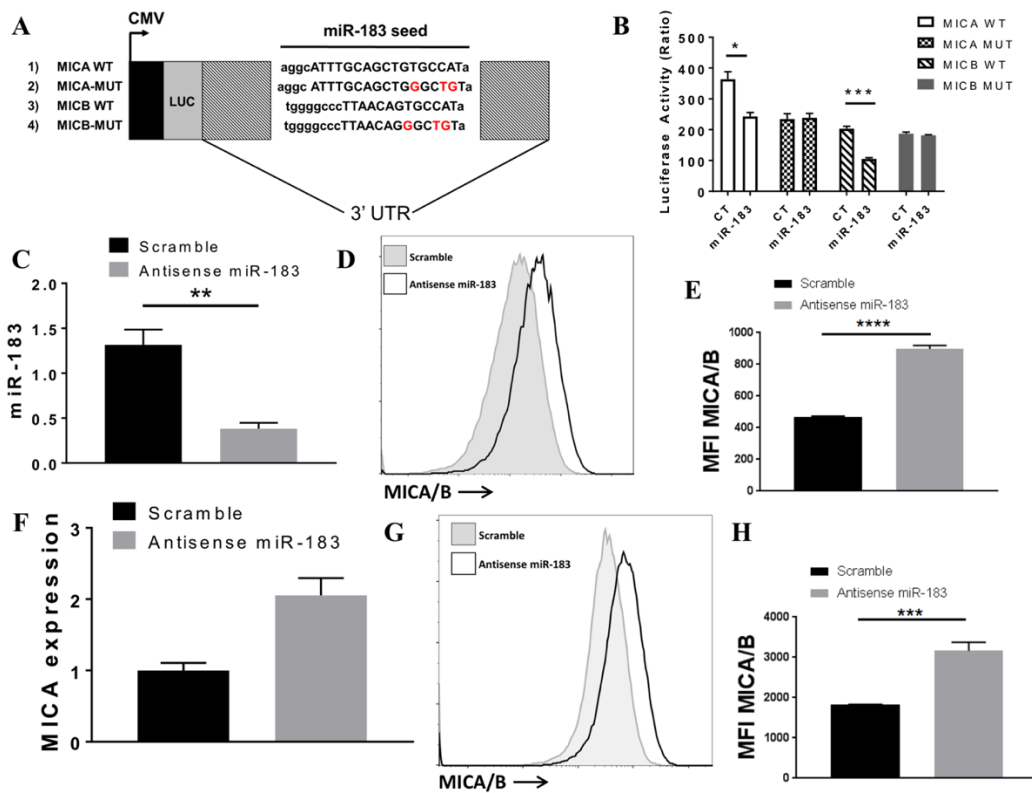


**Figure 5.** miR-183 targets the 3'UTR of MICA/B mRNA. (a) Schematic of luciferase reporter constructs carrying wild-type (WT) MICA or MICB 3'UTR as well as mutated (MUT) MICA or MICB 3'UTR. The miR seed sequences are depicted as capital letters and the mutated nucleotides are in red. CMV, cytomegalovirus promoter; LUC, luciferase. (b) 293T cells were transfected with luciferase constructs containing MICA-WT, MICA-MUT, MICB-WT or MICB-MUT (500ng), renilla luciferase (5ng) together with miR-183 (25nM). After 24 h, the cells were lysed and quantified for firefly luciferase activity. (c) Lentiviral constructs containing scramble control or anti-sense miR-183 were transfected into H1355 lung tumor cells. qPCR analysis was conducted to confirm the downregulation of miR-183 expression by antisense miR-183 (d, e) Flow cytometric analysis using a monoclonal antibody that detects a common sequence in MICA and MICB indicated that antisense miR-183 transfected H1355 tumor cells upregulated MICA/B expression. D is a representative staining of MICA/B. (f, g, h) H1299 lung tumor cells also transfected with antisense miR-183 showed upregulation of both MICA mRNA by qPCR and protein by flow cytometry analysis. G, H is a representative staining of MICA/B. Each of the experiments is representative of at least 3 experiments performed.

## **TGF $\beta$ drives miR183 expression to downregulate MICA/B**

We had earlier documented that TGF $\beta$  was highly elevated in lung tumor cell lines as well as primary lung tumor tissues (35). In fact, we reported the novel observation that TGF $\beta$  can induce miR-183 from NK cells leading to the loss of a critical adaptor protein required in mediating tumor lysis. This is highly relevant to all aspects of cancer immunology and immunotherapy, as NK cells are critical to antitumor immunity. Since we showed that the exposure of TGF $\beta$  reduces the effectiveness of NK cells, which induces miR-183 and thus suppresses NK cells, we felt that this topic deserved more attention. Relevant to our past work and thus current study, TGF $\beta$  has additionally been reported by others to downregulate NKG2D ligands (204). Based on the conclusions of the above cited works, and the knowledge that TGF $\beta$  is elevated in lung cell lines, we thus endeavored to explore whether TGF $\beta$  was involved in inducing miR-183 expression in the tumor cell themselves, consequently leading to suppression of MICA/B. The novelty of this concept lies in the ability of the lung cancer cells to contribute to tumor induced immune suppression. Thus, to pursue this exciting concept, we transfected H1355 lung tumor cells with shRNA TGF $\beta$  or scramble control shRNA prior to analysis of miR-183 and MICA/B expression. We first confirmed that TGF $\beta$  mRNA was effectively knocked down by shRNA TGF $\beta$  transfection, as compared to the scramble control (**Fig. 6A**). Loss of TGF $\beta$  resulted in a corresponding reduction in miR-183 expression (**Fig. 6B**). In contrast, TGF $\beta$  depletion led to increased MICA/B expression, with MFI rising from 659 in scramble control-shRNA transfected cells to 1077 in the shRNA TGF $\beta$ -transfected cells (**Fig. 6C, 6D**). We reproduced similar results in H1299 lung tumor cells. Depletion of TGF $\beta$

with specific shRNA (**Fig. 6E**) also caused significant depletion of miR-183 in H1299 cells (**Fig. 6F**), accompanied by an upregulation of MICA/B (**Fig. 6G, 6H**). Since lentiviral transfection can induce a type I interferon response, we utilized a pan-Type I Interferon neutralizing antibody (209) to ensure that our observed biologic effects were due to the silencing of TGF $\beta$ , and not to secondary viral transfection effects or type I interferon itself. The results were consistent with that of the original experiment, where the loss of TGF $\beta$  led to increased MICA/B expression by flow cytometry the H1299 cell line(**Fig. 7B, 7C**). Thus, TGF $\beta$  appears to induce miR-183 which can bind the 3'UTR of MICA/B to disrupt its expression, and this phenomenon is not Type I interferon dependent.

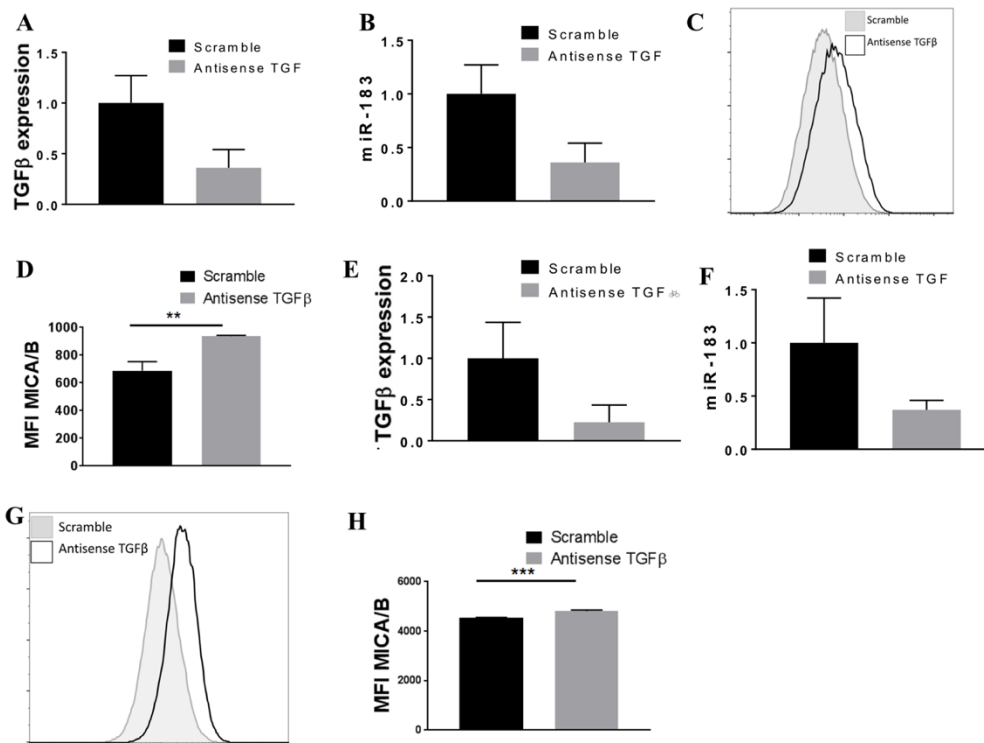


**Figure 6.** TGF $\beta$  suppresses MICA/B expression via miR-183. (A, B) H1355 tumor cells were transfected with antisense TGF $\beta$  or scramble control prior to analysis of TGF $\beta$  mRNA or miR-183 by qPCR. Reduced TGF $\beta$  expression correlated with reduced miR-183 expression in these cells. (C, D) In these same cells, flow cytometric analysis and the mean fluorescence intensity indicated that antisense TGF $\beta$ -transfected cells expressed higher levels of MICA/B than scramble control. C, D is a representative staining of MICA/B. (E, F, G, H) The experiments in H1355 tumor cells were repeated in H1299 tumor cells and confirmed that antisense TGF $\beta$  transfection reduces TGF $\beta$  mRNA with a corresponding downregulation of miR-183, accompanied by heightened expression of MICA/B in tumor cells. G, H is a representative staining of MICA/B. Each of the experiments is representative of at least 3 experiments performed.

## H1299

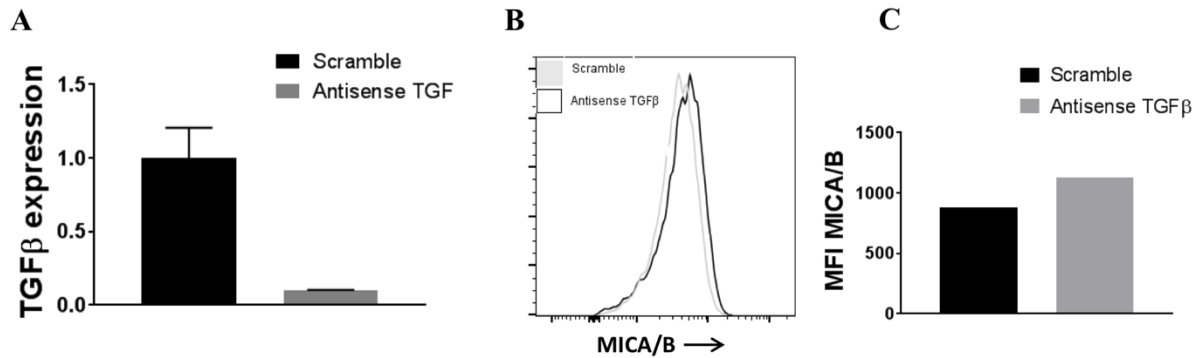


**Figure 7.** TGF $\beta$  suppresses MICA/B expression via miR-183 in the absence of Type I interferon. H1299 tumor cells were transfected with antisense TGF $\beta$  or scramble control prior to experimentation. Analysis of TGF $\beta$  mRNA was performed via qPCR on the transfected cell lines. In these same cells, MICA/B was analyzed via flow cytometry. The TGF $\beta$  mRNA was decreased in the antisense TGF $\beta$  transfected cell lines (A), and the MFI of MICA/B was increased in the TGF $\beta$  knockdown (B, C). The cells were treated with IFN blocking antibody for 30 minutes prior to analysis. Each of the experiments is representative of at least 3 experiments performed.

### miR-183 expression blocks NKG2D-mediated lysis of tumor cells

To analyze the biological consequence of miR-183 expression in tumor cells, we next assessed the sensitivity of lung tumor cells to NKG2D-mediated lysis by cytotoxic immune cells. First, we assessed the MHC class I expression of tumor cell lines, as MHC class I presence is important for NK response. We examined healthy peripheral blood mononuclear cells (PBMC) as a positive control, K562 immortalized myelogenous leukemic cells as a negative control, and H1299 and H1355 lung tumor cells. We found moderate expression in H1355, and higher expression in H1299 cells (**Fig. 8**). These cell lines are thus class I competent, a factor that is prominent because lung tumor cells often lose class I expression as a mechanism of tumor immune escape (210). NK cells sense and detect MHC Class I, and through the missing-self hypothesis, recognize and

eliminate cells missing Class I(211). NK cells, however, cannot be used as effector cells to study NKG2D-specific lytic events, because IL-2 used to culture human NK cells induces not only high levels of NKG2D but also upregulated other activating NK receptors such as activating Killer Immune Receptors (aKIRs) (212), NKp44 (213), NKG2C (214), and NKG2E (215), which recognize tumor-associated ligands unrelated to MICA/B. To overcome this obstacle, we generated cytotoxic CD8<sup>+</sup> T cells by first purifying CD8<sup>+</sup> T cells via negative selection from normal peripheral blood mononuclear cells and then placing them in culture for 7 days with anti-CD3/CD28 containing medium plus IFN $\gamma$ . We demonstrated that such short term stimulation induces primarily NKG2D but no other activating receptors, including NKp44, NKp46, KIR2DS4, or NKG2C (**Fig. 9A**). Indeed, these CD8<sup>+</sup> T cells lysed H1355 lung tumor cells which could be effectively blocked by anti-NKG2D (**Fig. 9B**). The T cell receptor on CD8<sup>+</sup> T cells is not involved because H1355 tumor cells are allogeneic to the T effector cells and have no matching MHC-Class I (216). We next transfected antisense miR-183 into H1355 tumor cells and tested their susceptibility to lysis by CD8<sup>+</sup> T cells. In 2 separate normal donors, we found that CD8<sup>+</sup> T cells had markedly increased tumoricidal activity against H1355 mir-183 transfected tumor cells, as compared to scramble control (**Fig. 9D, 9E**). To prove that this relationship between mir-183 and MICA/B sensitizes effector cells, we transfected H1299 and H1355 tumor cells with a vector to overexpress MICA/B. As expected, the tumor lysis phenotype was similar (**Fig. 9C**). The CD8<sup>+</sup> T cells had a similar trend in tumoricidal activity as did the antisense miR-183 transfected cells. This confirms that this relationship does indeed work both ways. Taken together, these results indicate that miR-183 suppression, either

by means of silencing mir-183 or overexpressing MICA/B in tumor cells sensitizes them to be better recognized by T cells via the NKG2D-MICA/B pathway.

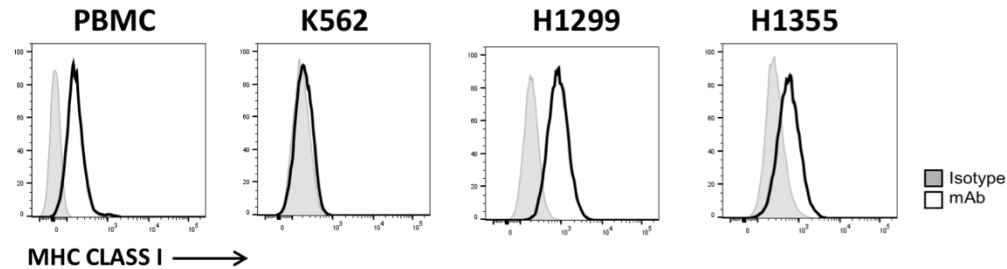


**Figure 8.** MHC Class I expression on Tumor Cell lines. Healthy PBMC, leukemic K562 cells, H1299 and H1355 lung tumor cells were analyzed for class I competence. PBMC were used as a positive control, K562 as negative compared to isotype control. H1299 have moderate-to-high levels of MHC class I, and H1355 moderate compared to isotype control.

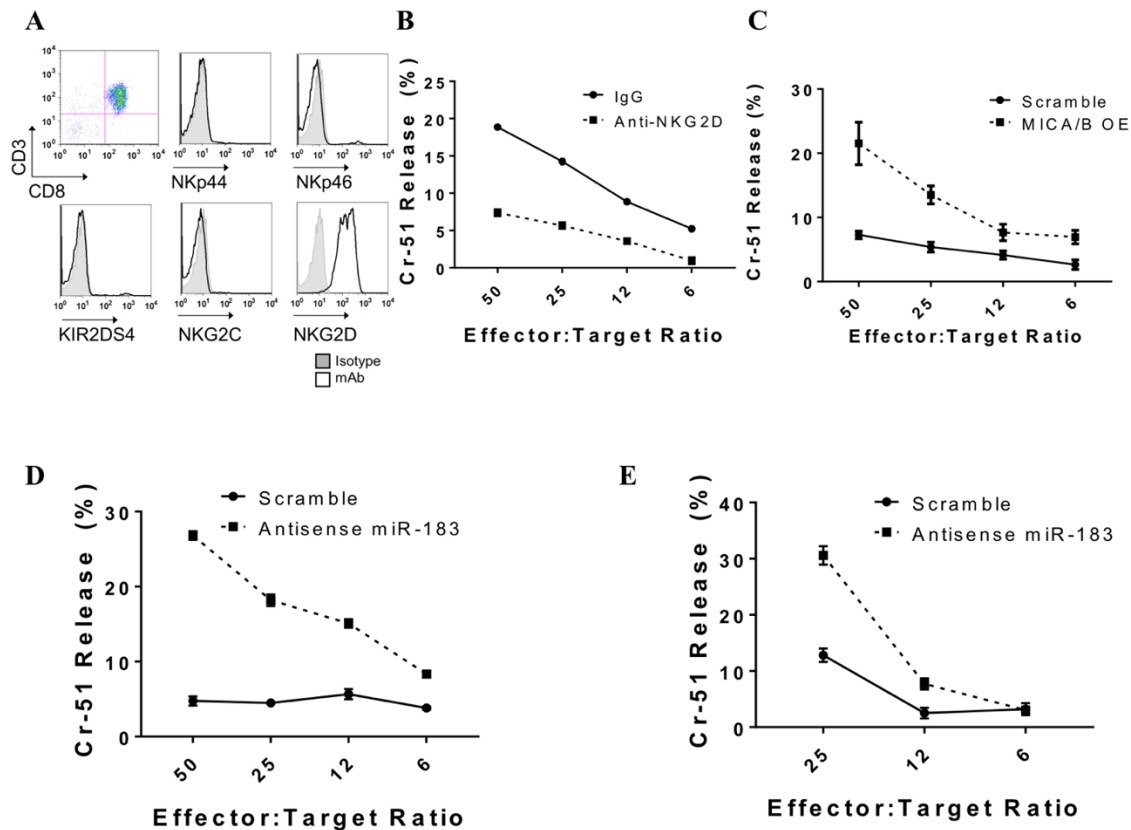


**Figure 9.** Depletion of miR-183 in tumor cells enhances sensitivity to lysis by activated T cells. (a) CD8<sup>+</sup> T cells, purified by negative selection from normal peripheral blood mononuclear cells, were activated with IFN $\gamma$  and anti-CD3/CD28 and cultured in IL2 for 7 days. Flow cytometric analysis indicated that such short term culture induced only NKG2D but not the other NK receptors on the T cells. (b) Short term-activated CD8<sup>+</sup> T cells kill H1355 tumor cells in a 5 h Cr release assay, which can be blocked by anti-NKG2D. (c) Short term-activated CD8<sup>+</sup> T cells were transfected with MICA/B overexpressing vector or scramble control, and then tested for cytotoxicity against H1299 tumor cells. MICA/B transfected tumor cells were more susceptible to lysis than scramble control, indicating overexpression of MICA/B in tumor cells increases sensitivity to lysis by activated T cells. (d, e) Short term-activated CD8<sup>+</sup> T cells from 2 separate donors were transfected with antisense miR-183 or scramble control, and then tested for cytotoxicity against H1355 tumor cells. Antisense miR-183 transfected tumor cells were more susceptible to T cell lysis than scramble control.

## ***Discussion***

In this study, we provide firm evidence of a novel molecular process that promotes immune escape in human lung tumor cells. It identifies a new link between TGF $\beta$  and miR-183 that drives repression of a critical NK ligand, MICA/B, causing the loss of detection by immune cells expressing its receptor, NKG2D. Immunohistochemical assessment of tissues from lung cancer patients with either adenocarcinoma or squamous cell carcinoma indicated a lack of MICA/B expression while meta-analysis of the TCGA database for human lung adenocarcinoma and squamous carcinoma revealed that both lung tumor types display a high expression of miR-183. In light of the reverse correlation of MICA/B expression with miR-183, we conducted a search for miR binding sites in the 3'UTR of both MICA and MICB and identified a 7-mer binding sequence that tightly complements the mature 22 nucleotide miR-183 in MICA and an even longer 9-mer sequence that completely mirrors miR-183 in MICB. Using luciferase reporter constructs carrying the MICA or MICB 3'UTR, we were able to demonstrate that miR-183 effectively repressed MICA and MICB. Sequence-specific mutation of the binding site on MICA and MICB further corroborated the requirement of miR-183 in regulating MICA/B in these reporter constructs. Besides such molecular elucidation of miR-183 binding to the MICA/B 3'UTR, analysis of the biological process in H1355 lung tumor cells indicated that antisense miR-183 transduction can upregulate MICA/B expression and sensitize these cells to lysis by activated allogeneic T cells expressing NKG2D. This process was reproduced in another lung tumor cell line, H1299. Use of short term activated allogeneic T cells allowed for the recognition of tumor cells by NKG2D without TCR which is self-MHC Class I specific. It also circumvents the issue posed by activated NK cells which



express other activating receptors such as aKIRs, NKp30, NKp44, NKG2C that could mask specific MICA/B-targeted killing (189, 190). We also provide evidence of the role of TGF $\beta$  in initiating the process, by demonstrating that anti-sense TGF $\beta$  transfection into human lung tumor cells can downregulate miR-183 expression, with corresponding increase in MICA/B expression.

Earlier studies have reported that MICA can be controlled by several other miRs, namely miR-10, miR-20, miR-93, miR-106, miR-373, miR-520 (217, 218) . However, these miRs were uncovered through the TargetSCAN algorithm to search for miR consensus sites on the 3'UTR of the MICA/B gene and are not linked to the tumor microenvironment. It is not known if any of these miRs are inducible by TGF $\beta$ , as we have shown for miR-183 expression in our lung tumor system. One interesting observation pertaining to MICA regulation is the report that IFN $\gamma$  can repress MICA via miR-520 (219). Thus, these other miRs may respond to signals unrelated to TGF $\beta$ . Shedding of MICA/B is another process utilized by tumor cells but it is still not settled whether shed MICA/B blocks or enhances NKG2D-mediated NK lysis (201-203). This shedding phenomenon could explain our consistent observation of better detection of cytoplasmic MICA/B by western blot analysis than by flow cytometric analysis of surface MICA/B.

One of the hallmarks of cancer is immune escape (171). Our work constitutes the first report of a tumor-promoting miR, namely miR-183, which can also drive immune escape of tumor cells. In addition to numerous reports of the ability of miR-183 to enhance tumor progression via direct interference with key regulators of cell survival and proliferation, we show here that miR-183 expressed within lung tumor cells can repress MICA/B expression to avoid detection by NKG2D<sup>+</sup> CD8<sup>+</sup> T cells. This dual effect of miR-

183 on tumor cells can be a powerful driver of tumor cell progression. Remarkably, there is a third property of miR-183 that we have recently uncovered. Rather than a direct effect on tumor cells, we reported that TGF $\beta$ -inducible miR-183 can repress NK cells within the tumor microenvironment. Here, miR-183 targets a separate NK lytic mechanism unrelated to the MICA/B/NKG2D ligand/receptor system. In this case, the ligation of TGF $\beta$  transcriptionally induces miR-183 in NK cells, and it is this NK-associated miR-183 that specifically represses DAP12, a vital adaptor protein, required to anchor numerous NK activating receptors on the cell surface, including activating Killer Immune Receptors (KIRs) (212), NKp44 (213), NKG2C (214), and NKG2E (215). It is to be noted that the ligands for these receptors are entirely different from MICA/B and ULBPs1-6. Activatory KIRs specifically target classical MHC-I molecules, thus facilitating the recognition of allogeneic tumor cells, useful in bone marrow transplantation in the allogeneic setting (220). NKG2C and NKG2E primarily recognize HLA-E, which belongs to the MHC-I heavy chain family, but bind a restricted subset of peptides derived from the leader peptides of other MHC-I molecules (221). HLA-E is often overexpressed in malignant cells, rendering them sensitive to NK lysis (222). The ligand for NKp44 is unclear, although viral hemagglutinin and heparin derivatives have been reported to bind NKp44 (223) (224). However, anti-NKp44 can dampen NK lysis of various tumor types, suggesting a putative common ligand expressed on tumor cells. MiR-183 repression of DAP12 can thus have a potent effect on NK cells, suppressing a variety of activating receptors to essentially blind them to the tumor cells.

The lesson learnt from our studies of miR-183 on immune modulation, together with other reports on tumor cell proliferation and metastasis, is profound. The tumor cell,

working through TGF $\beta$ , is endowed with a powerful transcriptional regulator in miR-183 with three essential subversive properties. First, miR-183 can target endogenous genes to favor aggressive growth. Second, it can dial down NK ligands, such as MICA/B, to avoid immune detection by a highly potent NK receptor, NKG2D, that is expressed on both activated NK and CD8<sup>+</sup> T cells. NKG2D is also present on  $\gamma\delta$ T cells which infiltrate a number of human solid cancers (225). Third, miR-183 can not only modulate the tumor itself to hide from the immune system, it can also disarm the surrounding NK cells by targeting yet another NK recognition system through repression of DAP12 that anchors multiple NK receptors, including KIRs, NKp44, NKG2C and NKG2E. It is notable that tumor cells have evolved to regulate only DAP12 in NK cells instead of its associated NK receptors, leaving them intact but cloistered in the cytoplasm, representing an economic means to silence NK cells. In the context of the NKG2D receptor, tumor cells opted to utilize miR-183 to repress its ligands, MICA/B. Tumor-associated miR-183 thus represents a global strategy by the tumor to disable immune recognition by innate immune receptors and simultaneously promote tumor growth. Whether this TGF $\beta$ /miR-183 network is operative in other tumor types has not yet been explored but it seems possible that it is a common strategy of most tumor cells, given the abundance of reports on TGF $\beta$  and miR-183 co-expression in breast, colorectal, hepatic, pancreatic and prostate cancer.

## **Materials and methods**

### **Cell culture and reagents**

H1299, H1355, H1155, A549, and H2170 human lung tumor cells were maintained in 10% (vol/vol) FBS, RPMI (Thermo Fisher Scientific) supplemented with 1% Pen/Strep, 1% L-glutamine (Thermo Fisher Scientific), and 1% MEM Non-Essential Amino Acids Solution (NEAA) (Corning). HBE4 human lung epithelial cells transformed with E6/E7 of the Epstein-Barr virus (American Type Culture Collection) were maintained in 10% (vol/vol) FBS Keratinocyte SFM supplemented with cholera toxin (CTX 10 ng/mL), bovine pituitary extract (50 ng/ml), and epidermal growth factor (5 ng/ml). MiaPaCa and PANC-1 human pancreatic ductal adenocarcinoma cell lines (American Type Culture Collection), Wi-38 human lung cells, HeLa human cervical adenocarcinoma cells, and K562 human chronic myelogenous leukemia cells were maintained in were maintained in 10% (vol/vol) FBS, Dulbecco's Modified Eagle's Medium (DMEM) (Thermo Fisher Scientific) supplemented with 1% Pen/Strep, 1% L-glutamine (Thermo Fisher Scientific), and 1% MEM Non-Essential Amino Acids Solution (NEAA) (Corning).

Primary cytotoxic T lymphocytes (CTLs) were obtained from peripheral blood of healthy donors from OneBlood. CD8<sup>+</sup> T cells were purified from peripheral blood mononuclear cells by negative selection (CD8<sup>+</sup> T cell Isolation Kit; Miltenyi Biotech). Purifications yielded >95% CD8<sup>+</sup>CD3<sup>+</sup> cells by FACS analysis. Cells were then incubated overnight at 37°C in culture media supplemented with 10% FBS RPMI (Thermo Fisher Scientific), 1% NEAA (Corning), 1% Sodium Pyruvate (NaPyr) (Corning), 1% Pen/Strep, 1% L-glutamine (Thermo Fisher Scientific), MycoZap-PR reagent (Lonza), and IFN $\gamma$  (1000 units/ml),

followed by activation with anti-CD3/anti-CD28 and expansion in recombinant human IL-2 (100 U/mL) for 6 days.

### **Flow cytometry analysis**

For analysis of surface receptors,  $1 \times 10^6$  cells of each cell line were stained with 5  $\mu$ l anti-human PE-conjugated antibody to MICA/B (eBioscience; clone 6D4) or 2.5  $\mu$ l PE-conjugated antibody to HLA-ABC (BD: Clone W6/32). Following incubation with anti-MICA/B antibody or anti-HLA-ABC, cells were washed and resuspended in FACS buffer (1X PBS containing 2% BSA and 0.1% sodium azide) and acquired on a LSR II Flow Cytometer (BD Biosciences). Primary CTLs were stained with the following antibodies: CD8-FITC (BD Pharmingen; clone SK1), CD3-PE (Biolegend; clone SK7), NKp44-APC (R&D Systems; clone 253415), NKp46-APC (BD Pharmingen; clone 9-E2), KIR2DS4-APC (R&D Systems; clone 179315), NKG2C-APC (R&D Systems; clone 134591), and NKG2D-APC (BD Pharmingen; clone 1D11). Data were analyzed using FlowJo version 10 and figures were prepared in GraphPad Prism 7.

### **Type I interferon neutralization**

For neutralizing of Type I interferon, cells were treated with Human Type 1 Interferon Neutralizing Antibody (PBL Assay Science) for 30 minutes at a concentration of 1:50. After incubation at 37°C, cells were harvested and washed, and used for further downstream assays. Data were analyzed, and figures were prepared in GraphPad Prism 7.

## **Chromium release assay**

Chromium release assay was performed as described.<sup>17</sup> Anti-sense miR-183 lentiviral transduced H1299 or H1355 cells were used as targets. Targets were labeled with 200 $\mu$ Ci of Na [<sup>51</sup>Cr] chromate (Amersham) for 1 hr at 37°C. Target cells were then washed and plated at  $5 \times 10^3$  cells/well with CD8<sup>+</sup> T cells to give an effector/target ratio of 50/1 to 6/1 in a round bottom microtiter plate. After incubation at 37°C for 5 hr, supernatants were harvested and counted in a  $\gamma$ -counter. The percent specific <sup>51</sup>Cr release was then calculated as: [(experimental cpm – spontaneous cpm)/total cpm incorporated] x 100. All determinations were performed in triplicate, and the SEM of all assays was calculated typically ~5% of the mean or less. Figures were prepared in GraphPad Prism 7.

## **Quantitative RT-PCR**

To detect mature microRNA (miR) transcripts, PCR was performed with Taqman reagents (Thermo Fisher Scientific). Purified RNA was reverse transcribed with primer for has-miR-183 (miR-183) and RNU6B followed by real-time PCR amplification with 6-carboxyfluorescein-conjugated primers for miR-183 and RNU6B in TaqMan Universal PCR Master Mix, no AmpErase UNG (Thermo Fisher Scientific). Experimental miRs were normalized to RNU6B. To detect MICA, MICB and TGF $\beta$  transcripts, total RNA was extracted using Trizol Reagent (Thermo Fisher Scientific). Total RNA was then reverse transcribed using the qScript cDNA Supermix (Quanta). Real-time PCR amplification was performed with primers specific for the respective mRNA, using the Power SYBR Green Master Mix (Thermo Fisher Scientific). Relative fold changes in expression were

determined by using the comparative cycle threshold method ( $2^{-\Delta\Delta CT}$ ). Figures were prepared in GraphPad Prism 7.

### **Immunohistochemical staining of lung TMAs**

Tissue cores (0.6 mm) from 59 adenocarcinoma (ADC), 67 squamous cell carcinoma and 14 normal adjacent human lung tissues purchased from US Biomax were fixed in 10% (vol/vol) neutral buffered formalin for construction of a tissue microarray (TMA). Sections of the TMA (4  $\mu$ m) were stained for MICA/B expression as described using anti-MICA/B (R&D Systems)<sup>17</sup> at a dilution of 1:100, for 2 h at room temperature with the Ventana automated immunostainer Discovery XT (Ventana Medical Systems, Tucson, AZ). As a negative control, non-immune mouse sera were used, omitting the MICA/B antibody during the primary antibody incubation step. The slides were read by a certified pathologist and co-author (DC) in a blinded fashion and the MICA/B protein expression levels were measured using the Allred semiquantitative scoring system.<sup>41</sup>

### **Bioinformatics analysis of miR binding**

Analysis of the MICA (NM\_000247) and MICB (NM\_005931) 3'UTR was performed using the publically available algorithm miRANDA (microRNA.org) or TargetScan.

### **Cloning, transfection and luciferase assay**

The oligonucleotide containing the MICA or MICB 3' UTR (synthesized by Integrated DNA Technologies) was amplified by RT-PCR (HotStar Mastermix, Qiagen). Amplified products were run on a 1% agarose gel, and extracted using QIAquick Gel Extraction Kit,

Qiagen) and subcloned into the pMIR-Report luciferase vector (Promega) to generate either MICA or MICB-luciferase reporter vector. The scrambled miR-183 seed-site sequence was generated by Mutagenex. The constructs were verified for correct insert sequence and orientation by DNA sequencing. For luciferase reporter assays, 293 cells were grown (70% confluent) in 12-well plates and transfected (Lipofectamine 2000; Thermo Fisher Scientific) with reporter constructs (500 ng per well), renilla luciferase (5 ng per well), and premiR-precursors (25 nm) (Applied Biosystems). At 24 h later, cells were lysed, and luciferase activity was quantified (Dual-Luciferase Reporter Assay; Promega) on a single automatic injection luminometer (Turner Biosystems). Ratios of renilla to firefly luciferase were quantified, and quadruplicates were averaged; experimental miRs were normalized to control scramble miRs. Figures were prepared in GraphPad Prism 7.

### **Lentiviral transfection of cell lines**

HIV-based lentiviral expression constructs (purchased from SBI) containing miR-183 (pCDH-CMV-MCS-EF1), antisense miR-183 (pGreenPuro shRNA), or scramble control were packaged with third-generation packaging plasmids (PMD-g, PMD-Lg, Rev; a kind gift of Todd Fehniger, Washington University St. Louis) in 293T cells. For TGF $\beta$  shRNA, plasmids (psi-LVRH1GP) were purchased from GeneCopoeia and packaged as mentioned above. Viral supernatants were harvested, filtered, and concentrated (Lenti-X concentrator; Clontech). H1355 or H1299 cells ( $5 \times 10^5$  cells per well in a 6-well plate) were spin-transduced with lentiviral particles at a multiplicity of infection (MOI) of 20 in RPMI. After two infections, cells were maintained in 10% (vol/vol) FBS RPMI



supplemented with 1% Pen/Strep, 1% L-glutamine (Thermo Fisher Scientific), and puromycin to select for transduced cells.

### **Analysis of published lung cancer datasets**

Expression of miR-183 and let7 in human ADC and SQU lung cancer in comparison to normal tissues were analyzed using the publicly available Cancer Genome Atlas (TCGA) directories:

LUAD:[https://tcgadata.nci.nih.gov/tcgadata/ftp\\_auth/distro\\_ftpusers/anonymous/tumor/luad/cgcc/bcgsc.ca/illuminahiseq\\_mirnaseq/mirnaseq/bcgsc.ca\\_LUAD.IlluminaHiSeq\\_miRNASeq.Level\\_3.1.12.0/](https://tcgadata.nci.nih.gov/tcgadata/ftp_auth/distro_ftpusers/anonymous/tumor/luad/cgcc/bcgsc.ca/illuminahiseq_mirnaseq/mirnaseq/bcgsc.ca_LUAD.IlluminaHiSeq_miRNASeq.Level_3.1.12.0/)

LUSC:[https://tcgadata.nci.nih.gov/tcgadata/ftp\\_auth/distro\\_ftpusers/anonymous/tumor/lusc/cgcc/bcgsc.ca/illuminahiseq\\_mirnaseq/mirnaseq/bcgsc.ca\\_LUSC.IlluminaHiSeq\\_miRNASeq.Level\\_3.1.7.0/](https://tcgadata.nci.nih.gov/tcgadata/ftp_auth/distro_ftpusers/anonymous/tumor/lusc/cgcc/bcgsc.ca/illuminahiseq_mirnaseq/mirnaseq/bcgsc.ca_LUSC.IlluminaHiSeq_miRNASeq.Level_3.1.7.0/).

TCGA IlluminaHiSeq miRNASeq level 3 data were downloaded from the open http directory of the TCGA data portal. The level 3 (normalized) miRNA quantification data analyses were utilized: LUAD = 1.12.0, LUSC = 1.7.0. Sample counts were as follows: LUAD (tumor = 422, normal = 46); LUSC (tumor = 332, normal = 45). Figures were prepared in R.

## CHAPTER THREE:

### MICRORNA-155 GOVERNS SHIP-1 EXPRESSION AND LOCALIZATION IN NK CELLS AND REGULATES SUBSEQUENT INFILTRATION INTO MURINE AT3 MAMMARY CARCINOMA

**A note to the reader:** this chapter has been previously published in a research article in *PLoS ONE*, Kandell et. al. 2020 (226).

#### ***Introduction***

Natural Killer (NK) cells are a subset of lymphocytes that produce pro-inflammatory cytokines such as IFN $\gamma$  and perforin, and kill target cells through an array of germline encoded receptors. NK cell activation is a finely tuned balance between positive (activating) and negative (inhibitory) signals. Ligands for these activating receptors are found on malignant or virally infected cells, which also frequently downregulate MHC (227). A robust NK cell response in cancer patients correlates with a positive prognosis (228, 229), and these clinical data translate to animal studies showing that NK cell depletion or inactivation increases tumor burden and worsens prognosis (230, 231). This highlights the important role of NK cells in antitumoral defense. NK are found within tumor infiltrating lymphocytes (TIL), however they are often rendered dysfunctional by means of the tumor (24). In the context of disease, NK cells quickly respond to chemokine signals such as that of the abundantly produced chemoattractant CCL2 (232-234) elicited by malignant cells or other inflammatory leukocytes, making them early-responders at the scene of a challenge. While previous studies have shown that CCL2 is required for NK cell-mediated clearance of viral infections (235), information about NK cell chemotaxis in

the context of breast tumor challenge is limited compared to T cell trafficking in the disease, and NK trafficking in other tumor types such as colon (236).

One class of regulators involved in diverse cellular processes are microRNAs (miRs), a class of small noncoding RNAs that post-transcriptionally represses gene expression by binding to transcripts exhibiting sequence homology, and inducing transcript degradation or inhibiting translation (237). Deficiency of Dicer, an RNase required for functional miRNA maturation, leads to defective NK cell development, solidifying the importance of miRNA regulation within NK cells (238). In particular, microRNA-155 (miR-155) is expressed in NK cells and other leukocytes (239, 240), where it is upregulated by inflammatory stimuli like Toll-like receptor ligands, IFN $\beta$ , TNF $\alpha$  and IFN $\gamma$  (241), and is robustly induced in response to activating cytokines IL-12 and IL-18 (242). Several genes have been identified as functional targets of miR-155, including SH2-containing inositol polyphosphate 5-phosphatase (SHIP-1) (44), which negatively regulates IFN $\gamma$  production in NK cells (242, 243). Additionally, SHIP-1 regulates the actin cytoskeleton at various levels by interacting with filamin-1, a scaffolding protein that organizes actin filaments in ruffle formation during chemotaxis (244, 245). Illustrating this relationship, decreases in filamin-1 or SHIP-2, a SHIP-1-related inositol phosphatase, leads to reduced F-actin polymerization in response to endothelial growth factor stimulation (246). Furthermore, SHIP-1 is involved in the regulation of migration of murine neutrophils in response to chemoattractive agents (247). Taken together, these data support a role for SHIP-1 not only in the regulation of cytokine secretion, as shown by Trotta et. al. (242) but also cell motility.

MiR-155 is processed from the transcript of *bic*, a non-protein-coding gene (248). To study the physiological function of *bic*/miR-155 in NK cells, we utilized the *bic*/miR-155-deficient mouse (miR-155<sup>-/-</sup>) (242, 248). Previous work has elucidated roles of miR-155 in NK cells both in vitro and in vivo, but impairments in chemotaxis are relatively unexplored. These works have shown that miR-155 is important for NK cell biology in vivo, showing such defects as impaired Interferon Gamma production and homeostatic proliferation (45, 49, 242). However NK cells from miR-155<sup>-/-</sup> mouse spleen displayed normal frequencies, and displayed a similar percentage of CD94, a marker of activation.(49). MiR-155 has also been shown to play a significant role in actin polymerization through the activity of SHIP-1 (242). Given that miR-155 has not been shown to affect NK cytotoxicity (49), we hypothesized that accelerated tumor growth in mice may be due to reduced migratory capacity secondary to defects in actin polymerization in NK cells. To examine this, we isolated NK cells from mice genetically lacking miR-155, and conducted a series of functional assays, as well as chemotaxis, transwell assays, and demonstrate that miR-155 may regulate chemotaxis and subsequent NK tumor infiltration downstream of SHIP-1 in mammary carcinoma.

## **Results**

### **NK cells in *bic*/miR-155<sup>-/-</sup> mice retain normal cytotoxic function**

MiR-155 has myriad roles in NK cell functionality, and thus we examined the miR-155<sup>-/-</sup> mouse to interrogate this population. NK cells in these miR-155<sup>-/-</sup> mice displayed normal levels of cytotoxicity receptors and frequencies in the spleen when compared to wildtype, similar to what has been previously characterized (49, 242). Our results were

similar to the findings cited, whereby the percentage of splenic NK cells was equivalent in miR-155<sup>-/-</sup> and WT mice, as assessed by NK1.1/DX5 co-expression (227) (**Fig. 10A, 10B**), suggesting that miR-155 does not play a role in NK cell development or homeostasis. NK are typically activated in inflammatory conditions. We thus assessed the cytotoxic potential of these cells post-activation with IL-2. This cytokine was chosen as the standard for in vitro NK activation, though other gamma chain cytokines are sufficient. (249). Splenic NK cells were purified by negative selection, activated with IL-2 (100 U/ml) for 72 h, and assessed for functional phenotype by means of their activating receptors by flow cytometric analysis and additionally, cytotoxicity towards tumor targets. To this end, chromium release assay was performed, and similar lytic function towards YAC-1 murine lymphoma targets, as well as C57BL/6 syngeneic AT3 murine mammary carcinoma targets were seen in both WT and miR-155<sup>-/-</sup> derived cells (**Fig. 10D**). We found no differences in cell surface expression that might impair cytolytic function, as miR-155<sup>-/-</sup> NK cells did not show defects in expression of the activating receptors NKp46, NKG2D or 2B4 (**Fig. 10C**). Despite possessing comparable direct lytic function and an intact activating receptor phenotype, other properties of NK cells equally important for effective rejection of cancer can be affected by miR-155 deficiency. To follow this further, we were particularly interested in dysregulation of the previously identified miR-155 target, SHIP-1 (44), as SHIP phosphatase activity negatively regulates NK function.

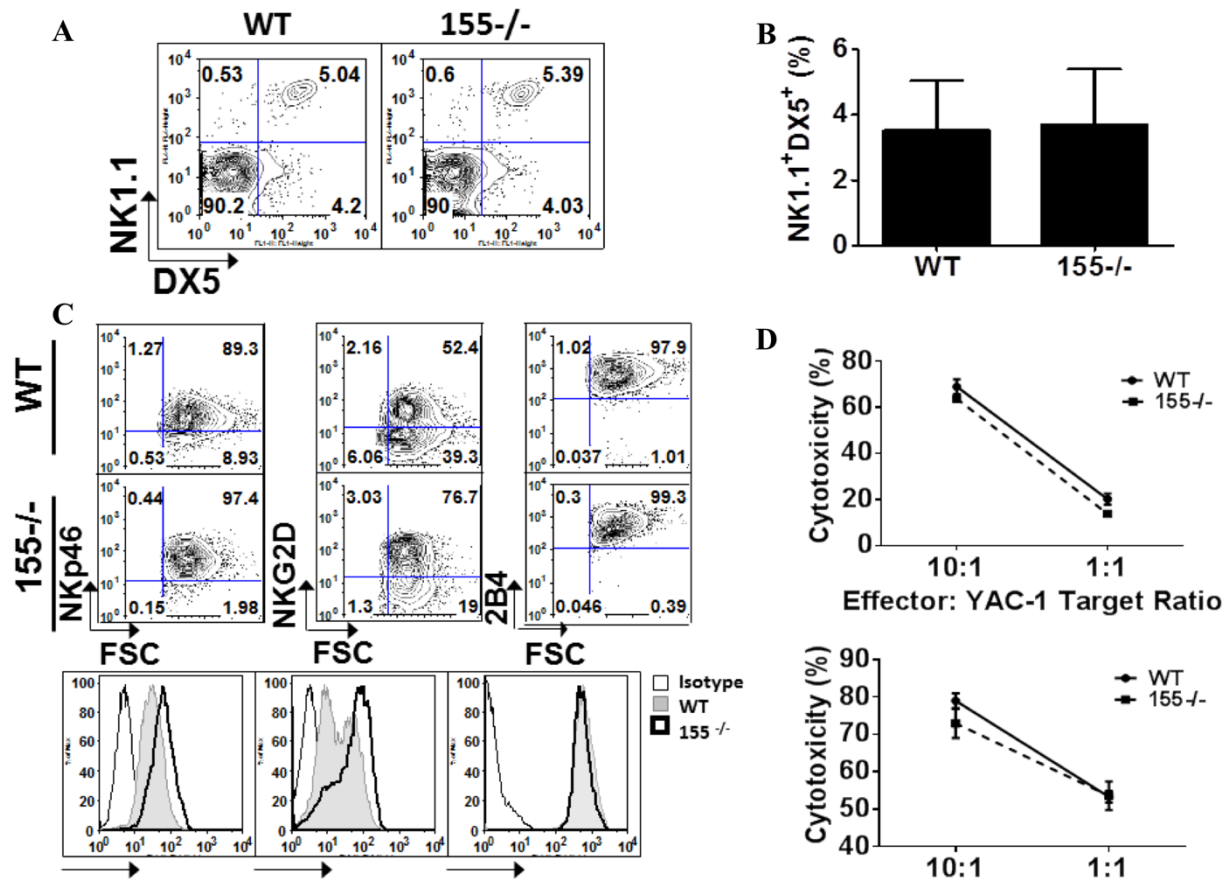


**Figure 10.** Characterization of miR-155<sup>-/-</sup> NK cells. Phenotypic and functional analysis of steady state splenic NK cells. Data shown is representative of 3 experiments performed. A) Splens of WT or miR155<sup>-/-</sup> mice (N=3 spleens/strain) were harvested, pooled, and stained with anti-mouse NK1.1 and DX5. B) Percentage of splenic NK cells (NK1.1+/DX5+). C) NK Activating Receptor Phenotype was analyzed by flow cytometry using anti-mouse NKp46, NKG2D and 2B4. D) <sup>51</sup>Cr-release assay of freshly isolated splenocytes with YAC-1 lymphoma cells and AT3 mammary carcinoma cells as targets.

### miR-155 is linked to SHIP1 and influences chemotaxis

Since SHIP-1 is a defined target of miR-155, and given the previous work on miR-155 regulation of SHIP-1 in NK cells (45, 49, 242), we assessed the level of total SHIP-1 in purified NK. Through this, we found that SHIP-1 was upregulated in purified NK cells of miR-155<sup>-/-</sup> mice (**Fig. 11A, 11B**). We additionally performed immunofluorescence on NK cells isolated from WT or miR-155<sup>-/-</sup> mice, and found increased cell-surface localization of SHIP-1 in cells lacking miR-155<sup>-/-</sup> (**Fig. 11C, 11D**), suggesting that not only

is SHIP-1 upregulated, but may be ideally localized to mediate signaling. Collectively, the data above indicate that miR-155-deficient mice exhibit no defect in direct-lytic NK cell tumoricidal function, yet express heightened levels of SHIP-1, which is likely to have consequences on NK functionality.

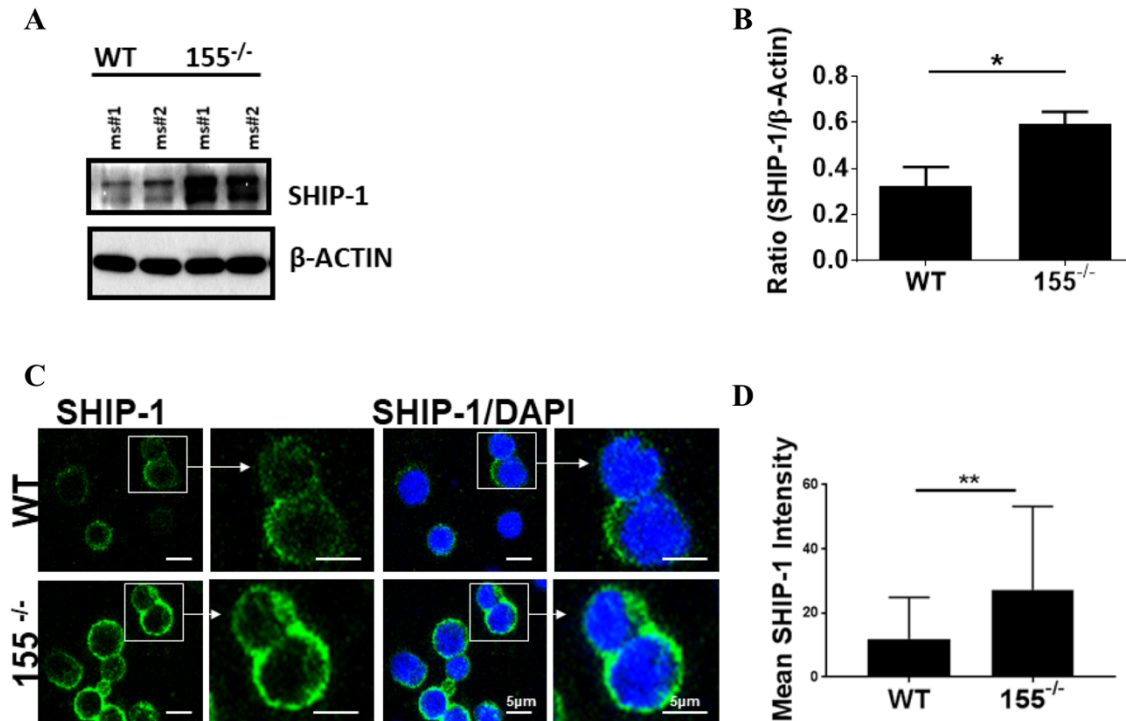


**Figure 11. miR-155<sup>-/-</sup> NK cells overexpress SHIP-1 and do not polymerize actin.**

IL-2 activated NK cells were generated from purified splenic wild-type or miR-155<sup>-/-</sup> NK cells. A) SHIP-1 immunoblot analysis of wild-type (lanes 1-2) or miR-155<sup>-/-</sup> (lanes 3-4). IL-2 activated NK cells were derived from four mice per strain. B) Quantification of the mean ratio of SHIP-1 to actin from densitometry of immunoblots. C) IL-2 activated NK cells immunostained for SHIP-1. Data shown is a representative of three experiments performed unless otherwise stated. D) Quantification of mean SHIP-1 membrane intensity from confocal microscopy as in panel C.

In mammalian cells, SHIP-1 is constitutively associated with filamin-1, a scaffolding protein that organizes polymerized actin filaments into orthogonal angles (244, 245). Additionally, SHIP-1 negatively regulates phosphoinositide 3-kinase (PI3K) signaling by hydrolyzing phosphatidylinositol 3,4,5-triphosphate (PiP<sub>3</sub>), the second messenger of PI3K that is critical for actin mobilization (250). SHIP-1-mediated hydrolysis of PiP<sub>3</sub> results in

phosphatidylinositol 4,5-triphosphate (PIP<sub>2</sub>) accumulation. Since PIP<sub>3</sub> is required for events driving ruffle formation and chemotaxis, loss of this phospholipid subsequently reduces F-actin formation and thus migration (245). SHIP1 has been found to be involved in all aspects of the NK life cycle (251). With this abundance of information regarding the relationship between NK cells and SHIP-1, we postulated that the abundance of SHIP-1 could negatively regulate actin polymerization in NK cells. Since polymerization of actin is required for cellular motility, we reasoned that the chemotaxis to tumor-derived factors could be affected by miR-155 deficiency. To address this question, we chose chemokine (C-C motif) ligand 2 (CCL2; also called monocyte chemoattractant protein-1 (MCP-1)) as a chemokine stimulus. CCL2 is often overproduced in the tumor microenvironment, including that of breast (252), and attracts T cells, monocytes, and NK cells (235, 253). Because CCL2 receptor (CCR2) is upregulated on NK cells after activation, we measured responsiveness to CCL2 chemotaxis after stimulation with IL-2 (232). We compared actin polymerization in CCL2-stimulated, purified NK cells from miR-155-deficient and WT animals by phalloidin staining (which detects filamentous (F)-actin) and subsequent confocal microscopic analysis. In response to CCL2 stimulation, WT NK cells robustly polymerized actin, as visualized by intense F-actin staining in focal pockets on the surface of the cells (**Fig. 12A**). In contrast, CCL2-treated miR-155<sup>-/-</sup> NK cells did not polymerize actin as compared to media control (**Fig. 12B**). Since F-actin polymerization in response to CCL2 stimulation was defective in those cells lacking miR-155, we hypothesized that miR-155-deficient NK cells may have a reduced capacity to migrate towards a chemokine gradient. To address CCL2 chemoattractive capacity, we measured migration of miR-155-deficient or WT NK cells towards a CCL2 stimulus in a Boyden chamber chemotaxis



assay. Using this system, we found that miR-155-deficient NK cells did not migrate towards a CCL2 stimulus, as did WT NK cells (**Fig. 12C**). As a confirmation that the cellular fitness is similar between the NK derived from these mice, a timecourse assay was performed to evaluate cell viability and marker of NK activation NKp46. The fitness of the WT and miR-155<sup>-/-</sup> cells were nearly identical. Viability in at all timepoints under the influence of CCL2 was ~95% for both groups, and NKp46 expression was unchanged at all timepoints. (**Figs. 13-15**). To rule out the possibility that the impaired directional movement was a result of defective CCL2 receptor density, we examined CCR2 expression amongst the strains. In WT mice, at baseline, there are more NK1.1+ CCR2+ NK cells than those of the 155<sup>-/-</sup> mice (13.7% vs 5.5%; N=3 mice/strain). However, CCR2 could be induced in both the wildtype and 155<sup>-/-</sup> NK cells upon stimulation with IL-2, as has been shown previously (232).(**Fig. 12D**). Nevertheless, despite comparable receptor expression post-stimulation, miR-155 deficient NK cells remained unresponsive to CCL2, suggesting that the impaired chemotaxis may be a result of dysfunctional actin polymerization. Because SHIP-1 is involved in directional migration and is overexpressed in miR-155<sup>-/-</sup> NK cells, we sought to determine whether blocking the function of the phosphatase could rescue chemotaxis. We utilized the specific small molecule inhibitor 3- $\alpha$ -aminocholestane (3AC) to block SHIP-1 function (254). Inhibition of SHIP-1 activity indeed rescued the chemotaxis of miR-155<sup>-/-</sup> cells to a CCL2 stimulus in a dose-dependent manner (**Fig. 12E**). Collectively, these results suggest that SHIP-1 overexpression resulting from miR-155 deletion confers impaired chemotaxis to CCL2.

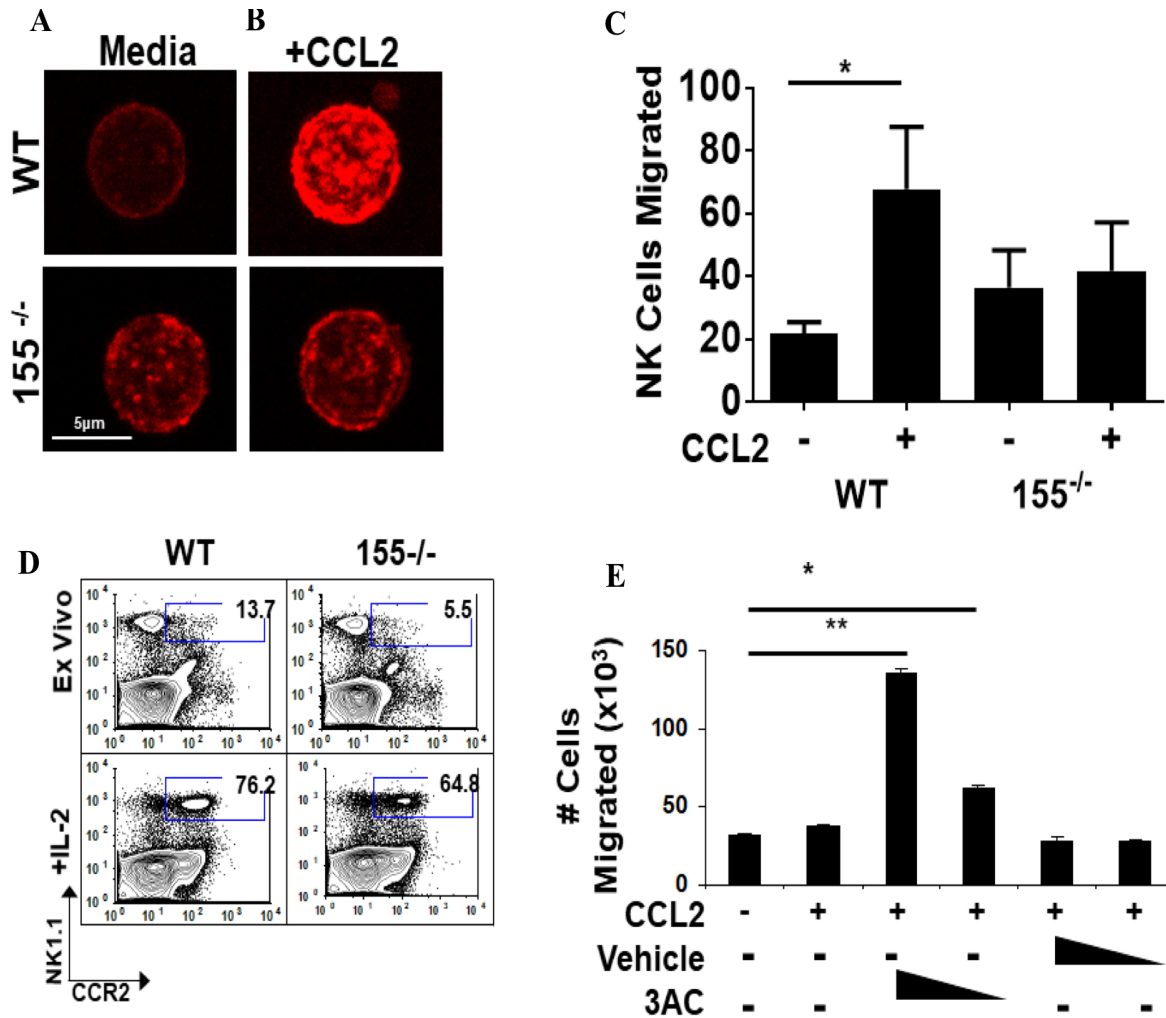


**Figure 12. miR-155<sup>-/-</sup> NK cells exhibit an altered response to CCL2.**

IL-2 activated NK cells were generated from WT or miR-155<sup>-/-</sup> purified splenic NK cells. Data shown is a representative of three experiments unless otherwise stated. A) Representative images of untreated or B) CCL-2-treated IL-2 activated cells stained with rhodamine-conjugated Phalloidin to detect F-actin. Magnification = 1833.3x; Scale bar = 2 µm. C) A Boyden chamber assay was utilized to detect IL-2 activated cell migration towards a CCL2 stimulus. Data shown is the absolute number of NK cells migrated toward the stimulus as determined by flow cytometry using CountBrite beads. D) Naïve or 24-hour IL-2 activated splenocytes were analyzed by flow cytometry for co-expression of NK1.1 and CCR2. E) Splenocytes were activated with IL-2 for 24h, followed by treatment with the SHIP-1 inhibitor, 3AC. A Boyden chamber assay was then utilized to detect cell migration towards a CCL2 stimulus. Data shown is the absolute number of NK cells migrated toward the stimulus as determined by flow cytometry using CountBrite beads. \**P* < 0.05, \*\**P* < 0.01, \*\*\**P* < 0.005

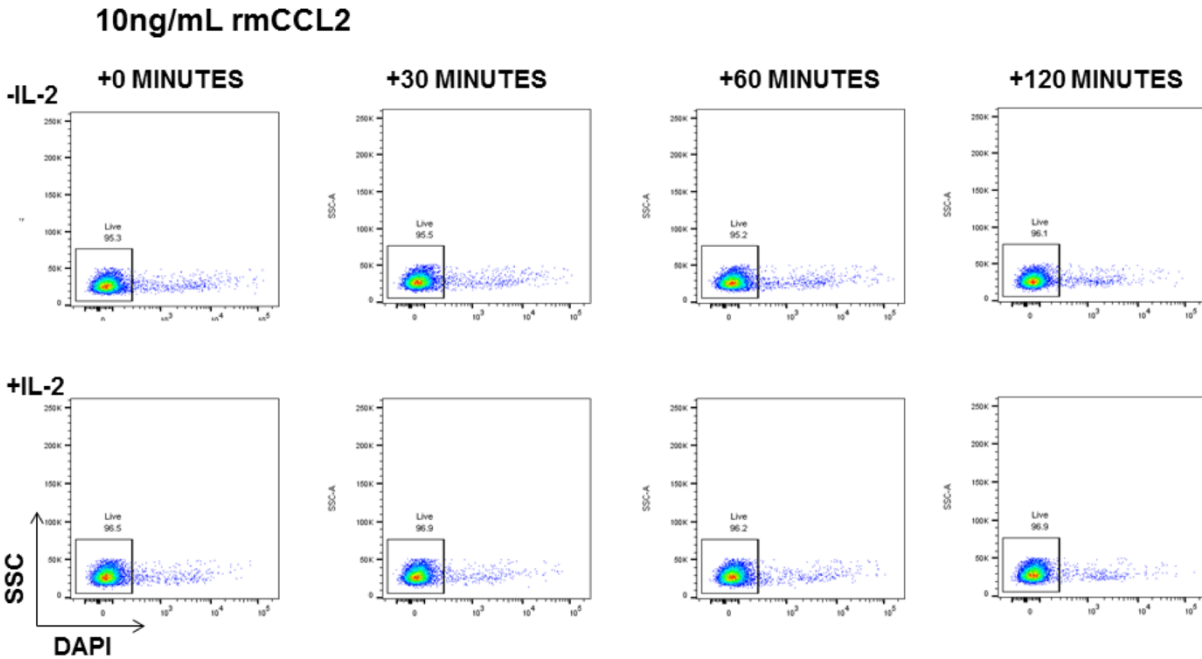


**Figure 13. Time Course Characterization of C57BL/6 (Wildtype) Derived Splenic NK cells.** NK cell viability over time (Basal, +30 minutes, +60 minutes, + 120 minutes) under the influence of IL-2 and/or CCL-2. Data shown is representative of 3 experiments performed. Viability was assessed using DAPI.

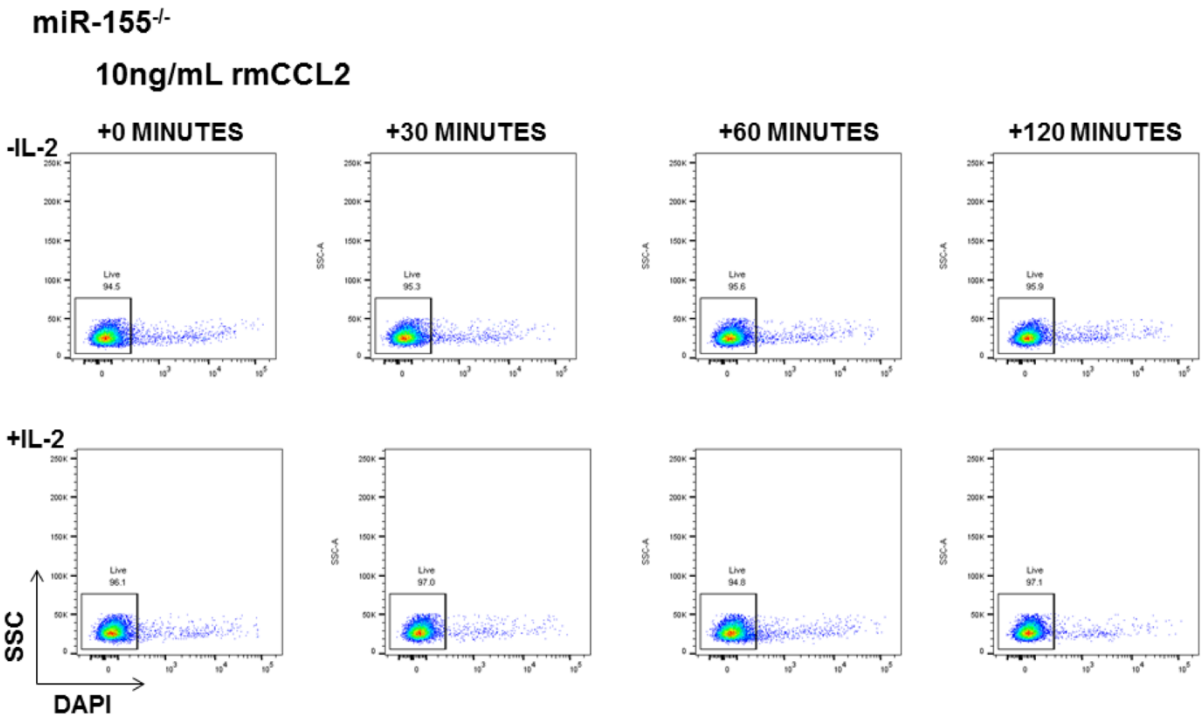


**Figure 14. Time Course Characterization of B6.Cg-MiR-155<sup>tm1.1Rsky/J</sup> (*bic/miR-155<sup>-/-</sup>*) derived Splenic NK cells.** NK cell viability over time (Basal, +30 minutes, +60 minutes, + 120 minutes) under the influence of IL-2 and/or CCL-2. Data shown is representative of 3 experiments performed. Viability was assessed using DAPI.

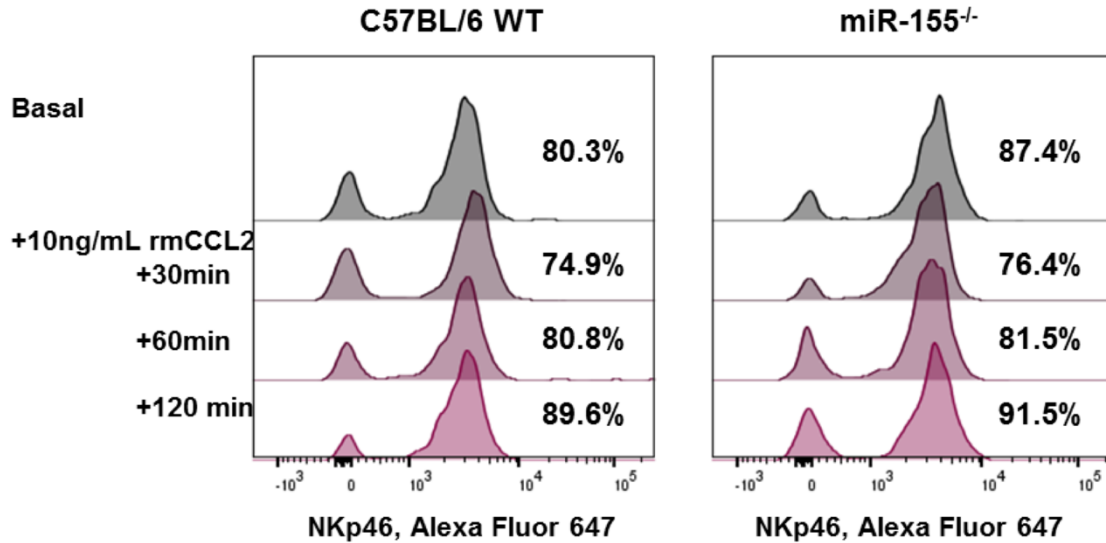


**Figure 15. Time Course Characterization of C57BL/6 (Wildtype) and B6.Cg-MiR-155<sup>tm1.1Rsky/J</sup> (*bic/miR-155<sup>-/-</sup>*) derived Splenic NK cells.**

NKp46 expression was assessed over time (Basal, +30 minutes, +60 minutes, + 120 minutes) under the influence of IL-2 and/or CCL-2. Data shown is representative of 3 experiments performed. Dead cells were excluded via DAPI. Gating scheme is live, singlets that are TCRB-NK1.1+NKp46+.

### miR-155 deficiency confers impaired NK cell tumor tropism in vivo

Since miR-155-deficient NK cells exhibit impaired chemotaxis to CCL2 ex vivo, we explored the possibility that they would also fail to traffic to a CCL2-rich tumor site. To test the in vivo relevance of miR-155 in NK cell tumor tropism, we first examined whether AT3 mammary carcinoma cells produce chemokines that induce NK homing. We characterized the cytokine and chemokine profile of AT3 cells by using an inflammatory cytokine cytometric bead array (CBA). As positive or negative controls, cytokine production from naïve or lipopolysaccharide (LPS)-stimulated C57BL/6 WT splenocytes was included in the CBA analysis. We found that AT3 produces copious amounts of CCL2 and marginal amounts of IL-6, but not other inflammatory factors such as IFN $\gamma$ , TNF $\alpha$ , or the immunosuppressive cytokine IL-10 (**Fig. 16A**). After confirming their CCL2 production, we examined the in vivo effect of miR-155 deficiency in rejection of AT3

tumors by assessing tumor burden and tumor-infiltrating leukocyte composition. Surprisingly, tumors from miR-155-deficient mice were significantly larger than tumors from WT mice (**Fig. 16B, 16C**). Furthermore, hematoxylin and eosin staining of tumor sections revealed that tumors from miR-155-deficient hosts exhibited a dense lawn of healthy tumor cells (**Fig. 16D**). In contrast, areas of tumor tissue necrosis and infiltrating lymphocytes were present in tumors from WT animals (**Fig. 16D**). We next isolated tumors and analyzed the TIL content by flow cytometry. The total leukocyte number was significantly lower in tumors derived from miR-155<sup>-/-</sup> background mice (**Fig. 17A**). The leukocyte number of splenic derived cells however was not significantly different between the two strains (**Fig. 17B**). We next evaluated NK cell, T cell and macrophage presence by NK1.1, TCR, and F4/80 staining. Unlike that of T cell and macrophage, NK cells were significantly lower in number in the miR-155 deficient hosts (Tumor-resident NK: miR-155<sup>-/-</sup> = 4.5% ± 0.9; WT = 11.4% ± 1.3). Splenic NK, T and macrophage numbers were equivalent. ((Splenic NK: miR-155<sup>-/-</sup> = 1.8% ± 0.3; WT = 2.0% ± 0.5) (Fig. 4C-D). Our flow cytometric analysis of these NK cells was confirmed with immunohistochemical staining of AT3 tumor sections from WT and miR-155<sup>-/-</sup> hosts for NK1.1+ NK cells. Immunohistochemistry of AT3 tumor sections from both strains showed noticeably more NK cells infiltrating AT3 tumors grafted in WT hosts (**Fig. 17E**). To quantify data from our immunostained tumor tissues, we scanned tumor sections (N=2 tumors/strain) with Aperio Scanscope and generated an algorithm in using Definiens TissueStudio Genie software to determine the percentage of NK1.1+ cells per total nuclei in each tumor section. Using this system, we indeed observed significantly fewer NK1.1+ cells in tumor

sections of 155<sup>-/-</sup> hosts (Fig. 17F). Collectively, these data suggest that miR-155 deficiency confers impaired NK cell tumor tropism in vivo.

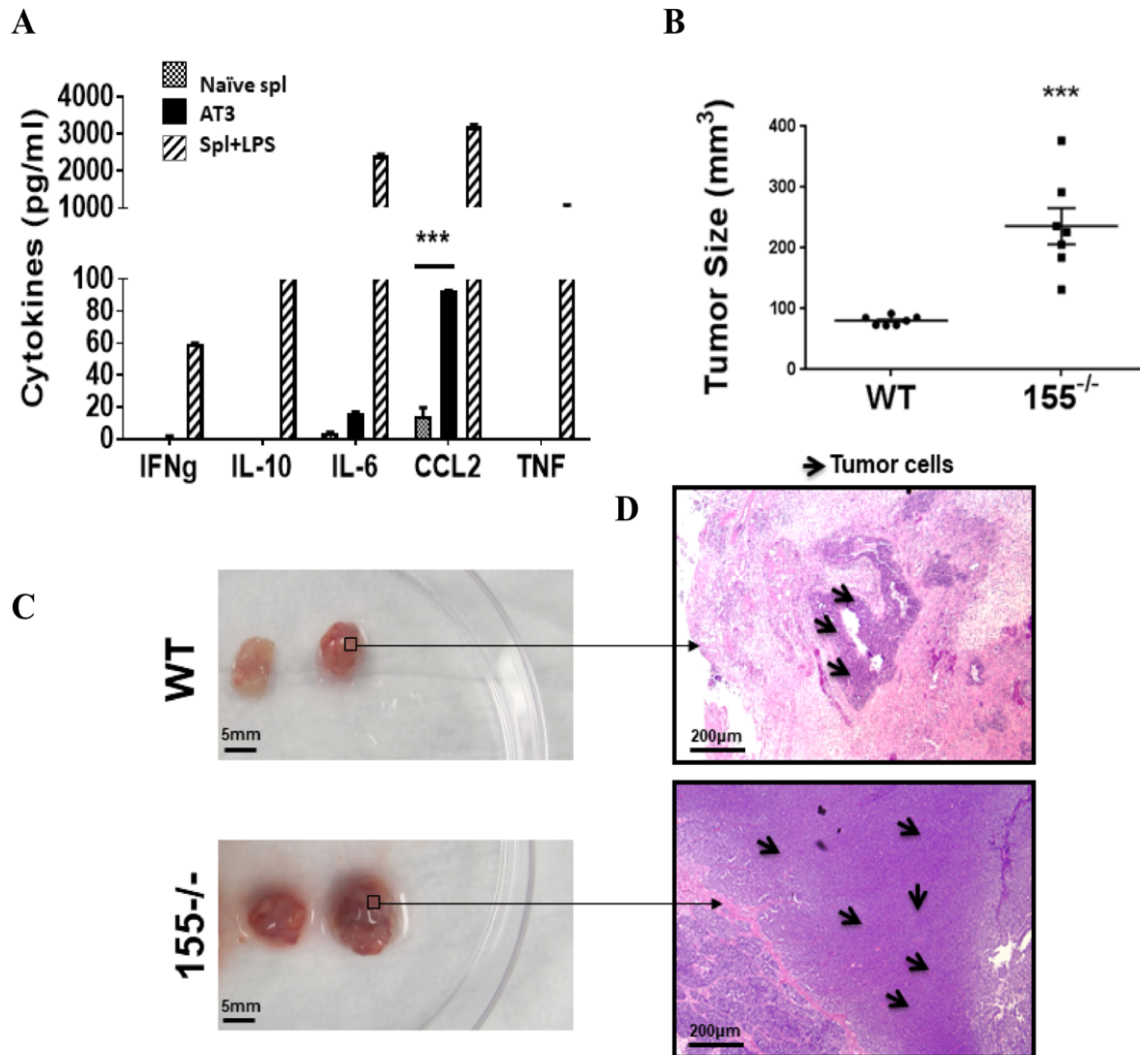


**Figure 16. AT3 tumor burden is higher in miR-155<sup>-/-</sup> hosts.**

A) Supernatants from AT3 tumor cell cultures (black bars), naïve WT splenocytes (stippled bars), or 24-hour LPS-stimulated splenocytes (grey bars) were collected and analyzed for cytokine production by CBA. B-D) AT3 tumor cells were injected subcutaneously into the flanks of WT or miR-155<sup>-/-</sup> mice. Four weeks after AT3 implantation, the mice were sacrificed and tumors were measured and dissected from surrounding tissues. B) MiR-155<sup>-/-</sup> tumor size compared to WT tumor size. C) Two representative AT3 tumors from each mouse strain with D) corresponding hematoxylin and eosin stained representative sections. Magnification = 100x; scale bar = 100  $\mu$ m. \* $P$  < 0.05, \*\* $P$  < 0.01, \*\*\* $P$  < 0.005

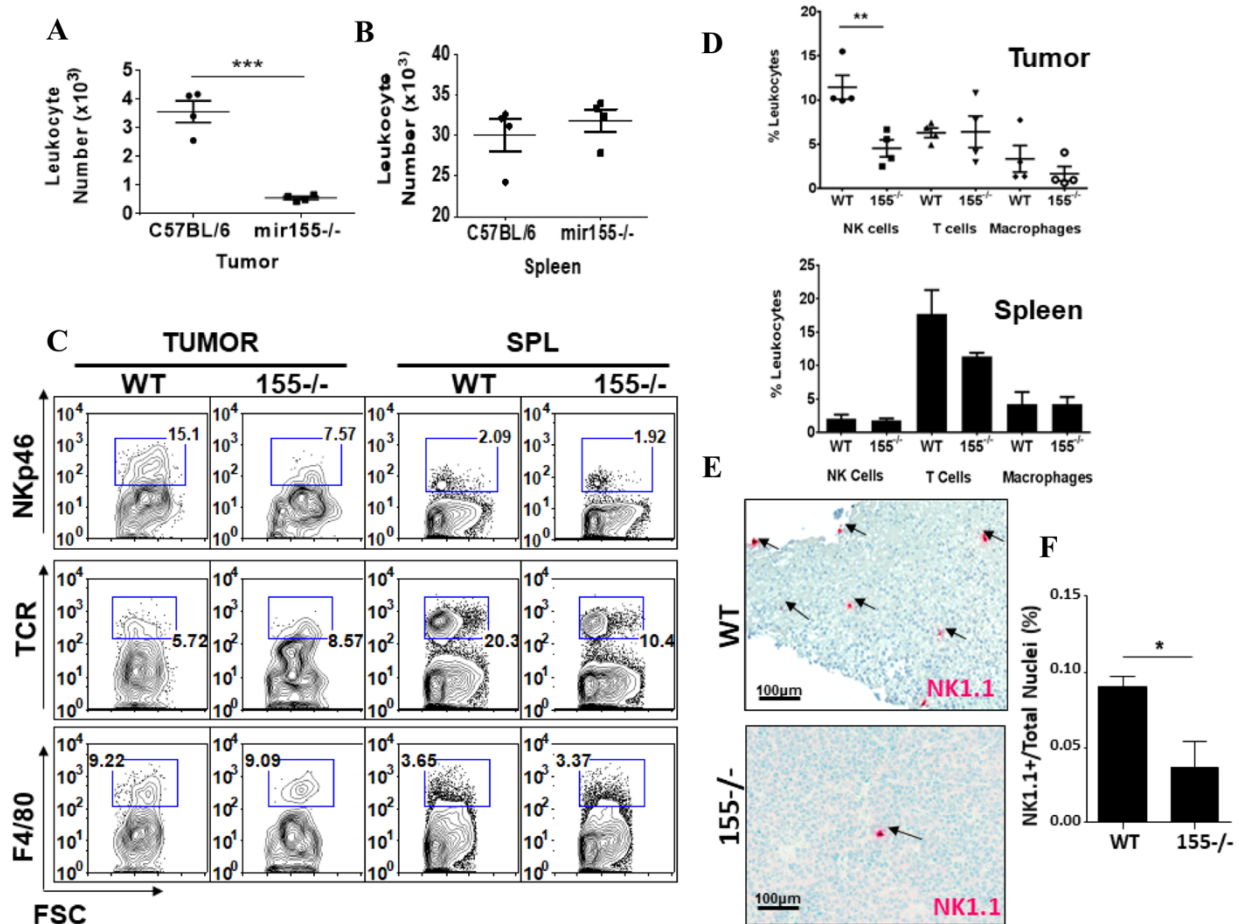


**Figure 17. NK cells fail to traffic to AT3 tumors in miR-155<sup>-/-</sup> hosts.**

AT3 tumor cells were injected subcutaneously into WT and miR-155<sup>-/-</sup> mice. Four weeks after AT3 tumor implantation, tumors and spleens were collected and homogenized to single cell suspension for analysis of TILs. Data shown is representative of three experiments. Percentage of NK cells in the tumor A) or spleen B) of tumor bearing mice averaged from 3 experiments. C, D) Representative flow cytometric contour plots and graphs of a single experiment (pooled from 3 mice per strain) showing NKp46<sup>+</sup> NK cells in tumor and spleen, as well as TCR<sup>+</sup> T cells and F4/80<sup>+</sup> Macrophage. E) AT3 tumors from WT or miR-155<sup>-/-</sup> hosts were fixed, paraffin-embedded and sectioned. The processed tissues were immunostained with anti-NK1.1 to detect intratumoral NK cells, and images of the whole tissues were captured with the Aperio scanning microscope. An imaging algorithm was generated to detect the number of NK1.1<sup>+</sup> cells in the tumor. Representative areas of AT3 tumors grafted in WT and miR-155-deficient mice and stained with hematoxylin and anti-NK1.1. Magnification = 200x; Scale bar = 50  $\mu$ m. F) The percentage of NK1.1<sup>+</sup> cells in tumors of WT and miR-155-deficient hosts as determined by an imaging algorithm from 2 tumors per strain. The data shown report the mean percentage of NK1.1<sup>+</sup> cells of the total nuclei count (as determined by hematoxylin stain) of each entire tumor section. \*P < 0.05, \*\*P < 0.01, \*\*\*P < 0.005

## Discussion

Here, we have shown that miR-155 deficiency in NK cells leads to SHIP-1 overexpression and that this, importantly, leads to faulty chemotaxis in vitro. In vivo, this results in defective tumor tropism and impaired tumor rejection. In this study, our results

show that the regulation of tumor infiltration and subsequent NK mediated tumor clearance and responsiveness is regulated by miR-155. With this study, we provide exciting evidence that negative regulation of the actin cytoskeleton via SHIP-1 has consequences in the context of tumor infiltration and cancer rejection. Our results provide novel evidence of a physiological role for SHIP-1 in NK cell tumor infiltration and implicate miR-155 in the regulation of NK cell chemotaxis.

miR-155 expression has a myriad of effects on multiple subsets of the immune system. miR-155 is essential for NK activation, and miR-155 deficiency decreases interferon gamma production. In terms of other subpopulations, miR-155 along with miR-21 have been shown to be involved with MDSC expansion (255), and miR-155 is required for B cell memory response (256). Additionally, miR-155 deficiency has been shown to enhance MDSC recruitment thus leading to enhancement of solid tumor growth (257). This previously published work may indicate potential non-NK reasons as to why the tumor burden was higher in the miR-155 mice. In the context of T cells which alongside NK cells are major players in antitumor immunity in the tumor microenvironment, miR-155 has been shown to be overexpressed in effector memory T cells, but not naïve or central memory T cells (48). In the context of viral infection, T cells have been shown to be defective in the absence of miR-155 (48). Since T cells have been shown to upregulate miR-155 upon activation and given the expression of miR-155 in effector memory T cells, miR-155 is thus an essential part of both innate and adaptive immunity. Given that the *bic/miR-155<sup>-/-</sup>* mouse used in our studies is not a conditional knockout within NK cells, but rather is a whole-body knockout, the T cell response in vivo may be influencing a substantial amount of the lack of antitumor immunity.



The gene targets of miR-155 in T cells and NK cells are similar. miR-155 in particular has been linked to pattern recognition receptor (PRR) pathways in NK cells, leading to regulation of type I interferon signaling (258). Similarly, in T cells, miR-155 has been shown to regulate type I interferon signaling, whereby there was increased type I signaling in miR-155 knockout T cells, and defects in proliferation. Type I interferon signaling can affect NK cells equally as it can T cells, leading to defects in STAT signaling, cytokine production, and overall effector function. In terms of Type II Interferons, Banerjee et. al. showed that in T cells, miR-155 skews T cell differentiation to Th1 by inhibiting interferon gamma (259). Contributing to this, miR-155 overexpression has also been shown to increase T-bet expression (260).

This is particularly relevant in the NK cell context given that interferon gamma production is one of the main ways that NK cells contribute to inflammation and cytotoxicity in the tumor microenvironment. The T cell response is also one that is slower to respond than that of NK. Thus, the chromium release assay results may be more representative of a true innate response, while the in vivo results may be more representative of what happens to the immune system as a whole over time. While it is outside of the context of this study, interrogating the T cell compartment in depth in this model would provide useful – evaluating both T cell memory phenotype and skewing/polarization.

SHIP-1 is involved in the cytoskeletal remodeling of mammalian cells, via regulation of the inositol phospholipids  $PIP_2$  and  $PIP_3$ . In WT cells, SHIP-1 expression is dampened by induction of miR-155. Since miR-155 depletes levels of SHIP-1,  $PIP_3$  accumulates at the membrane allowing positive signaling and cellular migration to occur.

We found that overexpression of SHIP-1 in NK cells resulting from miR-155 deficiency correlates with decreased motility and abnormal cytoskeletal rearrangement. Thus, miR-155-deficient NK cells may have disrupted motility due to overexpressed SHIP-1 resulting in a lack of PiP<sub>3</sub> and abundance of PiP<sub>2</sub> at the membrane. A further analysis of the miR-155-deficient NK cell cytoskeleton is warranted to determine the signaling proteins producing PiP<sub>3</sub> at the membrane and which actin remodeling proteins are directly associated with SHIP-1 in NK cells. Furthermore, whether SHIP-1 or PiP<sub>3</sub> are directly involved in actin polymerization in chemotaxing NK cells remains to be determined. Banh et. al. interrogated the effects of SHIP-1 on NK cell development and maturation and found that without SHIP-1, NK cells cannot reach the final stage of development and are functionally immature (43). In the context of our work, we found higher levels of SHIP-1 expression on miR-155<sup>-/-</sup> cells, with this SHIP-1 expression rendering the NK cells more dysfunctional. SHIP-1 is important to both development and function of NK cells and plays different roles in this regard. In our study we did not see impaired cytotoxicity in vitro, but significant impairments were seen in in vivo models, whereby the tumor burden was significantly higher and percentage of NK cells in both the tumor and spleen was decreased in the miR-155<sup>-/-</sup> mouse. It is important in this study to consider effects of the tumor microenvironment, which will be highly suppressive to NK cells. This may either be mediated by tumor cell-NK interaction or immune cell-NK interaction (ie. Treg-NK interaction). In a classical cytotoxicity assay, we perhaps did not see reduced cytotoxicity in the miR<sup>-/-</sup> conditions perhaps due to a lack of contextual cues signaling through SHIP-1 that may indeed be present in a physiologically relevant environment. A limitation of our work is the IL-2 activation of the isolated NK cells performed for all of the in vitro assays.

IL-2 may not be the predominant cytokine in a suppressed tumor microenvironment that may be skewed more toward a Th2 or suppressive environment driven by IL-10 and TGF $\beta$  (249, 257, 261). Clearly, further interrogation of miR-155 in the context of tumor induced immune suppression may be warranted.

## **Materials and Methods**

### **Mice, Cells, and Tumor Challenge**

C57BL/6 and B6.Cg-MiR-155<sup>tm1.1Rsky/J</sup> (*bic/miR-155<sup>-/-</sup>*) mice were purchased from Jackson Laboratory and housed in the Comparative Medicine Facility at the University of South Florida (USF). All experiments were approved by the Institutional Animal Care and Use Committee at USF. Mice were evaluated daily, and humanely euthanized via Carbon Dioxide inhalation. Autoclaved individually ventilated caging (IVC) units (Blueline, Tecniplast, Buguggiate, Italy) were used for all murine housing. A double-sided rack configuration with each rack holding 126 microisolation cages (63 cages per rack side) was used uniformly throughout the murine facility, and each pair of racks was ventilated and exhausted by a single air handling unit (AHU) trolley. Mice were fed an irradiated diet (Envigo, Teklad, Diet 2918) and housed on autoclaved pelleted paper bedding (Envigo, Teklad, 7084). Each cage was provided one nestlet for enrichment (Ancare, Bellmore, NY).

The AT3 mammary carcinoma line was a gift of Dr. Suzanne Ostrand-Rosenberg (University of Maryland, Baltimore, Maryland, United States of America). YAC-1 lymphoma cells were purchased from American Type Culture Collection (ATCC, Virginia,

United States of America). AT3 and YAC-1 lymphoma cells were cultured in RPMI supplemented with 10% FBS, 1% Penicillin-Streptomycin, and 1% L-glutamine. For the AT3 tumor challenge, AT3 cells were resuspended to  $1 \times 10^7$  c/ml in PBS. Age and sex-matched mice were injected subcutaneously in the right flank with 1 million cells/mouse, and tumors were visually monitored daily for four weeks prior to their sacrifice.

### **NK Cell Isolation**

Spleens were harvested from age and sex-matched mice and NK cells were purified with a NK cell negative selection kit (Miltenyi Biotech; 130-090-864). For each isolation, NK cells were determined to be >85% pure by NK1.1/DX5 co-expression. Purified NK cells were cultured in RPMI medium supplemented with 20% FBS, 1% nonessential amino acids, 1% sodium pyruvate, 1% Penicillin-Streptomycin, and 1% L-glutamine (Gibco). For production of activated NK cells, purified NK cells were cultured in the aforementioned media supplemented with 100 U/mL recombinant human IL-2 (Peprotech) for 3 d.

### **Flow Cytometry**

For steady state NK cell analysis, spleens were harvested from age and sex-matched mice, homogenized to single-cell suspension, and immediately stained with NK1.1-APC and DX5-FITC (BD Pharmingen; clones PK136, DX5) and 7-AAD (BD Pharmingen). For receptor phenotyping, 3 d IL-2 activated NK cells were stained with NKp46-FITC, NKG2D-PE, or 2B4-APC (eBioscience; clones 29A1.4, A10, eBio244F4) and 7-AAD. For determination of CCL2 expression, fresh splenic or 24-hour IL-2 [100 U/ml]-stimulated splenic cultures were stained with NK1.1-APC, CCR2-FITC (R&D Systems; FAB5538F)

and 7-AAD. In additional experiments, splenic cultures were stained with NK1.1-FITC, NKp46 AF647, TCRB PE, and DAPI was used for dead cell exclusion. For TIL isolation and analysis, spleens and tumors were harvested 4 wk post tumor cell injection. Spleens were homogenized to a single cell suspension and tumors were strained through 70 $\mu$ m strainers to a single cell suspension. The homogenized tissues were stained with NK1.1-APC, DX5-FITC, and 7-AAD. Samples were acquired on a BD FACSCalibur or BD FACSCanto II and analyzed with FlowJo software (BD). All data shown is gated on 7-AAD-negative events falling within the lymphocyte gate (denoted by Forward vs. Side Scatter). For detection of cytokines in tumor supernatants, the Mouse Inflammation Cytometric Bead Assay kit (BD Biosciences; cat#: 552364) was used per manufacturer instructions.

### **Chromium Release Assay**

A chromium-51 ( $^{51}\text{Cr}$ )-release assay was performed as described previously (262, 263), using YAC-1 or AT3 tumor cells as targets for IL-2 activated cells or freshly isolated splenocytes. Briefly, target tumor cells were labeled with 200  $\mu\text{Ci}$  of Na [ $^{51}\text{Cr}$ ] chromate (Amersham Corp., Arlington Heights, IL) in 0.2 ml of medium at 37°C for 1 h. The cells were then washed and added to effector cells at  $5 \times 10^3$  cells/ well in triplicate wells of a 96-well round-bottom plate, resulting in various E/T ratios in a final volume of 0.2 ml per well. After a 5-hour incubation at 37°C, 100  $\mu\text{l}$  of culture supernatants were harvested and counted in with a  $\gamma$ -counter. The percent specific  $^{51}\text{Cr}$  release was determined as described previously (262, 263) according to the equation: [(experimental cpm – spontaneous cpm)/total cpm incorporated]  $\times$  100. All determinations were done in

triplicate, and the SEM of all assays was calculated and was typically ~5% of the mean or less.

### **Migration assay**

Splenocytes from WT or 155<sup>-/-</sup> mice were incubated for 24 h with IL-2 (100 U/ml) to induce CCR2 surface expression. The cells were then washed and starved in serum and cytokine-free RPMI for 4 hours at 37°C. For inhibition of SHIP-1, the cells were serum and cytokine starved for three hours and pretreated with 3 $\alpha$ -aminocholestane (3AC) (Millipore; 565835) or ethanol vehicle for the final hour of starvation. The cell suspensions were then applied to the top wells of a 10-well Boyden chamber, with CCL2-supplemented [10 ng/ml] RPMI medium in the bottom chamber, separated by a 5- $\mu$ m pore size polyvinylidene fluoride membrane (Whatman). The apparatus was incubated at 37°C for 2 h. The migrated cells in the bottom wells were then harvested, resuspended to 500  $\mu$ l, and 50  $\mu$ L Countbright Absolute Counting Beads (Invitrogen; C36960) were added. For each sample, 20,000 beads were collected. Per manufacturer instruction, the absolute counts of migrated cells were determined by the following equation: Absolute # cells migrated = (# of Cell Events acquired on cytometer / 20,000 beads) x (50,000 beads/50  $\mu$ L).

### **Western blot analysis**

Cell lysates were acquired as previously described (263). Briefly, cells were pelleted and lysed in 1% NP-40, 10 mM Tris, 140 mM NaCl, 0.1 mM PMSF, 10 mM iodoacetamide, 50 mM Na fluoride, 1 mM EDTA, 0.4 mM Na orthovanadate, 10  $\mu$ g/ml leupeptin, 10

µg/pepstatin, and 10 µg/ml aprotinin, followed by centrifugation to remove nuclei and cell debris. Protein concentrations for each sample were calculated using the Bradford Bio-Rad protein assay. Protein lysates (80 µg/sample) were separated by gel electrophoresis through a 10% SDS-PAGE gel and were transferred overnight at 20 V/hr to a PVDF membrane. The membrane was then probed with anti-SHIP-1 (Santa Cruz Biotechnology; clone P1C1) followed by horseradish peroxidase-conjugated anti-mouse-IgG (GE Healthcare Life Sciences). The blot was developed with a SuperSignal West Femto chemoluminescent reagent (Thermo Scientific). As a protein loading control, the blot was stripped and reprobed for β-actin.

### **Immunohistochemistry**

Four weeks after tumor implantation, tumors were harvested, bisected, and fixed in 10% formalin. The tissues were then paraffin-embedded, cut into 5 µm sections and mounted onto slides. Representative sections were deparaffinized in two changes of xylene, rehydrated in changes of decreasing ethanol/water solutions, and treated with a citrate-based solution (pH 6.0) for antigen retrieval. The tissue samples were then blocked in 1.5% human serum followed by an avidin/biotin blocking kit (Vector Laboratories), and probed with a biotinylated anti-NK-1.1 (clone PK136, BD Biosciences) overnight at 4°C. Slides were then washed and probed with alkaline phosphatase-conjugated streptavidin (ABC kit; Vectastain) and developed with an avidin/biotin substrate kit (Vector Laboratories). The slides were then counterstained with Gill's Hematoxylin (Vector Laboratories), dehydrated, and mounted with Cytoseal (Thomas Scientific). The immunostained tumor tissues were scanned with the Spectrum Aperio Scanscope slide

scanner, and an algorithm to count immunostained NK1.1+ cells out of total nuclei (detected by hematoxylin) was generated using Definiens TissueStudio software. The percent of tumor infiltrating NK cells was determined with the following equation:  $((\text{number NK1.1+ cells} / \text{total number of nuclei in tissue}) * 100)$ . Alternatively, prior to antigen retrieval, some tumors were stained with Gill's hematoxylin and eosin, dehydrated, and mounted with Cytoseal.

### **Confocal Microscopy**

For F-actin staining, IL-2 activated NK cells were serum and cytokine-starved for 4 h. The cells were then left untreated or treated with 10 ng/ml recombinant mouse CCL2/MCP-1 (R&D Systems) for 30 minutes at 37°C. The cells were fixed in suspension with Fixation buffer (BD Biosciences) and  $2.5 \times 10^5$  cells were cytopun onto microscope slides (Shandon). The slides were then permeabilized with Permeabilization/Wash buffer (BD Biosciences) and stained with rhodamine-conjugated Phalloidin (Invitrogen) followed by mounting with Fluorescent Mounting Media (Vector Labs). The cells were visualized by confocal microscopy with a 63x oil objective on a Leica TCS SP5 Laser Scanning Confocal Microscope, and captured images were analyzed with LAS-AF software. Definiens Tissue Studio version 4.7 was used to analyze the images for green fluorescence intensity. First a nucleus detection algorithm was applied to the DAPI channel to segment nuclei based on intensity and size thresholds. Next a simple growth algorithm of 1 micron was applied to generate a cytoplasm around each nuclei. The intensity for green fluorescence was measure in each cell, nucleus, and cytoplasm.



## Statistics

Data are presented as means  $\pm$  standard error of the mean. Differences between individual groups were analyzed by Student's *t*-test using Graphpad Prism version 7.04. *P* values  $< 0.05$  were considered statistically significant. Significance was also confirmed with the Wilcoxon rank sum test.

## CHAPTER FOUR:

### S100A9 CONTRIBUTES TO T CELL DYSFUNCTION THROUGH ITS INTERACTION WITH RAGE IN MYELODYSPLASTIC SYNDROMES

#### *Introduction*

S100A9 drives the development of Myelodysplastic Syndrome (MDS) through expansion of Myeloid Derived Suppressor Cells (MDSC) and promotion of pyroptosis(60, 70) (**Fig. 18**). Despite the identified role of S100A9's effects on MDSC and hematopoietic stem and progenitor cells (HSPC), the role of S100A9 on disease progression due to effects on adaptive immunity are less clear. Here, we report for the first time of the substantial effects of S100A9 on T cell function in MDS that may lead to greatly impaired immunoresponsiveness in the disease. Danger Associated Molecular Pattern (DAMP) S100A9 is a known ligand for the Pattern Recognition Receptor (PRR) Receptor for Advanced Glycation Endproducts (RAGE) (264). This is the first study to investigate S100A9's effects on RAGE in MDS. We endeavored to understand a seeming lack of T cell response in the disease, and given our work and understanding of S100A9, asked whether S100A9 would adversely affect T cell function. We identified, through this work, a mechanism of T cell dysfunction that may lead to a lack of responsiveness in the context of a disease known to overexpress the RAGE ligand S100A9. Capitalizing on this

checkpoint can perhaps rescue T cells to a more functional state in the disease by blocking RAGE.

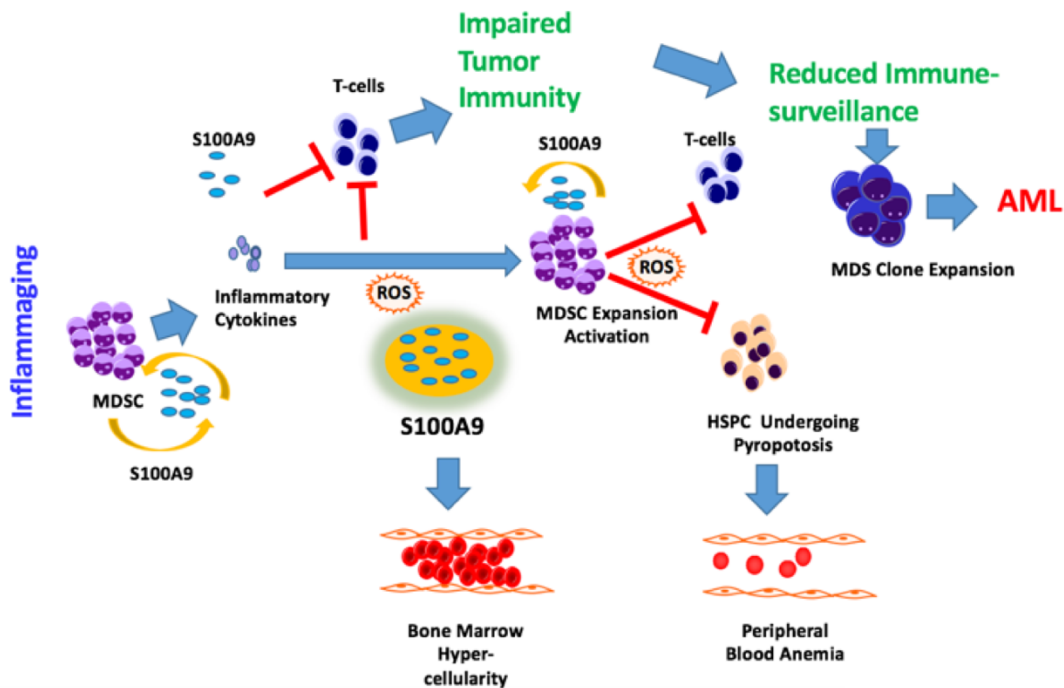


**Figure 18:** The Role of S100A9 in Myelodysplastic Syndromes. S100A9 increases MDSC expansion and activation, which can block T cell functionality. Additionally, S100A9 leads to the production of other proinflammatory cytokines, as well as induces pyroptosis. Collectively, these lead to impaired tumor immunity, and reduced immune surveillance through bone marrow hypercellularity and peripheral blood anemia secondary to MDS clone expansion.

## Results

### T cells from MDS Patients are antigen experienced and functionally normal

We obtained peripheral blood and bone marrow mononuclear cells from MDS patients as well as those from healthy age-matched controls. We first wanted to characterize the T cell compartment in the disease in order to determine if the T cells are functionally and phenotypically normal in this state of pathology. We chose to focus our

phenotyping predominately on bone marrow mononuclear cells as that is the primary site of the disease and pathology in MDS. Prior to this, we obtained MDS PBMC to interrogate.

We first examined 3 low-risk (IPSS-0) and 3 intermediate risk (IPSS-3) PBMC's from consenting patients. Extensive phenotyping was performed by flow cytometry using a BD LSR II SORP. When compared to the healthy donors, the MDS patients had less naïve T cells, and more effector memory, defined by CD45RA and CD62L expression (**Fig. 19A**). This is representative of a more antigen experienced state and is expected in the context of disease. Uniquely, though, while the healthy donors had an even mix of naïve, central and effector memory T cells, the MDS patients had very few naïve T cells. This indicates that these T cells in these patients have been activated at some point, but does not indicate that they are presently activated or not. The low risk patients had more of a T effector memory re-expressing CD45RA (TEMRA) phenotype, while the intermediate risk patients had a predominately effector memory phenotype (**Fig. 19B-19E**). The phenotype of the low risk patients may be representative of an exhausted phenotype, or perhaps more of an activated phenotype. Confirming this with CD69 expression indicates that at rest, the CD8 compartment of the low risk patients is activated, but this is not seen in the intermediate risk patients (Data not shown). There may be a shift in memory phenotype or trafficking in response to disease progression in MDS.

We sought to activate these T cells and found that they are functionally normal in response to strong stimulation through the TCR and costimulation (anti-CD3/28) + IL-2. Checkpoint receptors are conventionally studied in the context of an “exhausted” T cell. Here, we sought to study the checkpoints PD-1, CTLA4, LAG-3, and TIM-3 as markers

of activation, as they are upregulated sharply after T cell activation. We found that normal and MDS PBMC all upregulate PD-1, LAG-3 and TIM-3 in response to activation, as well as CD69 (**Fig. 20**). This indicates that there may not be a functional defect in these cells in response to normal activation. This does beg the question as to whether the T cells in MDS are receiving strong stimulation through their TCR to begin with, but in ex vivo assays, they do respond well to stimulation.

In order to study the disease more accurately, we interrogated the same parameters as above with bone marrow. In a previous work by our group, we identified that there were less CD3% cells in the bone marrow of MDS patient (**Fig. 21A**). In this current work, significantly ( $p < 0.001$ ) less T cells (by percent, not absolute number) were found by flow cytometry, using live, singlet, CD3+s to gate. Within this population, significantly ( $p < 0.0001$ ) less naïve T cells were found (using CD45RA and CD62L as above), and significantly ( $p < 0.001$ ) more TEMRA T cells were found (**Figs. 21B, 21E**). There was no significant difference between the TCM and TEM populations, though the trend appears to be an increase in both of these populations (**Figs. 21C, 21D**). These are all indicative of an antigen experienced T cell repertoire, similar to that of the blood in these patients. Unlike the PBMC, the patients did not have a higher expression of CD69, indicating that in the bone marrow, the T cells did not exhibit an activated profile (**Fig. 22E**). Similar to the peripheral blood, the BM T cells responded to activation by upregulating PD-1, LAG-3 and TIM-3 (**Figs. 22A-22D**). Cytometric Bead Arrays (CBA) for cytokines associated with Th1, Th2, and Th17 (IL-2, TNF $\alpha$ , IFN $\gamma$ , IL-4, IL-6, IL-10, IL-17) cells show that these T cells can be stimulated to produce normal levels of cytokine compared to their healthy counterparts (Data not shown).

This data above shows that the T cells in MDS are functionally responsive to activation, are antigen-experienced, and may not be abnormal as one would expect to see in a conventional suppressive tumor microenvironment. Given that the disease does not affect the lymphoid compartment normally, this may be expected, however we felt it was important to determine what this immunosuppressive microenvironment is doing to the T cells, since they do not appear to be activated fresh from isolation. Thus, we still sought to determine what could be possible mechanisms for a lack of responsiveness of the T cells in the disease.

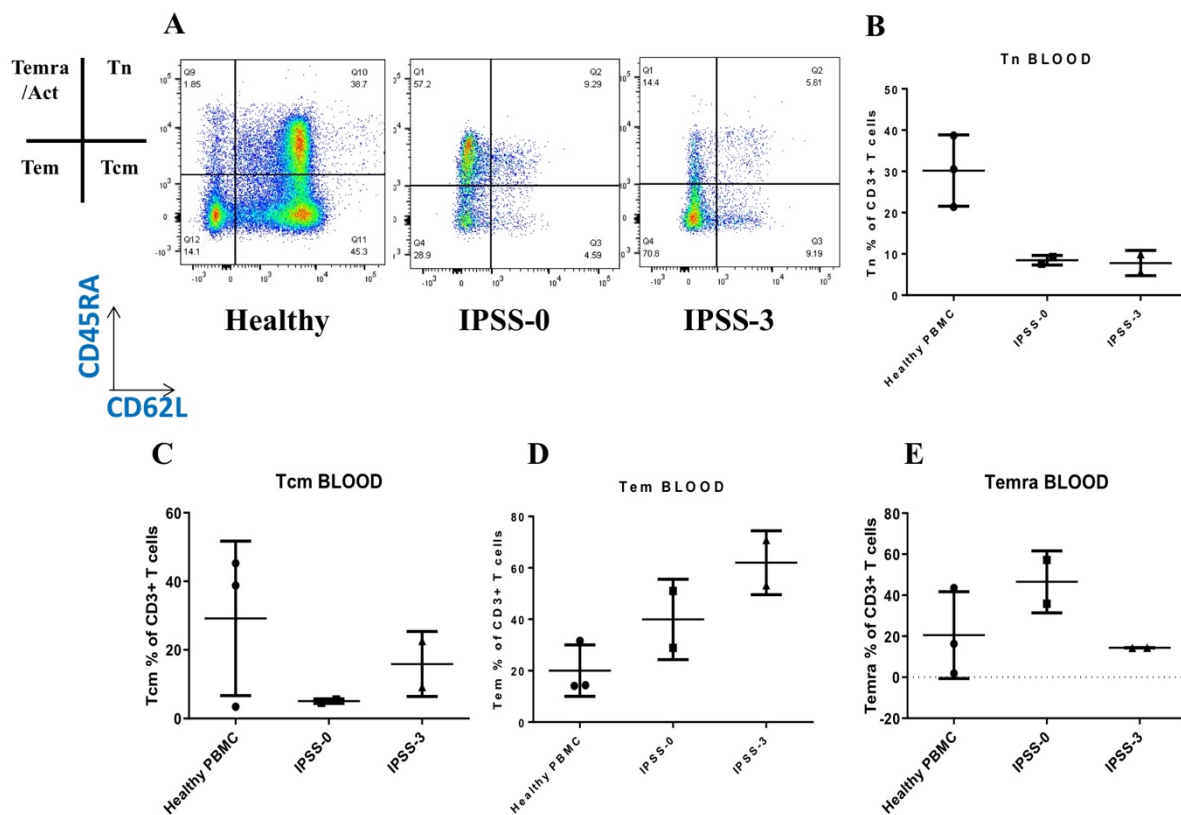


**Figure 19.** Phenotypic Characterization of Healthy and MDS PBMC. n=3 healthy, n=2 IPSS-0, n=2 IPSS-3; Gating was performed utilizing Live, Singlet, CD3+ Cells and defining these memory populations by CD45RA and CD62L. A) Representative flow staining of Healthy, IPSS-0 and IPSS-3 PBMC samples. B) % of Naïve T cells of CD3+ T cells in Healthy and MDS PBMC. C) % of Central Memory T cells of CD3+ T cells in Healthy and MDS PBMC. D) % of Effector Memory T cells of CD3+ T cells in Healthy and MDS PBMC. E) % of T Effector Memory Re-Expressing CD45RA (Temra) of CD3+ T cells in Healthy and MDS PBMC.

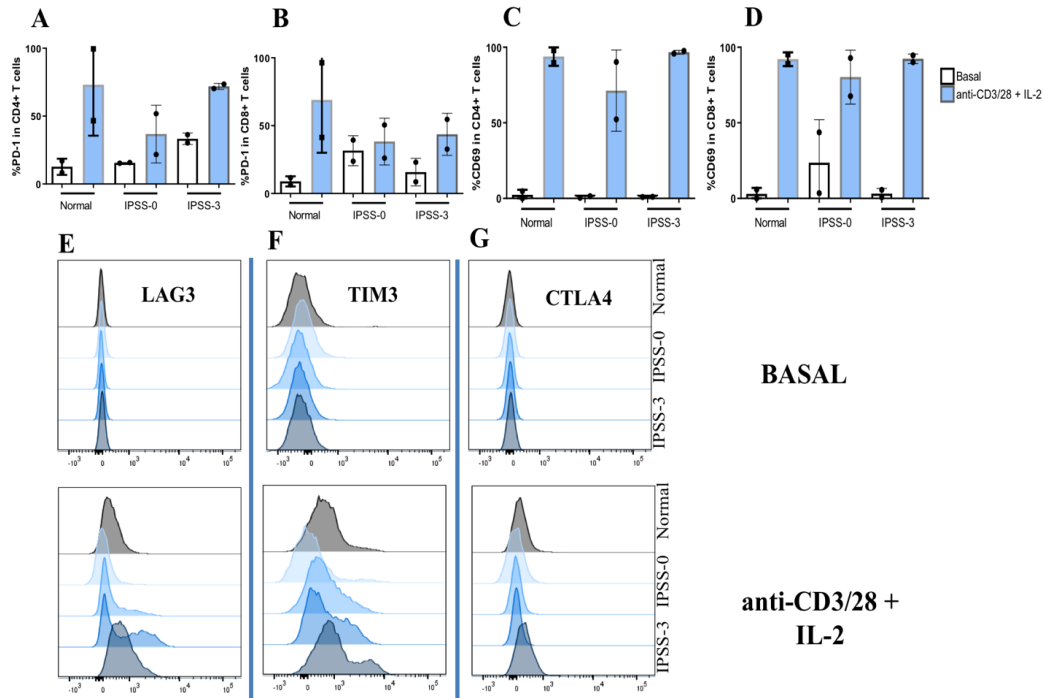


**Figure 20.** Phenotypic Characterization of Healthy and MDS PBMC. n=3 healthy, n=2 IPSS-0, n=2 IPSS-3; T cells were activated or not with anti-CD3/28 + IL-2 and analyzed by flow cytometry. Upstream gating was performed utilizing Live, Singlet, CD3+ Cells. A) %PD-1 in CD4+ T cells before and after activation with anti-CD3/28 + IL-2. B) %PD-1 in CD8+ T cells before and after activation with anti-CD3/28 + IL-2. C) %CD69 in CD4+ T cells before and after activation with anti-CD3/28 + IL-2. D) %CD69 in CD8+ T cells before and after activation with anti-CD3/28 + IL-2. LAG3(E), TIM-3(F), and CTLA-4(G)- Expression before (top panel) and after (bottom panel) activation with anti-CD3/28 + IL-2.

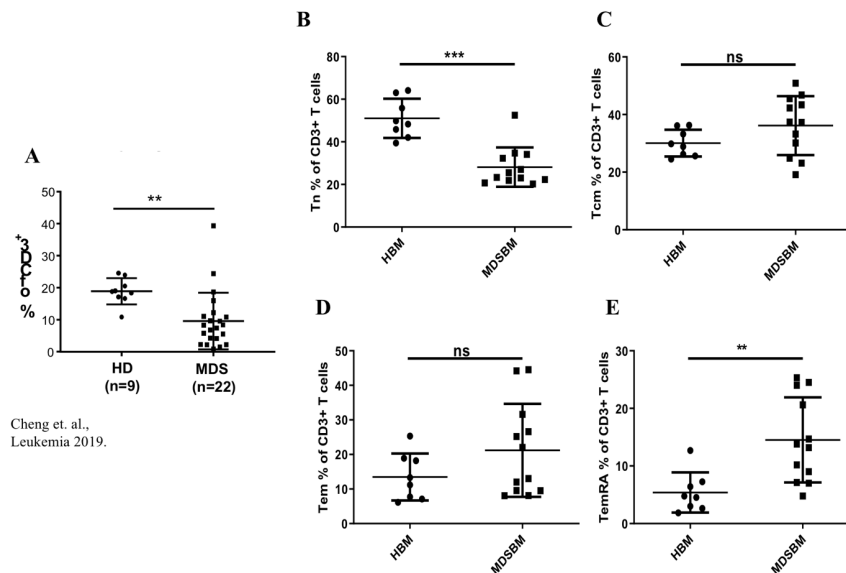


**Figure 21.** Phenotypic Characterization of Healthy and MDS BMMNC. Upstream gating was performed utilizing Live, Singlet, CD3+ Cells. A) %T cells within total live cells in HBM vs MDS-BMMNC. B) % of Naïve T cells within CD3+ T cells in HBM vs MDS-BMMNC. C) % of Central Memory T cells within CD3+ T cells in HBM vs MDS-BMMNC. D) % of Effector Memory T cells within CD3+ T cells in HBM vs MDS-BMMNC. E) % of T Effector Memory Re-Expressing CD45RA (TemRA) T cells within CD3+ T cells in HBM vs MDS-BMMNC.

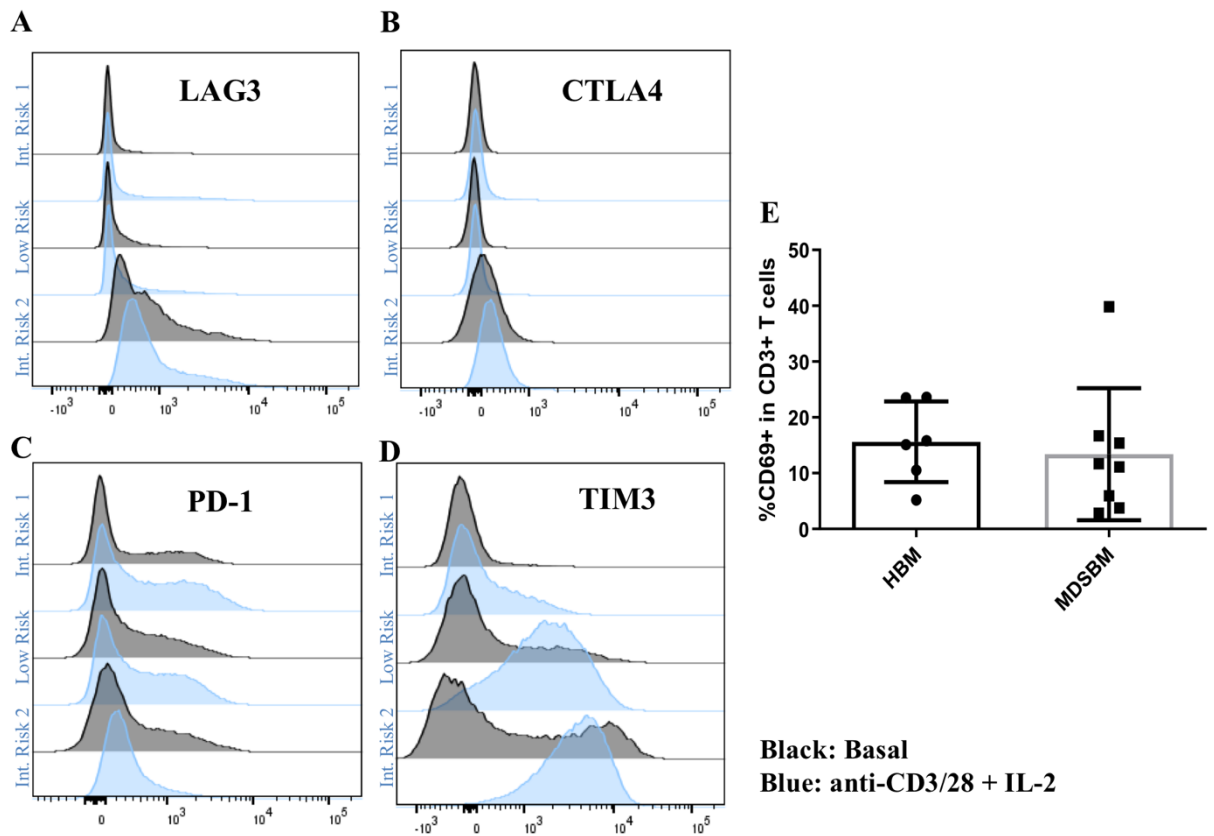


**Figure 22.** Phenotypic Characterization of Healthy and MDS BMMNC. Upstream gating was performed utilizing Live, Singlet, CD3+ Cells. T cells were activated or not with anti-CD3/28 + IL-2 and analyzed by flow cytometry. Black histograms represent basal, unactivated T cells. Blue histograms represent T cells activated with anti-CD3/28 + IL-2. Expression of (A) LAG3, (B) CTLA4, (C) PD-1, and (D) TIM-3 within CD3+ T Cells before (black) and after (blue) activation with anti-CD3/28 + IL-2 for two intermediate-risk and one low-risk MDS patient. E) % of CD69 within CD3+ T cells in basal HBM and MDS-BMMNC Cells.

## S100A9 is a major source of inflammation in the MDS Bone Marrow

### Microenvironment and suppresses T cell proliferation

Our group has shown that S100A9 is highly expressed in the plasma of MDS bone marrow, and in particular in lower risk disease. It drives the production of CD33+ MDSC, impairing tumor immunity, and contributes to increased rates of apoptosis through its promotion of pyroptosis via an IL-1B and Caspase-3 mediated mechanism (60, 70, 111). Since S100A9 promotes inflammation via engagement of multiple immune-related pathways, we sought to understand what functional effects S100A9 has on T cells. We



hypothesized that S100A9 activates T cells and promotes a highly inflammatory immune response. To study the basic science of what effect a DAMP has on T cell biology, we utilized healthy donor PBMC predominately, as well as MDS BM.

We first chose to interrogate proliferation, as T cells proliferate rapidly after TCR engagement and cytokine stimuli. Cell trace violet is a lipophilic dye similar in function to CFSE that is taken up by the parental cell using a conventional flow cytometry staining method, and the dye is divided evenly between daughter cells. Thus in a conventional flow plot, the brightest peak is the parental cells, and all the peaks to the left (at dimmer MFIs) represent the daughter cell divisions. Given the expectation of a PRR to initiate an immune response, we were shocked to find that PBMC are completely halted in their division after the first generation of division. Anti-CD3/28 + IL-2 treated PBMC proliferated normally (**Fig. 23A**), but those with recombinant human S100A9 (rhS100A9) in the culture experienced proliferative arrest (**Fig. 23B**). We confirmed this result in MDS BM, where the proliferation was arrested in a notable way, but not to the same degree as it was in PBMC (**Fig. 23C**). We hypothesized that these MDS BM T cells were already previously exposed to S100A9, thus the stimuli was not as much of a stressor to the cells as it was the healthy PBMC, where they wouldn't have had as much exposure to this DAMP. We questioned next whether the cells are dying or undergoing apoptosis that would lead to this halt in proliferation. We found that T cells not activated treated with S100A9 did not die nor were they undergoing conventional mechanisms of apoptosis as evaluated with 7AAD and Annexin V via flow cytometry (**Figs. 24A, 24C**). Activated T cells displayed normal levels of apoptosis upon activation, and this was not increased when treated with rhS100A9 (**Figs. 24B, 24D**). This indicates that these cells are healthy, not dying, and not

undergoing apoptosis and that this is not a mechanism for the decreased proliferative response. In order to further evaluate potential mechanisms for this, we evaluated the cell cycle using DNA binding dye 7AAD. This is a mechanism of intracellular staining by flow cytometry that allows us to visualize the cell cycle. This is a stoichiometric method of analysis, whereby the cells in S phase will take up more dye than those cells in G1, and those in G2 will be even brighter. Cells at rest untreated or treated with rhS100A9 did not display any cell cycle profile as expected due to their lack of proliferation (**Figs. 24E, 24G**). Those treated with anti-CD3/28 + IL-2 have robust G1, S and G2 peaks (**Fig. 24F**). The cells treated with rhS100A9 surprisingly lacked a G2 peak, indicating a G1/S cell cycle arrest (**Fig. 24H**). Further analysis with cyclins would confirm this arrest. It is interesting that the cells were not seen to undergo apoptosis, however it is possible that they are undergoing repair mechanisms at the snapshot in time that the flow cytometry assay is capturing.

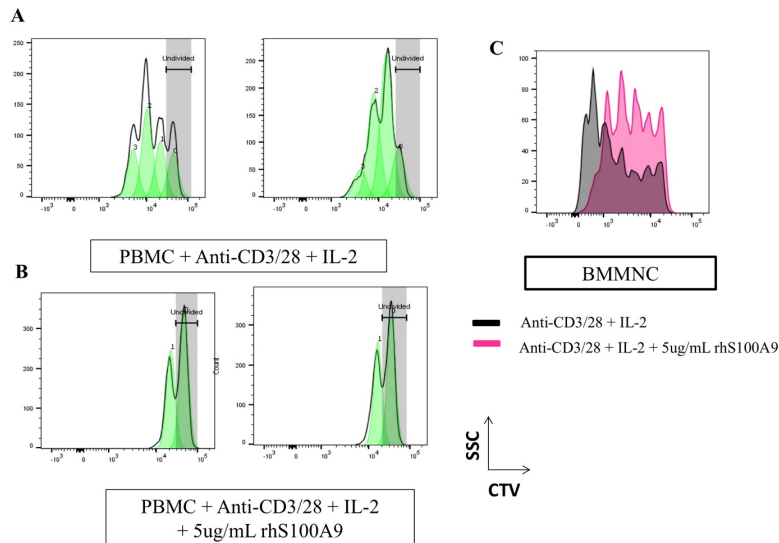


**Figure 23.** PBMC and BMMNC proliferation are inhibited by S100A9. Upstream gating was performed utilizing Live, Singlet, CD3+ Cells. T cells were activated or not with anti-CD3/28 + IL-2, with or without rhS100A9 (5ug/mL) and analyzed by flow cytometry. Staining was performed with Cell Trace Violet and stimulation was performed for four days. A) Two healthy PBMC donors activated with anti-CD3/28 + IL-2. B) Two healthy PBMC donors activated with anti-CD3/28 + IL-2 and 5ug/mL rhS100A9. C) BMMNC activated with anti-CD3/28 + IL-2 (black) and 5ug/mL rhS100A9 (pink).

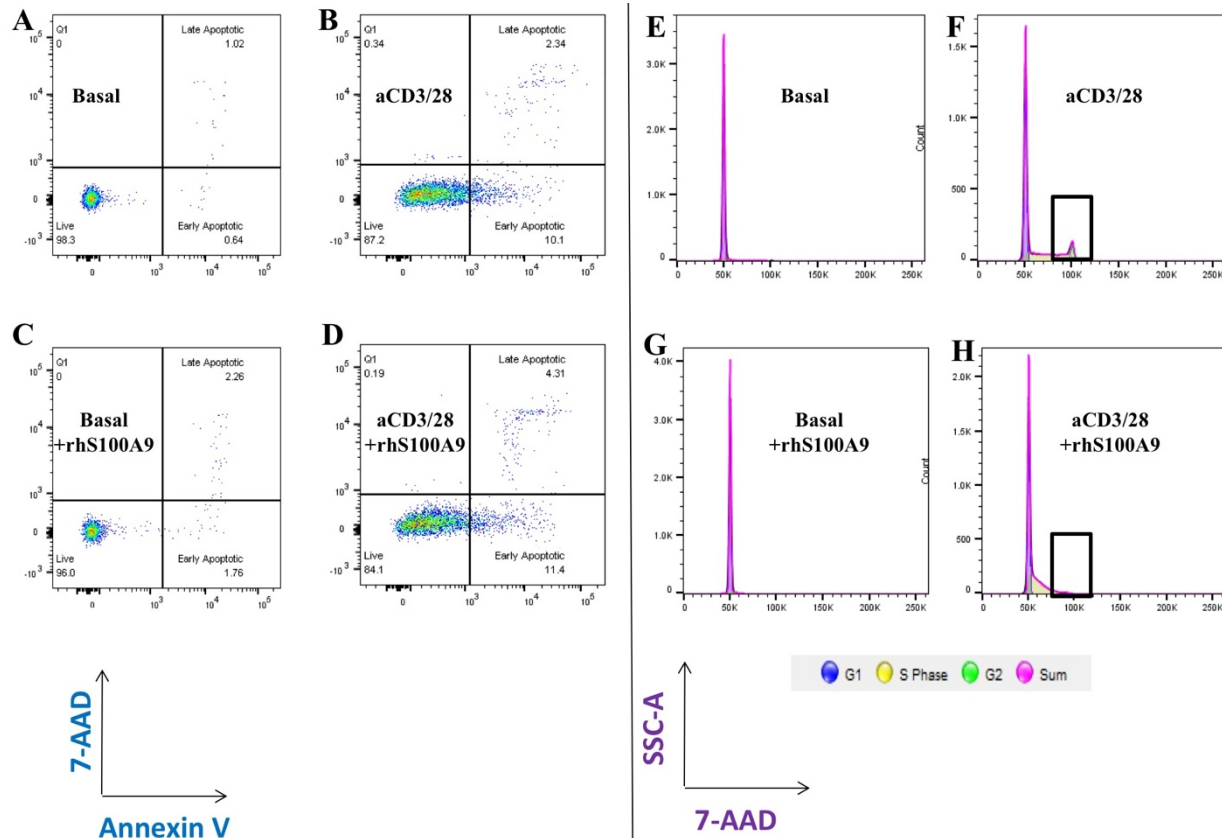


**Figure 24.** S100A9 does not induce cell death or apoptosis of PBMC but may induce cell cycle arrest. Upstream gating was performed utilizing Live, Singlet, CD3+ Cells. T cells were activated or not with anti-CD3/28 + IL-2, with or without rhS100A9 (5ug/mL) and analyzed by flow cytometry. Staining was performed with Annexin V and PI or 7AAD and stimulation was performed for four days. Apoptosis profile of: A) T cells without stimulation. B) T cells activated with anti-CD3/28 + IL-2. C) T cells without activation + rhS100A9 (5ug/mL). D) T cells activated with anti-CD3/28 + IL-2 + rhS100A9 (5ug/mL). Cell cycle profile of: E) T cells without stimulation. F) T cells activated with anti-CD3/28 + IL-2. G) T cells without activation + rhS100A9 (5ug/mL). H) T cells activated with anti-CD3/28 + IL-2 + rhS100A9 (5ug/mL).

In order to check for functionality of the T cells, we utilized an IFN $\gamma$  Enzyme Linked Immunosorbent Assay (ELISA). PBMC treated with anti-CD3/28 + IL-2 produced a robust amount of IFN $\gamma$ , and this was significantly halted with rhS100A9 treatment (**Fig. 25A**). We then confirmed our results with MDS BM, which were treated with either rhS100A9 or autologous serum, with S100A9 confirmed by ELISA. The rhS100A9 treatment of activated T cells led to significantly less IFN $\gamma$  production, and this was decreased even further when treated with autologous serum (**Figs. 25B, 25C**). This indicates that S100A9

may decrease the T cells functional abilities and outputs in vitro. We hypothesize that the reason for the autologous serum having a greater effect than the rhS100A9 is simply due to concentration. We utilize 5ug/mL of rhS100A9 in our assays, which was determined in a dose curve to be sufficient to suppress T cell responses, but patient serum typically has much more than this and can be upwards of 20ug/mL (**Fig. 25C**).

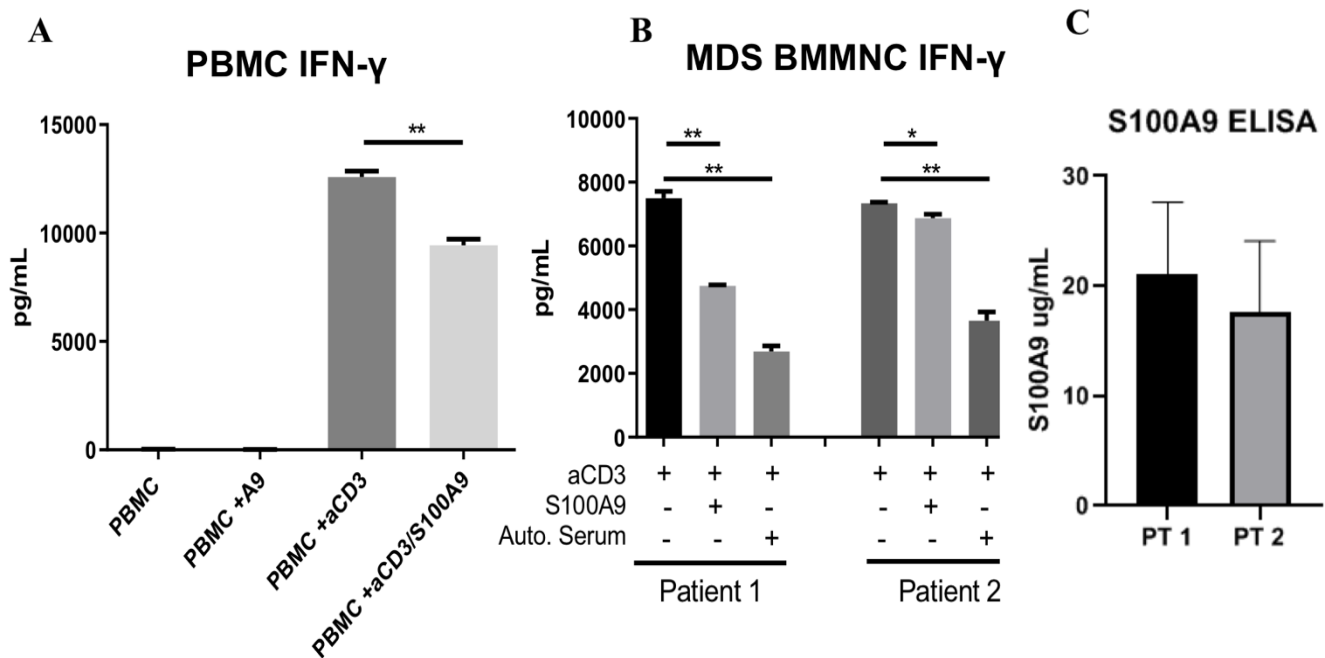


**Figure 25:** Interferon Gamma production is decreased with S100A9 treatment. A) Healthy Donor PBMC were treated with 5ug/mL rhS100A9, anti-CD3/28 + IL-2 alone or a combination of the two for four days. B) MDS BMMNC were activated with anti-CD3/28 + IL-2 with or without 5ug/mL rhS100A9 or autologous serum. C) S100A9 ELISA of autologous supernatant used to treat the MDS BMMNC.

In a conventional immune response, there is an inflammatory innate response that eventually leads to antigen presentation and an activated T cell response and more inflammation. In all of the assays above, the rhS100A9 treatment was given alongside the T cell activating conditions. One of the questions that we wanted to evaluate was whether or not it matters if the T cell is exposed to activation or the rhS100A9 treatment first. We speculated that the T cell would not be responsive to S100A9 once it was activated. HBM was utilized here, and IFN $\gamma$  again as an output. HBM treated with anti-CD3/28 + IL-2 a day prior to rhS100A9 treatment produced the most IFN $\gamma$ , confirming our thoughts about less sensitivity of the T cell to this signaling once it is already activated. When S100A9 was provided the day before anti-CD3/28 + IL-2, the result is similar to the two treatments being provided simultaneously, which is that the IFN $\gamma$  production is significantly lower. This indicates that this signaling may be most pertinent to the T cell only prior to activation (**Fig. 26A**). CD107a is a LAMP (lysosomal-associated membrane glycoprotein) that is used as a surrogate for T cell cytotoxicity, as its surface expression is induced during degranulation. S100A9 treatment the day prior to activation led to the highest percent of degranulating CD3+ T cells. Those treated with just anti-CD3/28 + IL-2 or simultaneous treatment showed 1/3 of the degranulation of those pretreated with S100A9. Thus the S100A9 may sensitize the T cells to killing (**Fig. 26B**). A potential reason for the discrepancy of less IFN $\gamma$  but more CD107a may be simply a CD4 vs CD8 phenomenon. Though CD8's produce cytokine, CD4's are the predominate cytokine producers in our assays. The larger focus is the degranulation, which is almost exclusively a CD8 T cell phenomenon. Strikingly, however, we found that the T cells pretreated with S100A9 displayed a higher percentage of CD4 T cells and that those CD4's were the

cells who were predominately degranulating (**Fig. 27**). We uniquely also found that the CD4's preactivated with rhS100A9 displayed the highest percentage of activation marker CD69 (**Fig. 27D**).

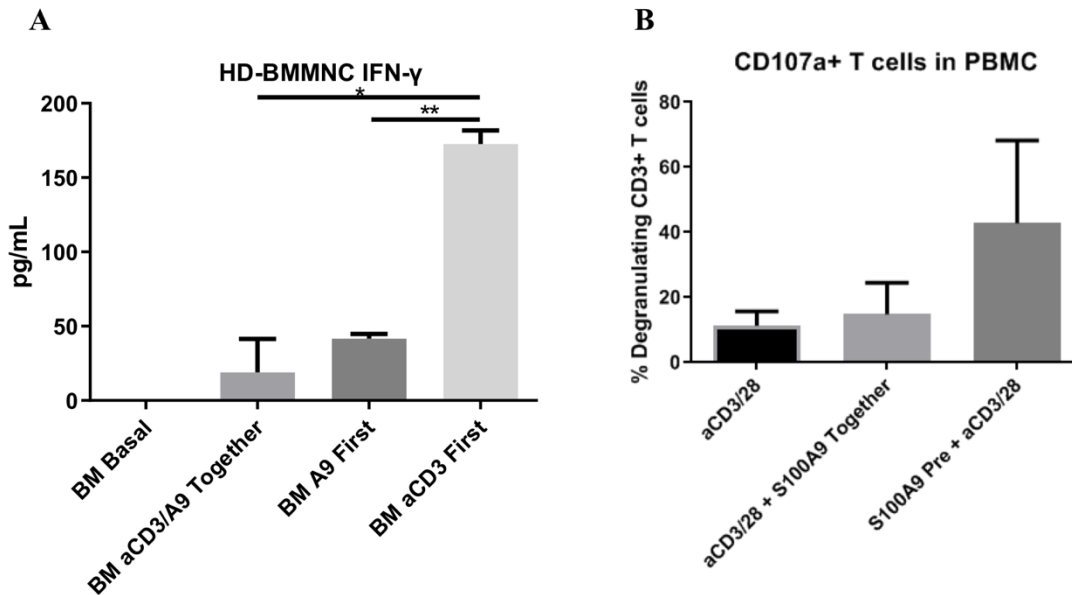


**Figure 26:** S100A9 pretreatment sensitizes the T cell to degranulate. A) BMMNC were untreated or treated with anti-CD3/28 + IL-2 and 5ug/mL rhS100A9 together, rhS100A9 first followed by anti-CD3/28 post-24 hours, or anti-CD3/28 first followed by rhS100A9 24 hours later for four total days. Supernatant was collected for ELISA. B) PBMC were activated with anti-CD3/28 + IL-2 with or without S100A9 or S100A9 24 hours prior to anti-CD3/28 treatment. Cells were collected and stained for CD107a within the CD3+ T cell compartment by flow cytometry four days later.

We next sought to determine how this mechanism of suppression signals. S100A9 is known to signal to NF-κB. Many aspects of the T cell immune response depend on NF-κB, including signaling through the TCR, so we performed flow cytometric analysis of phosphorylation (phosflow) to examine phosphorylated NF-κB p65 (pS529). T cell activation conditions surprisingly produced a higher % of phospho NF-κB in T cells, and S100A9 blunted this phospho-NF-κB signaling through the TCR (**Fig. 28**). This was another surprising finding, as we expected S100A9 to increase the phosphorylation of NF-κB, not blunt it. S100A9, while it has been shown to signal through NF-κB, has not

been shown to signal through NF- $\kappa$ B in T cells specifically. We speculate that there is a signaling aspect of this DAMP on T cells that is different than its typical signaling on monocytes.

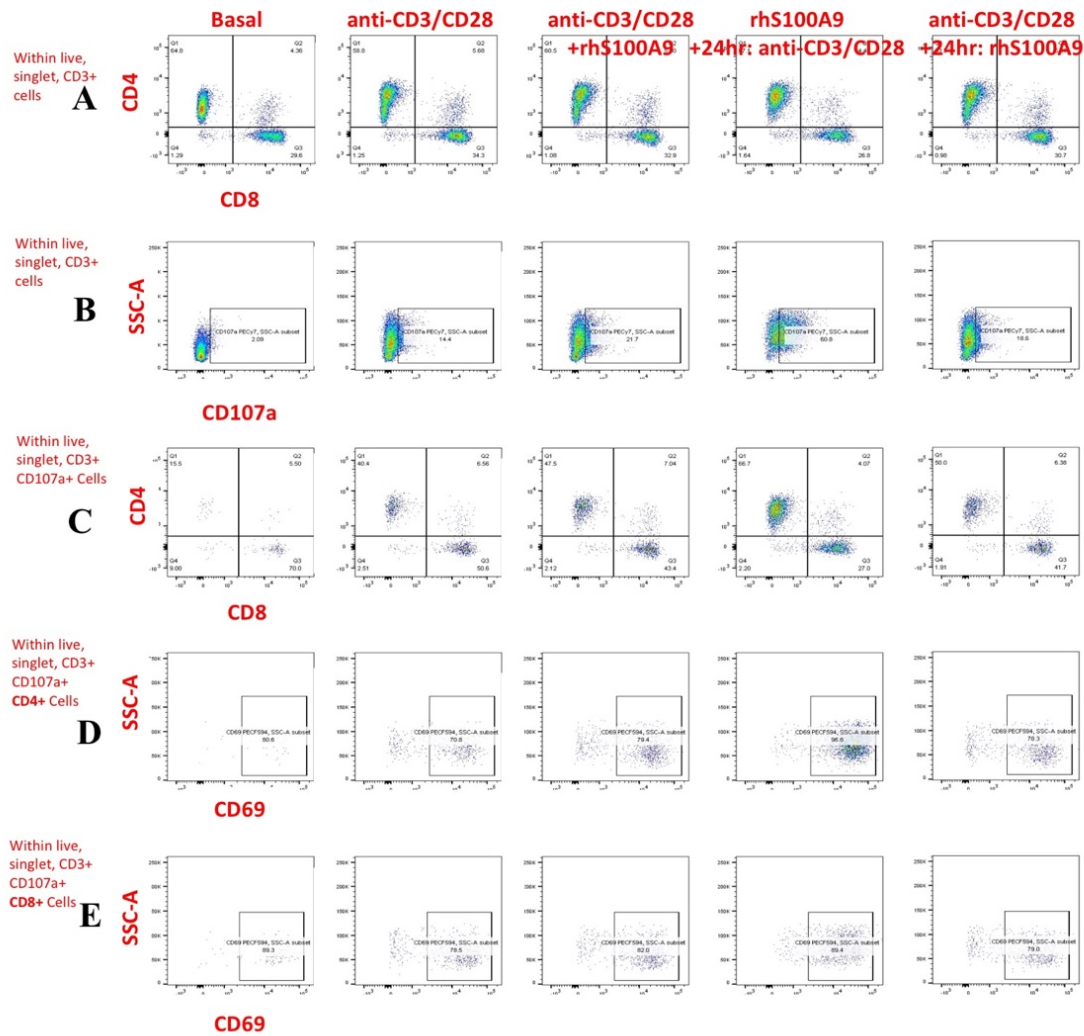


**Figure 27.** Schematic of T cell gating for degranulation. From Left to Right: Basal, anti-CD3/28 + IL-2, anti-CD3/28 + IL-2 + rhS100A9 together, rhS100A9 24 hours prior to anti-CD3/28, and anti-CD3/28 24 hours prior to rhS100A9. Treatment was performed for a total of four days prior to flow cytometry. From top to bottom: A) CD4 (y-axis) by CD8 (x-axis) within live, singlet, CD3+ T Cells. B) CD107a+ T cells within live, singlet, CD3+ T Cells. C) CD4 (y-axis) by CD8 (x-axis) within live, singlet, CD3+, CD107a+ T Cells. D) CD69+ T cells within live, singlet, CD3+ CD107a+ CD4+ T Cells. E) CD69+ T cells within live, singlet, CD3+ CD107a+ CD8+ T Cells.

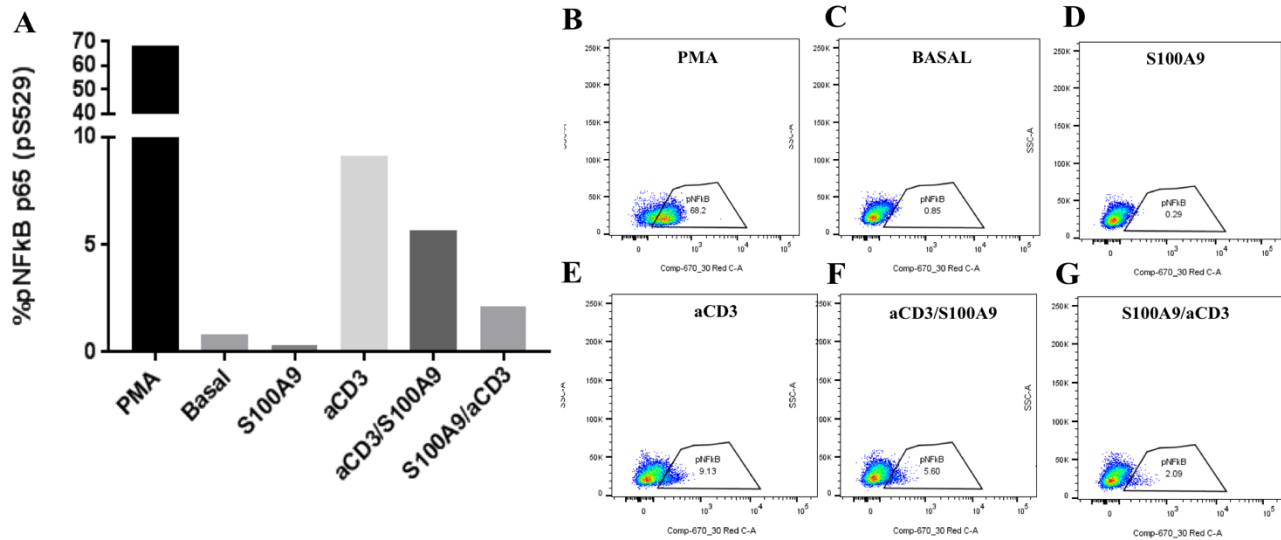


**Figure 28.** S100A9 decreases NF-κB phosphorylation through the TCR. T cells from Healthy Donor PBMC were treated for 15 minutes. A) Graphical representation of flow plots at right. B) PMA, positive control. C) Basal. D) 5ug/mL rhS100A9. E) anti-CD3/28 + IL-2. F) anti-CD3/28 + IL-2 prior to rhS100A9. G) rhS100A9 prior to anti-CD3/28 + IL-2.

## The Receptor for Advanced Glycation Endproducts (RAGE) is expressed on T cells and is activation responsive

After finding that S100A9 affects T cell proliferation, cytokine production and degranulation, we inquired as to what S100A9 could be signaling through on the T cell to mediate its effects. Receptors for S100A9 present on T cells include TLR4 and RAGE. We did not find robust expression of TLR4 on T cells unlike RAGE, and thus chose to focus on that receptor. RAGE is associated with inflammatory disease, aging and hyperglycemia, all characteristics of MDS biology.

We first investigated whether RAGE is expressed on healthy PBMCs and found that RAGE expression is high (~33%) and sharply decreases at 6 hours of activation with anti-CD3/28 + IL-2, and continues to decrease (**Fig. 29A**). RAGE is historically known to be expressed in the myeloid compartment, but we examined the CD3+ T cell



compartment and found RAGE to be bright and highly expressed (~50%), and similarly activation responsive as were total PBMCs (**Fig. 29B**). We confirmed RAGE expression by western blot in CD3+ T cells. (**Fig. 29C**). MDS PBMC displayed a similar phenomenon, whereby the % of RAGE+ T cells is high at basal levels, and decreased upon activation (**Fig. 30A**). Uniquely, though, MDS bone marrow displayed a different phenotype. HBM displayed low levels T cells that were RAGE positive, and MDS BM displayed consistently high levels of these RAGE positive T cells, regardless of disease staging (**Fig. 30B**). Given that the highest levels of S100A9 are found in the MDS Bone Marrow serum and comparatively lower levels are found in the MDS Peripheral Blood serum (Data not shown), this warranted further investigation as a potential mechanism of S100A9's effects on T cells in high concentration situations through RAGE.

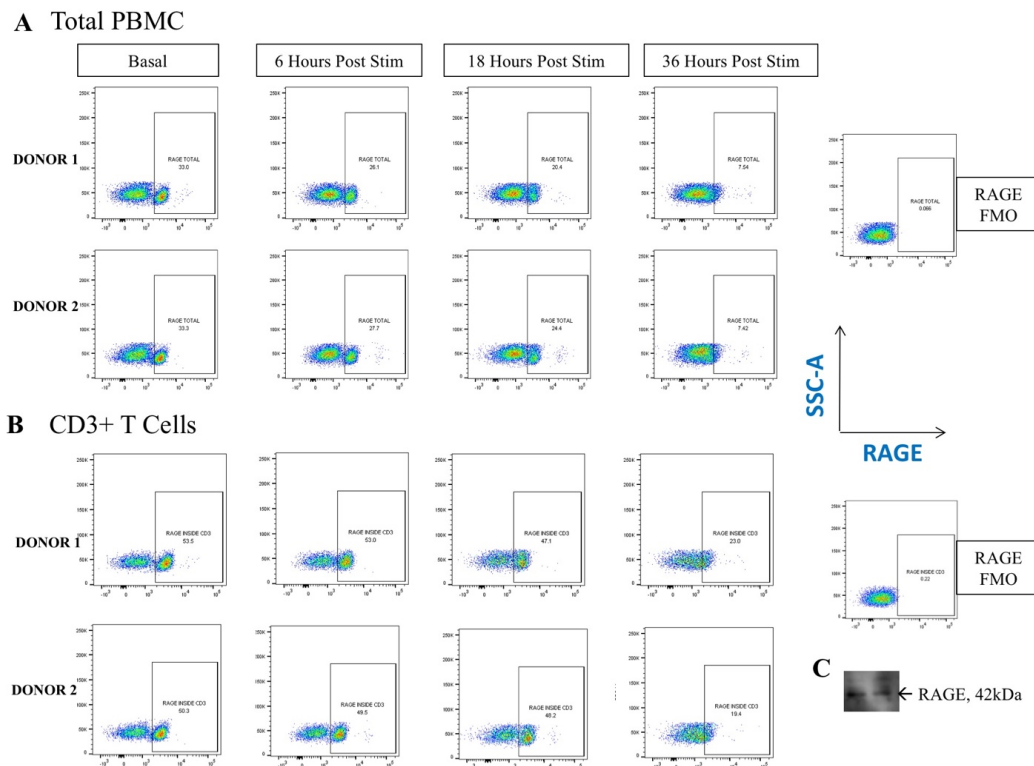


**Figure 29.** RAGE is expressed in PBMC and T cells and decreases after T cell activation. Two donor PBMC's were activated with anti-CD3/28 + IL-2. Flow for RAGE expression was performed at hour 0 and stimulation was removed at 6 hours. Flow was further performed at 6, 18 and 36 hours post-activation. FMOs are at right. A) Total PBMC. B) CD3+ T cells. C) Western Blot of two donors of basal, CD3+ T cells, blotted for anti-RAGE.

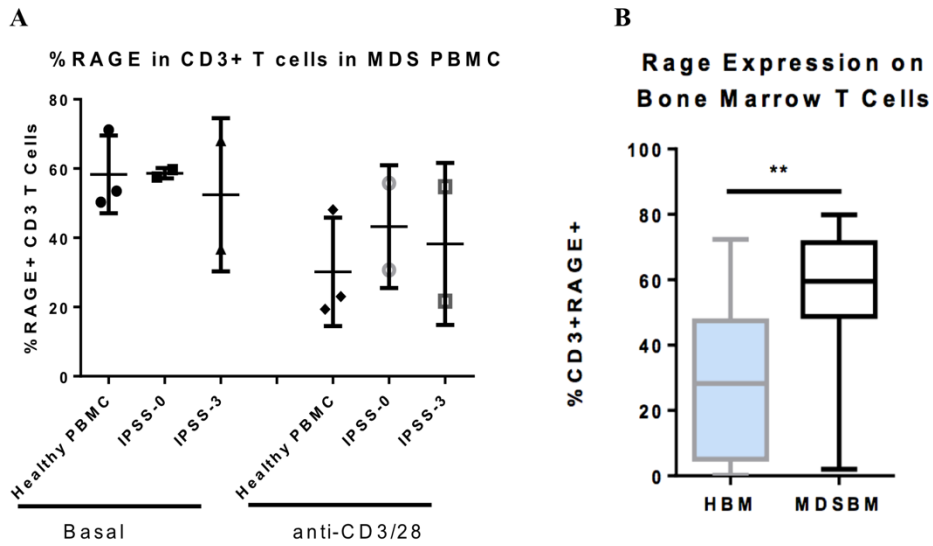


**Figure 30.** RAGE is expressed in MDS Patients. A) Donor PBMC were treated with anti-CD3/28 + IL-2 or not and analyzed for RAGE expression in healthy donor, IPSS-0 and IPSS-3 MDS patients. B) % of CD3+RAGE+ T Cells in HBM or MDS-BMMNC.

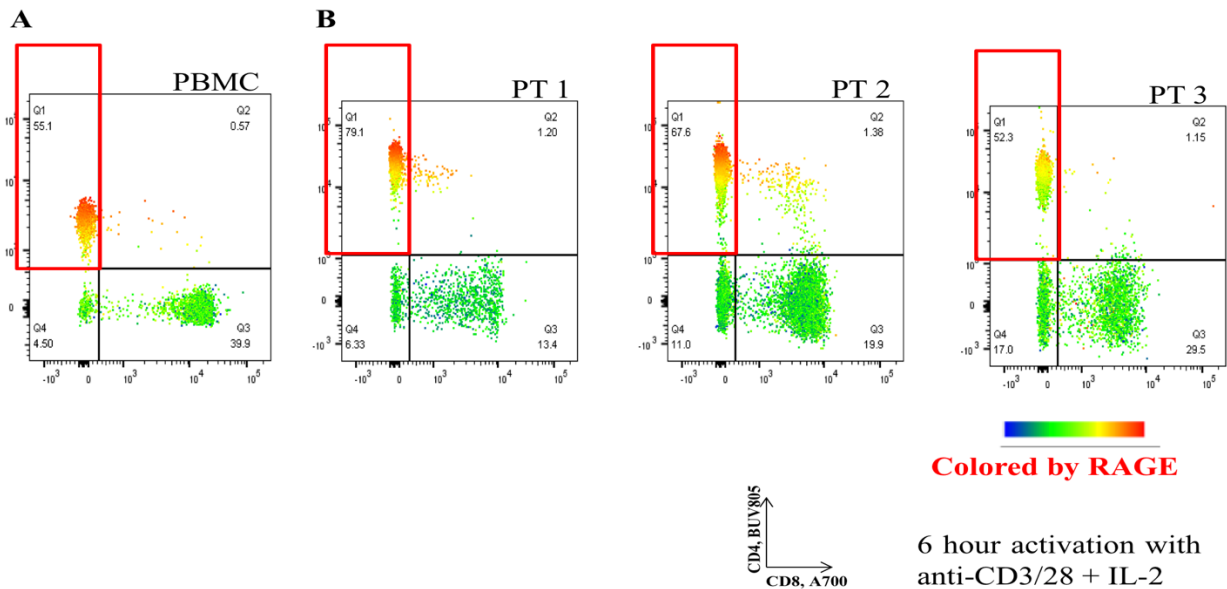


**Figure 31.** RAGE is restricted to the CD4 T Cell compartment. PBMC or MDS-BMMNC were activated for 6 hours with anti-CD3/28 + IL-2 for six hours and removed from stimulation. Upstream gating was performed on live, singlet, CD3+ T cells, and in the above, CD4 is on the Y-axis and CD8 on the X-axis. The flow plots are colored by RAGE MFI. A) Healthy Donor PBMC and B) 3 MDS-BMMNC Donors

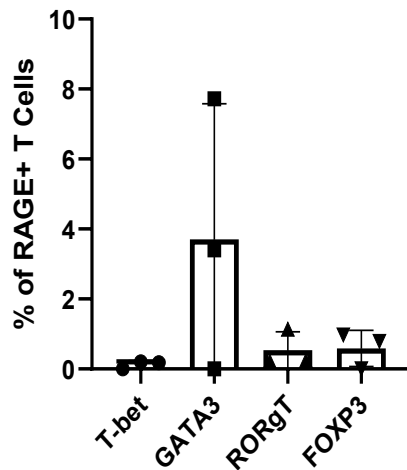


**Figure 32.** RAGE+ T Cells are Th2 polarized. Transcription factor staining was performed on isolated T cells. Live, singlet, CD3+ T cells were gated for T-bet, GATA3, RORγT and FOXP3.

Further interrogation of the phenotype of these CD3+ T cells led us to the CD4+ compartment, where the RAGE+ T cells are almost completely restricted (**Fig. 31**). In particular, they are restricted to the CD4hi median fluorescent intensity (MFI) cells. This is the same across patient BM and PBMC from both patient and healthy donor (**Fig. 31**). We found through transcription factor analysis of the bone marrow that these T cells are more of a Th2 polarized CD4 phenotype, expressing the GATA3 transcription factor, indicating the effects of any cognate RAGE ligand may be limited to the Th2 genetic program. (**Fig. 32**).

RAGE+ and RAGE- T cells were sorted from peripheral blood to high purity (**Figs. 33A-33C**). Performing cell trace violet staining as above led to the finding that the percent of RAGE+ T cells proliferating under normal activating conditions was higher in the RAGE+ population, and those RAGE+ T cells responded with a larger decrease in proliferation when treated with rhS100A9 than their RAGE- counterparts. It is important

to note that the RAGE- T cells were still suppressed by S100A9, perhaps due to its other receptors, but it was not to as extreme as a degree as those RAGE+ T cells (**Fig. 33D**).

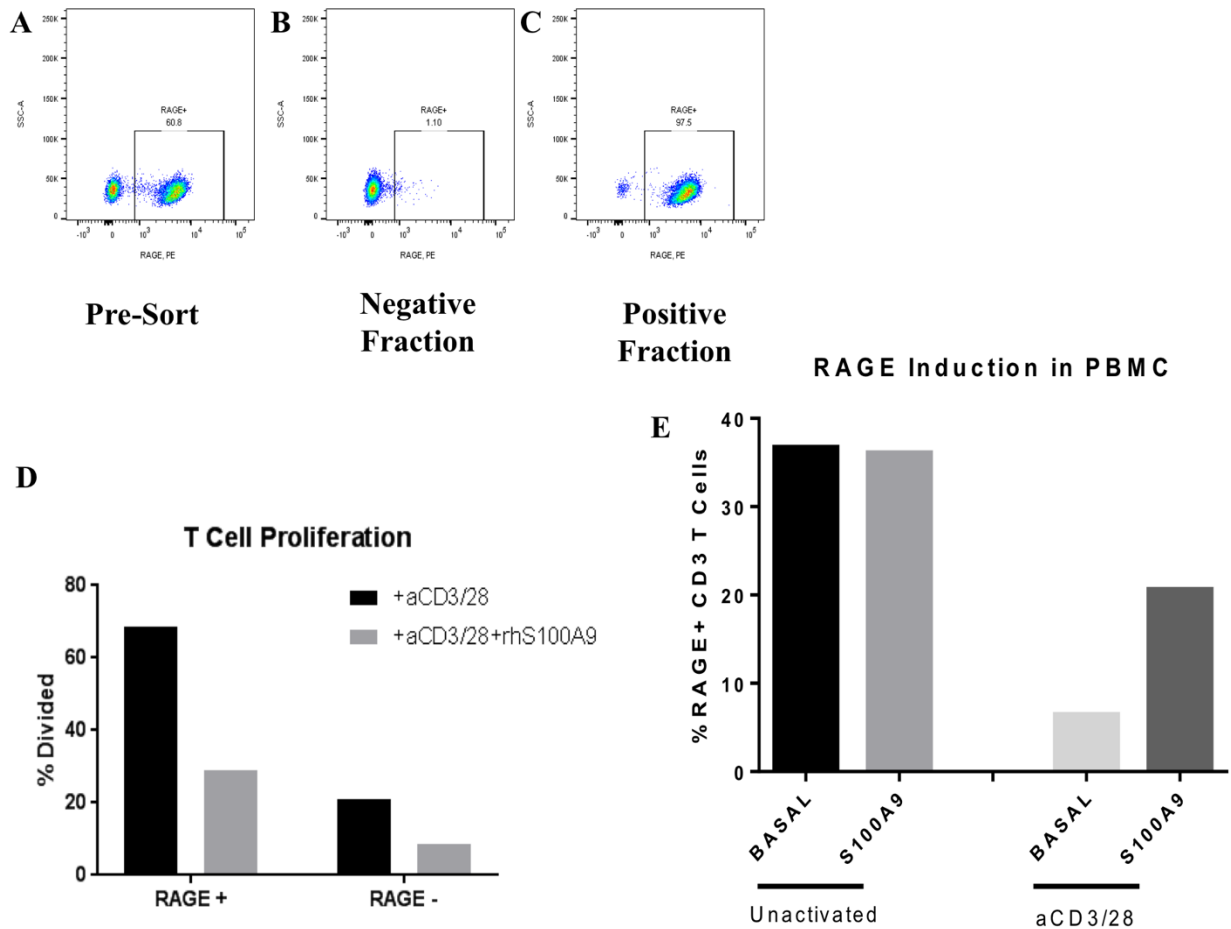


**Figure 33.** RAGE+ T cells are more proliferative and susceptible to S100A9 induced proliferative suppression. T cells were stained with RAGE-PE and sorted with anti-PE microbeads. A) Pre-sort T cell population. B) RAGE Negative T cell population. C) Pure RAGE Positive T cell population. D) % Divided T cells based on Cell Trace Violet Staining. E) Unactivated and anti-CD3/28 + IL-2 activated T cells treated or not with 5ug/mL S100A9 for 4 days and analyzed for RAGE by flow cytometry.

Both RAGE and S100A9 are known to be involved in positive-feedback loops promoting inflammation. After seeing such high levels of RAGE in MDSBM but not HBM, we asked whether S100A9 can induce RAGE expression in these T cells. In unactivated T cells, basal T cells had high RAGE, as did those treated with S100A9. Activated T cells showed a much-decreased %RAGE+ cells, and this more than doubled when S100A9 was added,

indicating a positive feedback loop (Fig. 32E). This indicates that these T cells are responsive to S100A9 treatment by upregulating RAGE which may uniquely allow them to sense more S100A9, and lead to a decrease in proliferation and inhibition of function and cytokine production. Knockdown to confirm this has been performed, and we expect to see reversal of these phenomena in future efforts. Schema below. (Fig. 34)

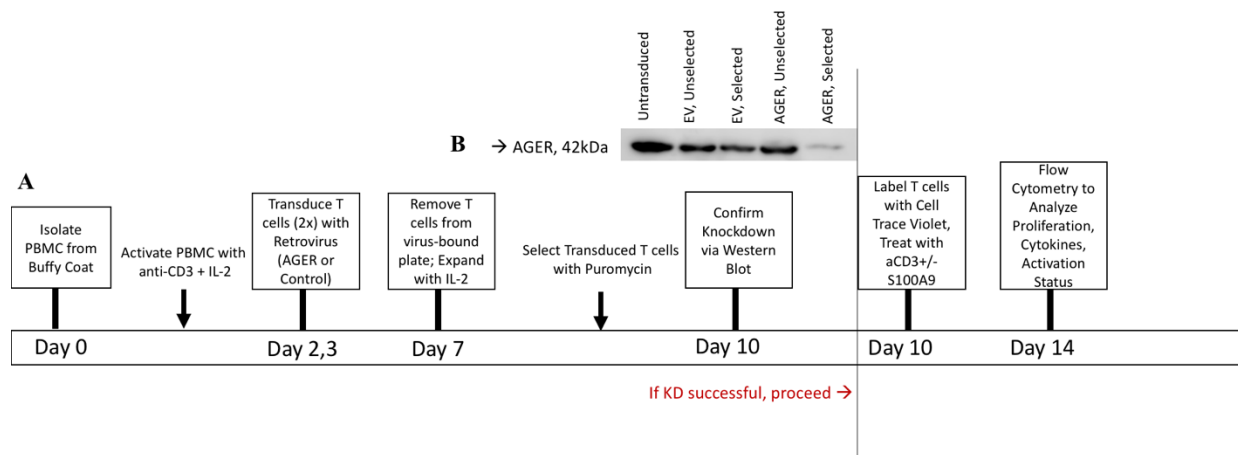


**Figure 34.** Schematic for RAGE (AGER) knockdown in T cells. A) Schematic. B) Successful knockdown of AGER gene.

## Discussion

Here we show that S100A9, a DAMP that has previously been unstudied in the context of adaptive immunity, inhibits T cell functionality. This is novel because rather than a myeloid cell-T cell interaction leading to the suppression of a T cell, it seems the myeloid produced factor is all the T cell needs to be suppressed enough to not proliferate. T cells in MDS appear to be normal in terms of their response to strong activation cues via checkpoint expression of PD-1, CTLA4, LAG-3 and TIM-3, and activation responsive gene CD69, but they differ in their expression of PRRs. The percentage of T cells is decreased in the disease and this may be due to apoptosis not induced by S100A9. The memory phenotype of MDS T cells is less polarized toward naïve and is more represented

by antigen experienced TCM, TEM and TEMRA T cells. The bone marrow is a home for long-term memory T cells, so this is partially expected, but also representative of a diseased phenotype and some sort of antigen experience throughout the T cells life. What is still unclear is whether the T cells natively have defects in proliferation inside these patient bone marrows. If antigen presentation is inhibited at all in the disease, then the T cells may not be able to receive strong stimulation through their TCR to begin with enough to show defects in proliferation. S100A9 does not induce T cell death in any way or conventional mechanisms of apoptosis. Interferon gamma is reduced in both healthy and patient samples with S100A9 indicating that this is potent enough to affect even healthy non-S100A9 conditioned cells. Preconditioning with S100A9 produces a T cell that degranulates more, and preconditioning with anti-CD3/28 + IL-2 leads to a T cell producing more IFN $\gamma$ . Additionally, S100A9 blunts phospho-NF- $\kappa$ B signaling through the TCR, and thus it may inhibit NF- $\kappa$ B target genes which are all important in the T cell immune response and thus this could be a potential mechanism for the inhibition of T cell function and cytokine production.

RAGE was found to be high on MDS PBMC and HD PBMC. Interestingly, MDS BM had high levels of RAGE expression, but HBM had much lower expression levels. The RAGE expression within the CD3+ compartment is restricted to CD4+s, particular those with the highest CD4 MFI. These CD4s, while not being the conventional cytotoxic cells, guide the immune response and shape the milieu of the bone marrow microenvironment through their cytokine production. Thus despite not directly killing the cancer cells themselves, they are an essential component of the microenvironment and cannot be overlooked in the disease. They may not fit into a specific lineage, though this

requires further study, they seem to have more of the transcription factor GATA3, indicating that they may be Th2 polarized. In the MDS BM microenvironment, this would be the expected cytokine anyway due to the IL-10, TGF $\beta$  driven exposure. We found that RAGE+ T cells are more proliferative than their RAGE- counterpart, however this may be due to the fact that RAGE+ T cells are CD4+ which are natively more proliferative than their CD8 counterparts. What is still difficult to understand is the dynamic RAGE expression and why it is high in both patient and healthy PBMC but high only in MDS BM but not HBM. It is reasonable that based on the feedback loop of RAGE expression found that S100A9 is able to drive RAGE expression, which can explain why MDS BM is higher in RAGE expression than the healthy counterparts, but this still does not explain what is occurring in the PBMC. It is possible that the dynamics of innate immunity are different in different locations, where there are different contextual cues, and the immune cells are expected to do different things.

It is not completely clear that these S100A9 induced phenomena are mediated through RAGE, however the convincing positive feedback loop and dynamic expression indicate that it is a likely binding partner. Previous studies have indicated that RAGE expression is high on T cells in inflammatory states, and we show for the first time that RAGE+ T cells are high in the inflammaging-associated disease MDS. What is still unknown is how this T cell is being shut down mechanistically, if there are different pathways affected by this S100A9/RAGE axis that are suppressive to the T cell and if these are altered in the disease or not.

In conclusion, T cells are profoundly affected by S100A9 treatment, and this may indicate how these T cells are suppressed in MDS. This mechanism of

immunosuppression offers hope in a disease that despite having many different treatment options still has poor outcomes. Targeting this axis could potentially lead to reinvigoration of the T cell compartment in the disease and better survival, leading to prevention of AML progression.

## ***Materials and methods***

### **Cell culture and reagents**

Peripheral Blood Mononuclear Cells were isolated from blood provided by healthy donors from OneBlood. All patients were recruited from the Malignant Hematology clinic at the H. Lee Moffitt Cancer Center & Research Institute. After obtaining written informed consent, patients were classified according to World Health Organization and International Prognostic Scoring System criteria. Healthy Bone Marrow Mononuclear Cells were obtained from StemExpress. Samples were diluted 2x using PBS and then isolated using Ficoll-Hypaque gradient centrifugation according to manufacturers guidelines. Red cells were lysed using Red Blood Cell Lysis Buffer (Sigma) according to manufacturers suggestions. Cells were counted and used for downstream assays without freezing.

### **T cell activation and culture**

T cells were activated with Human T-Activator Dynabeads (anti-CD3/CD28) (Invitrogen) at a 1:1 ratio. T cells were cultured in X-VIVO 15 Media (Lonza) with 300 IU IL-2 (Peprotech), 5% Human AB Serum (Access Biologicals), and 10% PSG (Gibco) **or**



RPML-1640 (Gibco) with 100 IU Human Interleukin-2, 10% Fetal Bovine Serum and 10% PSG (Gibco). T cells were treated with 5ug/mL recombinant Human S100A9 (Origene). In some experiments, fresh, autologous serum was used at 20% v/v. Bone marrow T cells were subject to Pan-T cell isolation (Miltenyi) according to manufacturers instructions.

### **Flow cytometry analysis**

All antibodies in all assays were pre-titrated prior to use according to best practices in the field. For analysis of surface receptors, 1e6 of the given sample was stained in a 7.5mm FACS tube (Falcon) with the pre-titrated concentration of antibody. Cells were washed 2x with PBS. Live/Dead staining (LD Aqua, LD Blue or LD Near Infrared, Invitrogen) was performed for 30 minutes at 4 degrees Centigrade, and washed twice with PBS. FC block was applied to the cells for 10 minutes prior to surface antigen staining. Cells were then stained with antibody cocktail alongside Brilliant Buffer Plus (BD). Cells were washed 2x with PBS and resuspended if only staining for surface antigens. For intracellular staining, cells were fixed and permeabilized using Fixation/Permeabilization Solution Kit (BD Cytotfix/Cytoperm) according to manufacturers instructions. For cytokine staining, cells were pre-treated for 6-8 hours with Golgistop (BD). Staining was performed using pre-titrated antibodies to intracellular antigens. Cells were washed 2-3x with PBS prior to acquisition on a BD LSR II SORP or BD FACS Symphony. Samples only interrogating cell surface antigens were ran fresh and not fixed. Transcription factor staining was performed using the BD Human FoxP3 Buffer Set according to manufacturers recommendation. Cell Trace Violet (Invitrogen) staining was performed according to manufacturers recommendation. Compensation was performed either with cells or

Ultracomp eBeads (Invitrogen). Consistency between experiments was tracked using 8 peak Rainbow Beads (Sphero). Data were analyzed using Flowjo Version 10 (BD) and graphed using Graphpad Prism Software Version 8. Prior to analysis, all gating upstream of the populations of interest followed the scheme: LYMPHOCYTES (FSC/SSC) → FSC SINGLETS (FSC-H/FSC-A) → SSC SINGLETS (SSC-H/SSC-A) → LIVE CELLS (SSC BY VIABILITY DYE).

### **Interferon Gamma Enzyme Linked Immunosorbent Assay**

Interferon Gamma ELISA (R&D) was performed according to manufacturers instructions. All samples and standards were ran in triplicate. Data were graphed and analyzed using Graphpad Prism Software Version 8.

### **Cytometric Bead Array**

BD Th1/Th2/Th17 CBA was performed according to manufacturers instructions and analyzed on a BD LSR II SORP. All samples and standards were ran in duplicate. Data were analyzed using Flowjo Version 10 (BD) and graphed using Graphpad Prism Software Version 8.

### **Western Blot**

Cells were lysed using RIPA (Thermo) with protease and phosphatase inhibitors (G bioscience) on ice for 30 minutes. Cell lysates were centrifuged at 13,000g for 30 minutes to remove debris. Protein concentration was determined using Bradford assay (Bio-Rad). 30ug of protein per lane was separated on 12% SDS-PAGE gels and subsequently

transferred using a Semi-Dry transfer to PVDF membranes, which were probed for anti-RAGE (Santa Cruz).

### **Virus Production and Transduction**

Short hairpin RNA (shRNA) targeting AGER (Advanced Glycation Endproduct Receptor) was purchased from Origene. This was packaged in the 293GP2 packaging system with VSV-G env protein (Takara). The retroviral supernatant was harvested and filtered using a 0.22um filter. T cells were activated for 48 hours prior to spinfection. The cells were allowed to rest for 3 days prior to downstream assay. T cells were selected using Puromycin for 3 days and knockdown was confirmed via western blot.

### **Statistical Analysis**

Data are presented as means  $\pm$  standard error of the mean. Differences between individual groups were analyzed by Student's *t*-test using Graphpad Prism version 8.3. *P* values  $\leq 0.05$  were considered statistically significant, where \* represents *p* values of  $\leq 0.05$ , \*\*  $\leq 0.01$ , and \*\*\*  $\leq 0.001$ . Significance was also confirmed with the Wilcoxon rank sum test.

## **CHAPTER FIVE: IMPLICATIONS AND FUTURE PERSPECTIVES**

Our understanding of the dynamic interplay between cancer and the immune system has greatly evolved in the past decades. Despite this, it can still be insurmountably difficult to predict the immune response to tumor. Treatments are changing, personalized medicine is evolving rapidly, and immunotherapy is coming of age, but there are still foundational basics that are not understood in terms of mechanisms of tumor induced immune suppression that lead to either innate failure of the immune system or therapeutic failure. This work focuses on the former – identifying mechanisms of tumor induced immune suppression that can lead to better therapeutics and can be capitalized upon for biomarker analysis in these patients.

Natural Killer cells and T cells are one of the power couples of the immune system, both providing highly effective effector lytic activities at earlier and later stages in the immune response, respectively, to any pathogen or transformed cell that dares to cross them. Unfortunately, they are both equally susceptible to multiple mechanisms of subversion, be it through checkpoint receptors, cytokines, or in this case, uniquely, miRs and PRRs.

NK cells, as one of the first lines of the effector response in the immune system are one of the first affected by these mechanisms employed by the tumor to subvert the immune response. Early on in the immune response, they are of the first to produce

interferon gamma and other cytokines in order to shape the subsequent effector response of the immune system. While NK cells are found within the tumor infiltrating lymphocytes, they are often those that are lacking in cytokine production and have insufficient production of lytic granules granzyme B and perforin (24). So, while they are able to infiltrate into the tumor, they may not be able to perform their effector functions. Due to their delicate response to a balance of activating and inhibitory signals, they are especially susceptible to changes in receptor/ligand interactions governed by the tumor. MICA/B, a NK2DG ligand is upregulated in multiple tumor types as well as more basic occurrences of cell stress as a mechanism to induce NK cell lytic activity via the MICAB/NKG2D axis (198-200).

TGF $\beta$  is highly overexpressed in the lung adenocarcinoma tumor microenvironment (35). TGF $\beta$  has been known for years to suppress NK cell functions, but its mechanism was largely unexplained until our group discovered that TGF $\beta$  reduces cell surface expression of NK receptors KIR2DS4 and NKp44, and abrogates expression of critical NK cell adaptor molecule DAP12. Our group found that miR-183 was sufficient to repress DAP12, but it was not known at this time if any other NK receptors or adaptor proteins were affected (35). This most current work shows that miR-183 also regulates NKG2D, making this phenomenon one that is relevant to both NK cell and activated T cell biology, given the activation responsive increase of NKG2D on both CD8 and Gamma/Delta T cells as well. MiR dysregulation has been found to affect all tumor types and most aspects of immunology as well (26, 27). It is worth exploring this pathway in other tumor types given the expression and dysregulation reported in non-immunology contexts with the role of the miR-183 family on prostate, breast and pancreatic cancers

(175, 180, 181). Our work integrates the use of lung cancer cell lines as well as primary patient samples which are extremely heterogeneous, making this a deeper analysis of this pathway than just using cell lines alone. This investigation indicates a real possibility for targeting this pathway for to increase immune surveillance and response in lung cancer.

Later work led us to study miR-155, which itself is an essential part of the immune response and is necessary for leukocyte functioning. While miR-155 expression is upregulated by inflammatory stimuli such as interferon gamma in promotion of an effector immune response, its expression is culled by conventionally suppressive cytokines like IL-10 (241, 242, 265, 266).

The first studies of this miR led to a miR-155 knockout mouse, which was characterized to have dysfunction across the B and T cell compartments (267). This miR was identified as one that is important in both homeostasis of the immune cell, but also is induced upon activation and cytokine exposure (45, 49, 242). Of the earliest targets identified of miR-155 was SHIP-1, and when miR-155 was overexpressed, SHIP-1 expression decreased (45). Since this miR is cytokine responsive, in a tumor microenvironment which may be dominated by a “cold” environment, NK cells may be more or less responsive, due to SHIP-1, downstream of inhibitory NK cell signaling.

Interestingly, we and others showed that miR-155 deficiency does not affect NK cytotoxicity despite being essential for NK cell cytokine production. In previous works, it was shown that miR-155 deficient mice lack viral-specific NK effector response compared to wildtype mouse response, and that these mice do not go on to develop NK memory at the contraction phase of the immune response. Additional targets of miR-155 affecting

NK cell function include Noxa and SOCS1, which were found to be elevated in miR-155 knockout mice similar to SHIP-1 (49). These results suggest that NK cells require miR-155 while resting and while activated, and that miR-155 effects multiple essential gene regulatory points throughout the life cycle and function of an NK cell. These all confirm the importance of the tight regulation of miR-155 levels being of the utmost importance for controlling the NK response not just to tumor, but in response to all threats, viral, tumor or otherwise. Thus, while these cells display normal cytotoxicity levels compared to wildtype NK cells in in vitro and in vivo assays, heightened SHIP-1 resulting in suboptimal antiviral response and a lack of NK memory may represent a form of immune suppression (49).

The current novelty presented here focuses on impairments in chemotaxis. SHIP-1 has been reported to negatively regulate PI3K signaling by hydrolyzing the mediators necessary for actin mobilization. SHIP-1 leads to loss of these mediators, and thus directly affects chemotaxis (254). In our work, we found less F-actin at the leading edge of the NK cells lacking miR-155, indicating impairments in actin polymerization, which is necessary for chemotaxis. CCL2 is a chemokine that is highly expressed in tumors (252). In the absence of miR-155, these knockout NK cells had comparable receptor expression of CCR2, but were not able to traffic into the CCL2+ tumor beds. Of course, trafficking is never as simple as a single chemokine axis, however it was compelling to see normal trafficking in the wildtype models. While the CCL2/CCR2 axis was chosen based on its expression levels in the chosen tumor model, other chemokines may be involved and affected. We found that blocking SHIP-1 rescued the chemotaxis of these cells, and in other works this has been shown to increase apoptosis of cancer cells. There are however

considerable risks with targeting SHIP-1 due to its myriad roles and regulatory processes. Regardless, SHIP-1 inhibitors 3AC and K190 have been investigated and led to less efficient immune responses which may be beneficial depending on the disease, but in other cases lead to activation induced cell death of the tumor cell (254, 268). Like many things in immunobiology, there exists a goldilocks zone of ideal activation versus inhibition. In situations such as hematopoietic malignancy where NK cells are too inflammatory, miR-155 expression dynamics may represent a unique mechanism by which NK cells can be shut down, and may be ideal in the bone marrow transplant field (251, 269). By upregulating SHIP-1, the NK cell is inhibited and is unable to produce sufficient cytokine to induce an immune response. Overwhelmingly, the key finding is that miR-155 can directly affect NK cell chemotaxis secondary to defects in actin polymerization, and that this may be targeted therapeutically, but it may be at the risk of the NK cell. Through the years, miR-155 has truly come of age as a potent regulator of both NK cells and T cells, but this represents the first investigating into actin polymerization and chemotaxis therein.

Therapies to target miR dysregulation are complex and lack extensive in vivo efficacy and safety testing. It is a well established lab procedure to block miRs in vitro by using complimentary oligonucleotides, but in vivo mechanisms are still being studied. Perhaps what is more relevant in the case of the miR-183 story is blocking TGF $\beta$  signaling. TGF $\beta$  can be blocked in vivo with small molecule inhibitors or antibodies to great antitumor effect, which could be relevant in this case and more simple than attempting to manipulate miRs (270). Regardless, this mechanism of basic immunology that we found to affect lung cancer has consequences translationally, and will be useful



for the development of further therapies. Dynamics of cytokine expression control the miR-155 story more, and thus controlling expression of this miR via cytokine exposure may be an option, as blocking this miR would not likely prove beneficial.

MDS immunobiology is complex and largely untouched outside of the context of myeloid cells. This is understandable given the location of the somatic mutations and the fact that the malignant clone does not often affect the lymphoid compartment. Here we show that there are mechanisms of T cell suppression that exist outside of the MDSC-T cell interaction studied almost exclusively in the disease. Our group has shown that S100A9 is overexpressed in the serum of MDS patients, particularly at the early stages of the disease (70). Previous work by our collaborators showed that T cells dynamically change with disease progression. The T regulatory compartment was studied and there was found to be a change from central memory Treg to effector memory Treg. By this point the equilibrium phase of immunoediting has past and the myeloblasts have accumulated to the point of immune escape and Treg expansion (61, 62). Since S100A9 has been seen to be higher in early disease stages but not late, it is possible that this DAMP affects T cell function at earlier stages, but by the point the disease has progressed past equilibrium, the S100A9/T cell interaction is a null point. Since one of the most important things to do is prevent disease progression, this is an exciting mechanism that is possibly more useful for early-stage disease. The hypothesis that this mechanism of T cell suppression could be allowing the malignant clone to grow unchecked later in the disease is compelling, but more work is needed.

Of the most unique findings of this story is the suppression of proliferation by S100A9. It is still incompletely understood as to why this DAMP, which for all intents

should promote an immune response, would be shutting down normal responses to T cell activation. Still, there is consideration that in vivo this may not occur given the number of positive activating signals a T cell would receive in addition to stimulation through the TCR, costimulation and cytokine in a healthy person, with a normal immune response. This does provide basic biologic insight both dependent and independent of activation. Cancer, however, changes the game in regard to all of these factors. Insight into the dynamics of T cell dysfunction provided by S100A9 was provided through the experiments that showed that T cells are sensitized to S100A9 if and only if the S100A9 is provided prior to stimulation through the TCR. It is not clear whether in MDS TCR stimulation is of sufficient strength to overcome all of the negative stimuli provided such as S100A9 in this case, especially when there are other immunosuppressive factors at play such as excessive TGF $\beta$  and IL-10, however these T cells ex vivo from the patients are absolutely not responsive to S100A9 prior to strong anti-CD3 activation coupled with cytokine. This is coupled with the unique finding of high levels of degranulation (CD107a+ cells) induced by S100A9 pretreatment only. The genetic programs endowed by S100A9 that lead to increased production of cytotoxic granules, but similarly less interferon gamma production seem to be at odds with one another, and the importance of further interrogating the transcriptome of these T cells responding to DAMPs in general cannot be understated. There are complexities of CD4 T cells that are just being touched upon, and it is important to think outside of the box in both basic immunobiology and in situations of this very complex disease.

RAGE expression on T cells is a novelty that has not been extensively explored outside of the context of diabetes (157-160). This work represents a first of its kind

exploration into the role of marrow infiltrating lymphocytes being suppressed by factors that should normally be immune-response promoting. Chapter 4 in particular lays the foundation for multiple therapies to be capitalized upon. This work has opened the door to more unanswered questions that include why the RAGE expression is so dynamic between blood and bone marrow, and whether or not it is enough to be used as a prognostic marker in the disease. RAGE inhibitors are being utilized in clinical trials to varying efficacy (Clinical Trial: NCT02080364 for TTP488 was terminated due to lack of efficacy) (271, 272), however it is unclear whether they specifically block the region of this complex binding PRR where S100A9 binds, or if they specifically just block the region in which advanced glycation endproducts and amyloid beta plaques bind. Development of a RAGE inhibitor that conformationally binds at the S100A9-binding site is thus crucial. Alternatives are the developments of S100A9 neutralizing antibodies for clinical use. This would perhaps be a broader spectrum approach for multiple malignancies since S100A9 is implicated in various pathologies.

The work reported here lays the groundwork for future studies of basic and translational immunology in a disease where this arm of the immune system is virtually untouched outside of the realm of therapeutics. Although adoptive cell therapies are at the forefront of everyone's mind, it is still of great importance to consider ways to reinvigorate the autologous immune system, since the only real curative therapy is allogeneic bone marrow transplant, a therapy which is high-risk, high-reward.

## References:

1. Abel AM, Yang C, Thakar MS, Malarkannan S. Natural Killer Cells: Development, Maturation, and Clinical Utilization. *Front Immunol.* 2018;9:1869. Epub 2018/08/29. doi: 10.3389/fimmu.2018.01869. PubMed PMID: 30150991; PMCID: PMC6099181.
2. Long EO, Kim HS, Liu D, Peterson ME, Rajagopalan S. Controlling natural killer cell responses: integration of signals for activation and inhibition. *Annu Rev Immunol.* 2013;31:227-58. Epub 2013/03/23. doi: 10.1146/annurev-immunol-020711-075005. PubMed PMID: 23516982; PMCID: PMC3868343.
3. Godfrey DI, Hammond KJ, Poulton LD, Smyth MJ, Baxter AG. NKT cells: facts, functions and fallacies. *Immunol Today.* 2000;21(11):573-83. Epub 2000/11/30. doi: 10.1016/s0167-5699(00)01735-7. PubMed PMID: 11094262.
4. Hu Z, Gu W, Wei Y, Liu G, Wu S, Liu T. NKT Cells in Mice Originate from Cytoplasmic CD3-Positive, CD4(-)CD8(-) Double-Negative Thymocytes that Express CD44 and IL-7Ralpha. *Scientific reports.* 2019;9(1):1874. Epub 2019/02/14. doi: 10.1038/s41598-018-37811-0. PubMed PMID: 30755654; PMCID: PMC6372634.
5. Poli A, Michel T, Theresine M, Andres E, Hentges F, Zimmer J. CD56bright natural killer (NK) cells: an important NK cell subset. *Immunology.* 2009;126(4):458-65. Epub 2009/03/13. doi: 10.1111/j.1365-2567.2008.03027.x. PubMed PMID: 19278419; PMCID: PMC2673358.
6. Melsen JE, Lugthart G, Lankester AC, Schilham MW. Human Circulating and Tissue-Resident CD56(bright) Natural Killer Cell Populations. *Front Immunol.* 2016;7:262. Epub 2016/07/23. doi: 10.3389/fimmu.2016.00262. PubMed PMID: 27446091; PMCID: PMC4927633.
7. Schmiedel D, Mandelboim O. NKG2D Ligands-Critical Targets for Cancer Immune Escape and Therapy. *Front Immunol.* 2018;9:2040. Epub 2018/09/27. doi: 10.3389/fimmu.2018.02040. PubMed PMID: 30254634; PMCID: PMC6141707.
8. Long EO, Rajagopalan S. Stress signals activate natural killer cells. *J Exp Med.* 2002;196(11):1399-402. Epub 2002/12/04. doi: 10.1084/jem.20021747. PubMed PMID: 12461075; PMCID: PMC2194264.
9. Chan CJ, Smyth MJ, Martinet L. Molecular mechanisms of natural killer cell activation in response to cellular stress. *Cell Death Differ.* 2014;21(1):5-14. Epub 2013/04/13. doi: 10.1038/cdd.2013.26. PubMed PMID: 23579243; PMCID: PMC3857624.
10. Topham NJ, Hewitt EW. Natural killer cell cytotoxicity: how do they pull the trigger? *Immunology.* 2009;128(1):7-15. Epub 2009/08/20. doi: 10.1111/j.1365-2567.2009.03123.x. PubMed PMID: 19689731; PMCID: PMC2747134.
11. Paul S, Lal G. The Molecular Mechanism of Natural Killer Cells Function and Its Importance in Cancer Immunotherapy. *Front Immunol.* 2017;8:1124. Epub 2017/09/29. doi: 10.3389/fimmu.2017.01124. PubMed PMID: 28955340; PMCID: PMC5601256.
12. Fauriat C, Long EO, Ljunggren HG, Bryceson YT. Regulation of human NK-cell cytokine and chemokine production by target cell recognition. *Blood.* 2010;115(11):2167-76. Epub

2009/12/08. doi: 10.1182/blood-2009-08-238469. PubMed PMID: 19965656; PMCID: PMC2844017.

13. Fehniger TA, Shah MH, Turner MJ, VanDeusen JB, Whitman SP, Cooper MA, Suzuki K, Wechsler M, Goodsaid F, Caligiuri MA. Differential cytokine and chemokine gene expression by human NK cells following activation with IL-18 or IL-15 in combination with IL-12: implications for the innate immune response. *Journal of immunology*. 1999;162(8):4511-20. Epub 1999/04/14. PubMed PMID: 10201989.

14. Crouse J, Xu HC, Lang PA, Oxenius A. NK cells regulating T cell responses: mechanisms and outcome. *Trends Immunol*. 2015;36(1):49-58. Epub 2014/11/30. doi: 10.1016/j.it.2014.11.001. PubMed PMID: 25432489.

15. Pallmer K, Oxenius A. Recognition and Regulation of T Cells by NK Cells. *Front Immunol*. 2016;7:251. Epub 2016/07/23. doi: 10.3389/fimmu.2016.00251. PubMed PMID: 27446081; PMCID: PMC4919350.

16. Sun H, Sun C. The Rise of NK Cell Checkpoints as Promising Therapeutic Targets in Cancer Immunotherapy. *Front Immunol*. 2019;10:2354. Epub 2019/11/05. doi: 10.3389/fimmu.2019.02354. PubMed PMID: 31681269; PMCID: PMC6812684.

17. Stojanovic A, Cerwenka A. Checkpoint inhibition: NK cells enter the scene. *Nat Immunol*. 2018;19(7):650-2. Epub 2018/06/20. doi: 10.1038/s41590-018-0142-y. PubMed PMID: 29915295.

18. Souza-Fonseca-Guimaraes F, Cursons J, Huntington ND. The Emergence of Natural Killer Cells as a Major Target in Cancer Immunotherapy. *Trends Immunol*. 2019;40(2):142-58. Epub 2019/01/15. doi: 10.1016/j.it.2018.12.003. PubMed PMID: 30639050.

19. Hsu J, Hodgins JJ, Marathe M, Nicolai CJ, Bourgeois-Daigneault MC, Trevino TN, Azimi CS, Scheer AK, Randolph HE, Thompson TW, Zhang L, Iannello A, Mathur N, Jardine KE, Kirn GA, Bell JC, McBurney MW, Raulet DH, Ardolino M. Contribution of NK cells to immunotherapy mediated by PD-1/PD-L1 blockade. *The Journal of clinical investigation*. 2018;128(10):4654-68. Epub 2018/09/11. doi: 10.1172/JCI99317. PubMed PMID: 30198904; PMCID: PMC6159991.

20. Mule JJ, Shu S, Rosenberg SA. The anti-tumor efficacy of lymphokine-activated killer cells and recombinant interleukin 2 in vivo. *Journal of immunology*. 1985;135(1):646-52. Epub 1985/07/01. PubMed PMID: 3889158.

21. Rosenberg SA, Mule JJ. Immunotherapy of cancer with lymphokine-activated killer cells and recombinant interleukin-2. *Surgery*. 1985;98(3):437-44. Epub 1985/09/01. PubMed PMID: 3898451.

22. Burger MC, Zhang C, Harter PN, Romanski A, Strassheimer F, Senft C, Tonn T, Steinbach JP, Wels WS. CAR-Engineered NK Cells for the Treatment of Glioblastoma: Turning Innate Effectors Into Precision Tools for Cancer Immunotherapy. *Front Immunol*. 2019;10:2683. Epub 2019/12/05. doi: 10.3389/fimmu.2019.02683. PubMed PMID: 31798595; PMCID: PMC6868035.

23. Hu Y, Tian ZG, Zhang C. Chimeric antigen receptor (CAR)-transduced natural killer cells in tumor immunotherapy. *Acta Pharmacol Sin*. 2018;39(2):167-76. Epub 2017/09/08. doi: 10.1038/aps.2017.125. PubMed PMID: 28880014; PMCID: PMC5800464.

24. Levi I, Amsalem H, Nissan A, Darash-Yahana M, Peretz T, Mandelboim O, Rachmilewitz J. Characterization of tumor infiltrating natural killer cell subset. *Oncotarget*. 2015;6(15):13835-43.

Epub 2015/06/17. doi: 10.18632/oncotarget.3453. PubMed PMID: 26079948; PMCID: PMC4537053.

25. O'Brien J, Hayder H, Zayed Y, Peng C. Overview of MicroRNA Biogenesis, Mechanisms of Actions, and Circulation. *Front Endocrinol (Lausanne)*. 2018;9:402. Epub 2018/08/21. doi: 10.3389/fendo.2018.00402. PubMed PMID: 30123182; PMCID: PMC6085463.

26. Iorio MV, Croce CM. MicroRNA dysregulation in cancer: diagnostics, monitoring and therapeutics. A comprehensive review. *EMBO molecular medicine*. 2012;4(3):143-59. doi: 10.1002/emmm.201100209. PubMed PMID: 22351564; PMCID: 3376845.

27. Frixa T, Donzelli S, Blandino G. Oncogenic MicroRNAs: Key Players in Malignant Transformation. *Cancers (Basel)*. 2015;7(4):2466-85. Epub 2015/12/24. doi: 10.3390/cancers7040904. PubMed PMID: 26694467; PMCID: PMC4695904.

28. Wang Y, Luo J, Zhang H, Lu J. microRNAs in the Same Clusters Evolve to Coordinately Regulate Functionally Related Genes. *Mol Biol Evol*. 2016;33(9):2232-47. Epub 2016/05/18. doi: 10.1093/molbev/msw089. PubMed PMID: 27189568; PMCID: PMC4989102.

29. Zhang XL, Pan SH, Yan JJ, Xu G. The prognostic value of microRNA-183 in human cancers: A meta-analysis. *Medicine (Baltimore)*. 2018;97(26):e11213. Epub 2018/06/29. doi: 10.1097/MD.00000000000011213. PubMed PMID: 29952976; PMCID: PMC6039630.

30. Yuan D, Li K, Zhu K, Yan R, Dang C. Plasma miR-183 predicts recurrence and prognosis in patients with colorectal cancer. *Cancer Biol Ther*. 2015;16(2):268-75. Epub 2015/01/30. doi: 10.1080/15384047.2014.1002327. PubMed PMID: 25629978; PMCID: PMC4622949.

31. Yang CL, Zheng XL, Ye K, Ge H, Sun YN, Lu YF, Fan QX. MicroRNA-183 Acts as a Tumor Suppressor in Human Non-Small Cell Lung Cancer by Down-Regulating MTA1. *Cell Physiol Biochem*. 2018;46(1):93-106. Epub 2018/03/28. doi: 10.1159/000488412. PubMed PMID: 29587281.

32. Ma Y, Liang AJ, Fan YP, Huang YR, Zhao XM, Sun Y, Chen XF. Dysregulation and functional roles of miR-183-96-182 cluster in cancer cell proliferation, invasion and metastasis. *Oncotarget*. 2016;7(27):42805-25. doi: 10.18632/oncotarget.8715. PubMed PMID: 27081087; PMCID: 5173173.

33. Derynck R, Akhurst RJ, Balmain A. TGF-beta signaling in tumor suppression and cancer progression. *Nat Genet*. 2001;29(2):117-29. Epub 2001/10/05. doi: 10.1038/ng1001-117. PubMed PMID: 11586292.

34. Suzuki HI. MicroRNA Control of TGF-beta Signaling. *Int J Mol Sci*. 2018;19(7). Epub 2018/07/01. doi: 10.3390/ijms19071901. PubMed PMID: 29958433; PMCID: PMC6073626.

35. Donatelli SS, Zhou JM, Gilvary DL, Eksioğlu EA, Chen X, Cress WD, Haura EB, Schabath MB, Coppola D, Wei S, Djeu JY. TGF-beta-inducible microRNA-183 silences tumor-associated natural killer cells. *Proceedings of the National Academy of Sciences of the United States of America*. 2014;111(11):4203-8. doi: 10.1073/pnas.1319269111. PubMed PMID: 24586048; PMCID: 3964044.

36. Mahesh G, Biswas R. MicroRNA-155: A Master Regulator of Inflammation. *J Interferon Cytokine Res*. 2019;39(6):321-30. Epub 2019/04/19. doi: 10.1089/jir.2018.0155. PubMed PMID: 30998423; PMCID: PMC6591773.

37. Tili E, Croce CM, Michaille JJ. miR-155: on the crosstalk between inflammation and cancer. *Int Rev Immunol.* 2009;28(5):264-84. Epub 2009/10/09. doi: 10.1080/08830180903093796. PubMed PMID: 19811312.
38. Papageorgiou SG, Kontos CK, Diamantopoulos MA, Bouchla A, Glezou E, Bazani E, Pappa V, Scorilas A. MicroRNA-155-5p Overexpression in Peripheral Blood Mononuclear Cells of Chronic Lymphocytic Leukemia Patients Is a Novel, Independent Molecular Biomarker of Poor Prognosis. *Dis Markers.* 2017;2017:2046545. Epub 2018/02/22. doi: 10.1155/2017/2046545. PubMed PMID: 29463948; PMCID: PMC5804407.
39. Narayan N, Bracken CP, Ekert PG. MicroRNA-155 expression and function in AML: An evolving paradigm. *Exp Hematol.* 2018;62:1-6. Epub 2018/03/31. doi: 10.1016/j.exphem.2018.03.007. PubMed PMID: 29601851.
40. Bayraktar R, Van Roosbroeck K. miR-155 in cancer drug resistance and as target for miRNA-based therapeutics. *Cancer Metastasis Rev.* 2018;37(1):33-44. Epub 2017/12/29. doi: 10.1007/s10555-017-9724-7. PubMed PMID: 29282605.
41. Mattiske S, Suetani RJ, Neilsen PM, Callen DF. The oncogenic role of miR-155 in breast cancer. *Cancer Epidemiol Biomarkers Prev.* 2012;21(8):1236-43. Epub 2012/06/28. doi: 10.1158/1055-9965.EPI-12-0173. PubMed PMID: 22736789.
42. Zheng Z, Sun R, Zhao HJ, Fu D, Zhong HJ, Weng XQ, Qu B, Zhao Y, Wang L, Zhao WL. MiR155 sensitized B-lymphoma cells to anti-PD-L1 antibody via PD-1/PD-L1-mediated lymphoma cell interaction with CD8+T cells. *Mol Cancer.* 2019;18(1):54. Epub 2019/03/31. doi: 10.1186/s12943-019-0977-3. PubMed PMID: 30925928; PMCID: PMC6441197.
43. Banh C, Miah SM, Kerr WG, Brossay L. Mouse natural killer cell development and maturation are differentially regulated by SHIP-1. *Blood.* 2012;120(23):4583-90. Epub 2012/10/05. doi: 10.1182/blood-2012-04-425009. PubMed PMID: 23034281; PMCID: PMC3512235.
44. O'Connell RM, Chaudhuri AA, Rao DS, Baltimore D. Inositol phosphatase SHIP1 is a primary target of miR-155. *Proceedings of the National Academy of Sciences of the United States of America.* 2009;106(17):7113-8. Epub 2009/04/11. doi: 0902636106 [pii] 10.1073/pnas.0902636106. PubMed PMID: 19359473; PMCID: 2678424.
45. Trotta R, Chen L, Costinean S, Josyula S, Mundy-Bosse BL, Ciarlariello D, Mao C, Briercheck EL, McConnell KK, Mishra A, Yu L, Croce CM, Caligiuri MA. Overexpression of miR-155 causes expansion, arrest in terminal differentiation and functional activation of mouse natural killer cells. *Blood.* 2013;121(16):3126-34. Epub 2013/02/21. doi: 10.1182/blood-2012-12-467597. PubMed PMID: 23422749; PMCID: PMC3630828.
46. Dudda JC, Salaun B, Ji Y, Palmer DC, Monnot GC, Merck E, Boudousquie C, Utzschneider DT, Escobar TM, Perret R, Muljo SA, Hebeisen M, Rufer N, Zehn D, Donda A, Restifo NP, Held W, Gattinoni L, Romero P. MicroRNA-155 is required for effector CD8+ T cell responses to virus infection and cancer. *Immunity.* 2013;38(4):742-53. Epub 2013/04/23. doi: 10.1016/j.immuni.2012.12.006. PubMed PMID: 23601686; PMCID: PMC3788592.
47. Tsai CY, Allie SR, Zhang W, Usherwood EJ. MicroRNA miR-155 affects antiviral effector and effector Memory CD8 T cell differentiation. *Journal of virology.* 2013;87(4):2348-51. Epub 2012/12/12. doi: 10.1128/JVI.01742-12. PubMed PMID: 23221547; PMCID: PMC3571487.

48. Gracias DT, Stelekati E, Hope JL, Boesteanu AC, Doering TA, Norton J, Mueller YM, Fraietta JA, Wherry EJ, Turner M, Katsikis PD. The microRNA miR-155 controls CD8(+) T cell responses by regulating interferon signaling. *Nat Immunol.* 2013;14(6):593-602. Epub 2013/04/23. doi: 10.1038/ni.2576. PubMed PMID: 23603793; PMCID: PMC3664306.
49. Zawislak CL, Beaulieu AM, Loeb GB, Karo J, Canner D, Bezman NA, Lanier LL, Rudensky AY, Sun JC. Stage-specific regulation of natural killer cell homeostasis and response against viral infection by microRNA-155. *Proceedings of the National Academy of Sciences of the United States of America.* 2013;110(17):6967-72. Epub 2013/04/11. doi: 10.1073/pnas.1304410110. PubMed PMID: 23572582; PMCID: PMC3637707.
50. Sullivan RP, Fogel LA, Leong JW, Schneider SE, Wong R, Romee R, Thai TH, Sexl V, Matkovich SJ, Dorn GW, 2nd, French AR, Fehniger TA. MicroRNA-155 tunes both the threshold and extent of NK cell activation via targeting of multiple signaling pathways. *Journal of immunology.* 2013;191(12):5904-13. Epub 2013/11/15. doi: 10.4049/jimmunol.1301950. PubMed PMID: 24227772; PMCID: PMC3863634.
51. Mohammad AA. Myelodysplastic syndrome from theoretical review to clinical application view. *Oncol Rev.* 2018;12(2):397. Epub 2019/01/05. doi: 10.4081/oncol.2018.397. PubMed PMID: 30607219; PMCID: PMC6291758.
52. Cogle CR. Incidence and Burden of the Myelodysplastic Syndromes. *Curr Hematol Malig Rep.* 2015;10(3):272-81. Epub 2015/07/03. doi: 10.1007/s11899-015-0269-y. PubMed PMID: 26134527; PMCID: PMC4553145.
53. Ma X. Epidemiology of myelodysplastic syndromes. *Am J Med.* 2012;125(7 Suppl):S2-5. Epub 2012/06/29. doi: 10.1016/j.amjmed.2012.04.014. PubMed PMID: 22735748; PMCID: PMC3394456.
54. Nazha A, Bejar R. Molecular Data and the IPSS-R: How Mutational Burden Can Affect Prognostication in MDS. *Curr Hematol Malig Rep.* 2017;12(5):461-7. Epub 2017/08/28. doi: 10.1007/s11899-017-0407-9. PubMed PMID: 28844082.
55. Nazha A. Does mutational burden add to other prognostic factors in MDS? *Best Pract Res Clin Haematol.* 2019;32(4):101098. Epub 2019/11/30. doi: 10.1016/j.beha.2019.101098. PubMed PMID: 31779975.
56. Singhal D, Wee LYA, Kutyna MM, Chhetri R, Geoghegan J, Schreiber AW, Feng J, Wang PP, Babic M, Parker WT, Hiwase S, Edwards S, Moore S, Branford S, Kuzmanovic T, Singhal N, Gowda R, Brown AL, Arts P, To LB, Bardy PG, Lewis ID, D'Andrea RJ, Maciejewski JP, Scott HS, Hahn CN, Hiwase DK. The mutational burden of therapy-related myeloid neoplasms is similar to primary myelodysplastic syndrome but has a distinctive distribution. *Leukemia.* 2019;33(12):2842-53. Epub 2019/05/16. doi: 10.1038/s41375-019-0479-8. PubMed PMID: 31089247.
57. Chung SS, Park CY. Aging, hematopoiesis, and the myelodysplastic syndromes. *Blood Adv.* 2017;1(26):2572-8. Epub 2018/01/04. doi: 10.1182/bloodadvances.2017009852. PubMed PMID: 29296910; PMCID: PMC5728633 interests. Off-label drug use: None disclosed.
58. Kovtonyuk LV, Fritsch K, Feng X, Manz MG, Takizawa H. Inflamm-Aging of Hematopoiesis, Hematopoietic Stem Cells, and the Bone Marrow Microenvironment. *Front Immunol.* 2016;7:502. Epub 2016/11/30. doi: 10.3389/fimmu.2016.00502. PubMed PMID: 27895645; PMCID: PMC5107568.



59. Kittang AO, Kordasti S, Sand KE, Costantini B, Kramer AM, Perezabellan P, Seidl T, Rye KP, Hagen KM, Kulasekararaj A, Bruserud O, Mufti GJ. Expansion of myeloid derived suppressor cells correlates with number of T regulatory cells and disease progression in myelodysplastic syndrome. *Oncoimmunology*. 2016;5(2):e1062208. Epub 2016/04/09. doi: 10.1080/2162402X.2015.1062208. PubMed PMID: 27057428; PMCID: PMC4801428.
60. Chen X, Eksioglu EA, Zhou J, Zhang L, Djeu J, Fortenbery N, Epling-Burnette P, Van Bijnen S, Dolstra H, Cannon J, Youn JI, Donatelli SS, Qin D, De Witte T, Tao J, Wang H, Cheng P, Gabrilovich DI, List A, Wei S. Induction of myelodysplasia by myeloid-derived suppressor cells. *The Journal of clinical investigation*. 2013;123(11):4595-611. doi: 10.1172/JCI67580. PubMed PMID: 24216507; PMCID: 3809779.
61. Mailloux AW, Sugimori C, Komrokji RS, Yang L, Maciejewski JP, Sekeres MA, Paquette R, Loughran TP, Jr., List AF, Epling-Burnette PK. Expansion of effector memory regulatory T cells represents a novel prognostic factor in lower risk myelodysplastic syndrome. *Journal of immunology*. 2012;189(6):3198-208. Epub 2012/08/10. doi: 10.4049/jimmunol.1200602. PubMed PMID: 22875800; PMCID: PMC3436939.
62. Mailloux AW, Epling-Burnette PK. Effector memory regulatory T-cell expansion marks a pivotal point of immune escape in myelodysplastic syndromes. *Oncoimmunology*. 2013;2(2):e22654. Epub 2013/03/26. doi: 10.4161/onci.22654. PubMed PMID: 23524348; PMCID: PMC3601152.
63. Greenberg PL. Apoptosis and its role in the myelodysplastic syndromes: implications for disease natural history and treatment. *Leukemia research*. 1998;22(12):1123-36. Epub 1999/01/28. doi: 10.1016/s0145-2126(98)00112-x. PubMed PMID: 9922076.
64. Kerbauy DB, Deeg HJ. Apoptosis and antiapoptotic mechanisms in the progression of myelodysplastic syndrome. *Exp Hematol*. 2007;35(11):1739-46. Epub 2007/11/03. doi: 10.1016/j.exphem.2007.09.007. PubMed PMID: 17976524; PMCID: PMC2131709.
65. Langemeijer SM, Mariani N, Knops R, Gilissen C, Woestenenk R, de Witte T, Huls G, van der Reijden BA, Jansen JH. Apoptosis-Related Gene Expression Profiling in Hematopoietic Cell Fractions of MDS Patients. *PloS one*. 2016;11(11):e0165582. Epub 2016/12/03. doi: 10.1371/journal.pone.0165582. PubMed PMID: 27902785; PMCID: PMC5130187.
66. Tsoplou P, Kouraklis-Symeonidis A, Thanopoulou E, Zikos P, Orphanos V, Zoumbos NC. Apoptosis in patients with myelodysplastic syndromes: differential involvement of marrow cells in 'good' versus 'poor' prognosis patients and correlation with apoptosis-related genes. *Leukemia*. 1999;13(10):1554-63. Epub 1999/10/12. doi: 10.1038/sj.leu.2401538. PubMed PMID: 10516757.
67. van de Loosdrecht AA, Vellenga E. Myelodysplasia and apoptosis: new insights into ineffective erythropoiesis. *Med Oncol*. 2000;17(1):16-21. Epub 2000/03/14. doi: 10.1007/bf02826211. PubMed PMID: 10713655.
68. Fontenay-Roupie M, Bouscary D, Guesnu M, Picard F, Melle J, Lacombe C, Gisselbrecht S, Mayeux P, Dreyfus F. Ineffective erythropoiesis in myelodysplastic syndromes: correlation with Fas expression but not with lack of erythropoietin receptor signal transduction. *British journal of haematology*. 1999;106(2):464-73. Epub 1999/08/25. doi: 10.1046/j.1365-2141.1999.01539.x. PubMed PMID: 10460607.

69. Sallman DA, Cluzeau T, Basiorka AA, List A. Unraveling the Pathogenesis of MDS: The NLRP3 Inflammasome and Pyroptosis Drive the MDS Phenotype. *Front Oncol.* 2016;6:151. Epub 2016/07/06. doi: 10.3389/fonc.2016.00151. PubMed PMID: 27379212; PMCID: PMC4909736.
70. Basiorka AA, McGraw KL, Eksioglu EA, Chen X, Johnson J, Zhang L, Zhang Q, Irvine BA, Cluzeau T, Sallman DA, Padron E, Komrokji R, Sokol L, Coll RC, Robertson AA, Cooper MA, Cleveland JL, O'Neill LA, Wei S, List AF. The NLRP3 inflammasome functions as a driver of the myelodysplastic syndrome phenotype. *Blood.* 2016;128(25):2960-75. Epub 2016/10/16. doi: 10.1182/blood-2016-07-730556. PubMed PMID: 27737891; PMCID: PMC5179338.
71. Germing U, Kobbe G, Haas R, Gattermann N. Myelodysplastic syndromes: diagnosis, prognosis, and treatment. *Dtsch Arztebl Int.* 2013;110(46):783-90. Epub 2013/12/05. doi: 10.3238/arztebl.2013.0783. PubMed PMID: 24300826; PMCID: PMC3855821.
72. Greenberg PL, Tuechler H, Schanz J, Sanz G, Garcia-Manero G, Sole F, Bennett JM, Bowen D, Fenaux P, Dreyfus F, Kantarjian H, Kuendgen A, Levis A, Malcovati L, Cazzola M, Cermak J, Fonatsch C, Le Beau MM, Slovak ML, Krieger O, Luebbert M, Maciejewski J, Magalhaes SM, Miyazaki Y, Pfeilstocker M, Sekeres M, Sperr WR, Stauder R, Tauro S, Valent P, Vallespi T, van de Loosdrecht AA, Germing U, Haase D. Revised international prognostic scoring system for myelodysplastic syndromes. *Blood.* 2012;120(12):2454-65. Epub 2012/06/29. doi: 10.1182/blood-2012-03-420489. PubMed PMID: 22740453; PMCID: PMC4425443.
73. Montalban-Bravo G, Garcia-Manero G. Myelodysplastic syndromes: 2018 update on diagnosis, risk-stratification and management. *Am J Hematol.* 2018;93(1):129-47. Epub 2017/12/08. doi: 10.1002/ajh.24930. PubMed PMID: 29214694.
74. Giagounidis A. Current treatment algorithm for the management of lower-risk MDS. *Hematology Am Soc Hematol Educ Program.* 2017;2017(1):453-9. Epub 2017/12/10. doi: 10.1182/asheducation-2017.1.453. PubMed PMID: 29222293; PMCID: PMC6142548 Celgene, and Acceleron.
75. Ma Y, Shen J, Wang LX. Successful treatment of high-risk myelodysplastic syndrome with decitabine-based chemotherapy followed by haploidentical lymphocyte infusion: A case report and literature review. *Medicine (Baltimore).* 2018;97(16):e0434. Epub 2018/04/19. doi: 10.1097/MD.00000000000010434. PubMed PMID: 29668607; PMCID: PMC5916686.
76. Tsuchioka T, Yokoi A, Uesugi M, Kishimoto M, Tochigi A, Suemori S, Tohyama Y, Tohyama K. Effects of DNA methyltransferase inhibitors (DNMTIs) on MDS-derived cell lines. *Exp Hematol.* 2013;41(2):189-97. Epub 2012/10/23. doi: 10.1016/j.exphem.2012.10.006. PubMed PMID: 23085465.
77. Silverman LR. DNA methyltransferase inhibitors in myelodysplastic syndrome. *Best Pract Res Clin Haematol.* 2004;17(4):585-94. Epub 2004/10/21. doi: 10.1016/j.beha.2004.08.010. PubMed PMID: 15494296.
78. Gore SD. New ways to use DNA methyltransferase inhibitors for the treatment of myelodysplastic syndrome. *Hematology Am Soc Hematol Educ Program.* 2011;2011:550-5. Epub 2011/12/14. doi: 10.1182/asheducation-2011.1.550. PubMed PMID: 22160088; PMCID: PMC3593590.
79. Stahl M, DeVeaux M, de Witte T, Neukirchen J, Sekeres MA, Brunner AM, Roboz GJ, Steensma DP, Bhatt VR, Platzbecker U, Cluzeau T, Prata PH, Itzykson R, Fenaux P, Fathi AT, Smith A, Germing U, Ritchie EK, Verma V, Nazha A, Maciejewski JP, Podoltsev NA, Prebet T, Santini V,

Gore SD, Komrokji RS, Zeidan AM. The use of immunosuppressive therapy in MDS: clinical outcomes and their predictors in a large international patient cohort. *Blood Adv.* 2018;2(14):1765-72. Epub 2018/07/25. doi: 10.1182/bloodadvances.2018019414. PubMed PMID: 30037803; PMCID: PMC6058241.

80. Glenthøj A, Orskov AD, Hansen JW, Hadrup SR, O'Connell C, Gronbaek K. Immune Mechanisms in Myelodysplastic Syndrome. *Int J Mol Sci.* 2016;17(6). Epub 2016/06/18. doi: 10.3390/ijms17060944. PubMed PMID: 27314337; PMCID: PMC4926477.

81. Epperson DE, Nakamura R, Sauntharajah Y, Melenhorst J, Barrett AJ. Oligoclonal T cell expansion in myelodysplastic syndrome: evidence for an autoimmune process. *Leukemia research.* 2001;25(12):1075-83. Epub 2001/10/31. doi: 10.1016/s0145-2126(01)00083-2. PubMed PMID: 11684279.

82. Talati C, Sallman D, List A. Lenalidomide: Myelodysplastic syndromes with del(5q) and beyond. *Semin Hematol.* 2017;54(3):159-66. Epub 2017/09/30. doi: 10.1053/j.seminhematol.2017.06.003. PubMed PMID: 28958290.

83. Bartenstein M, Deeg HJ. Hematopoietic stem cell transplantation for MDS. *Hematology/oncology clinics of North America.* 2010;24(2):407-22. Epub 2010/04/03. doi: 10.1016/j.hoc.2010.02.003. PubMed PMID: 20359634; PMCID: PMC2848960.

84. Falconi G, Fabiani E, Piciocchi A, Criscuolo M, Fianchi L, Lindfors Rossi EL, Finelli C, Cerqui E, Ottone T, Molteni A, Parma M, Santarone S, Candoni A, Sica S, Leone G, Lo-Coco F, Voso MT. Somatic mutations as markers of outcome after azacitidine and allogeneic stem cell transplantation in higher-risk myelodysplastic syndromes. *Leukemia.* 2019;33(3):785-90. Epub 2018/10/07. doi: 10.1038/s41375-018-0284-9. PubMed PMID: 30291338; PMCID: PMC6462855.

85. Kim M, Yahng SA, Kwon A, Park J, Jeon YW, Yoon JH, Shin SH, Lee SE, Cho BS, Eom KS, Lee S, Min CK, Kim HJ, Cho SG, Kim DW, Lee JW, Min WS, Lee SH, Kim YJ. Mutation in TET2 or TP53 predicts poor survival in patients with myelodysplastic syndrome receiving hypomethylating treatment or stem cell transplantation. *Bone Marrow Transplant.* 2015;50(8):1132-4. Epub 2015/05/12. doi: 10.1038/bmt.2015.110. PubMed PMID: 25961778.

86. Tamari R, Rapaport F, Zhang N, McNamara C, Kuykendall A, Sallman DA, Komrokji R, Arruda A, Najfeld V, Sandy L, Medina J, Litvin R, Famulare CA, Patel MA, Maloy M, Castro-Malaspina H, Giralto SA, Weinberg RS, Mascarenhas JO, Mesa R, Rondelli D, Dueck AC, Levine RL, Gupta V, Hoffman R, Rampal RK. Impact of High-Molecular-Risk Mutations on Transplantation Outcomes in Patients with Myelofibrosis. *Biol Blood Marrow Transplant.* 2019;25(6):1142-51. Epub 2019/01/10. doi: 10.1016/j.bbmt.2019.01.002. PubMed PMID: 30625392; PMCID: PMC6918823.

87. Feins S, Kong W, Williams EF, Milone MC, Fraietta JA. An introduction to chimeric antigen receptor (CAR) T-cell immunotherapy for human cancer. *Am J Hematol.* 2019;94(S1):S3-S9. Epub 2019/01/27. doi: 10.1002/ajh.25418. PubMed PMID: 30680780.

88. Sadelain M, Brentjens R, Riviere I, Park J. CD19 CAR Therapy for Acute Lymphoblastic Leukemia. *Am Soc Clin Oncol Educ Book.* 2015:e360-3. Epub 2015/05/21. doi: 10.14694/EdBook\_AM.2015.35.e360. PubMed PMID: 25993197.

89. Locke FL, Neelapu SS, Bartlett NL, Siddiqi T, Chavez JC, Hosing CM, Ghobadi A, Budde LE, Bot A, Rossi JM, Jiang Y, Xue AX, Elias M, Aycock J, Wiecek J, Go WY. Phase 1 Results of ZUMA-1: A Multicenter Study of KTE-C19 Anti-CD19 CAR T Cell Therapy in Refractory Aggressive

Lymphoma. *Mol Ther.* 2017;25(1):285-95. Epub 2017/01/28. doi: 10.1016/j.ymthe.2016.10.020. PubMed PMID: 28129122; PMCID: PMC5363293.

90. Neelapu SS, Locke FL, Bartlett NL, Lekakis LJ, Miklos DB, Jacobson CA, Braunschweig I, Oluwole OO, Siddiqi T, Lin Y, Timmerman JM, Stiff PJ, Friedberg JW, Flinn IW, Goy A, Hill BT, Smith MR, Deol A, Farooq U, McSweeney P, Munoz J, Avivi I, Castro JE, Westin JR, Chavez JC, Ghobadi A, Komanduri KV, Levy R, Jacobsen ED, Witzig TE, Reagan P, Bot A, Rossi J, Navale L, Jiang Y, Aycock J, Elias M, Chang D, Wieszorek J, Go WY. Axicabtagene Ciloleucel CAR T-Cell Therapy in Refractory Large B-Cell Lymphoma. *N Engl J Med.* 2017;377(26):2531-44. Epub 2017/12/12. doi: 10.1056/NEJMoa1707447. PubMed PMID: 29226797; PMCID: PMC5882485.

91. Stevens BM, Zhang W, Pollyea DA, Winters A, Gutman J, Smith C, Budde E, Forman SJ, Jordan CT, Purev E. CD123 CAR T cells for the treatment of myelodysplastic syndrome. *Exp Hematol.* 2019;74:52-63 e3. Epub 2019/05/29. doi: 10.1016/j.exphem.2019.05.002. PubMed PMID: 31136781.

92. Baumeister SH, Murad J, Werner L, Daley H, Trebeden-Negre H, Gicobi JK, Schmucker A, Reder J, Sentman CL, Gilham DE, Lehmann FF, Galinsky I, DiPietro H, Cummings K, Munshi NC, Stone RM, Neuberg DS, Soiffer R, Dranoff G, Ritz J, Nikiforow S. Phase I Trial of Autologous CAR T Cells Targeting NKG2D Ligands in Patients with AML/MDS and Multiple Myeloma. *Cancer immunology research.* 2019;7(1):100-12. Epub 2018/11/07. doi: 10.1158/2326-6066.CIR-18-0307. PubMed PMID: 30396908.

93. Ryckman C, Vandal K, Rouleau P, Talbot M, Tessier PA. Proinflammatory activities of S100: proteins S100A8, S100A9, and S100A8/A9 induce neutrophil chemotaxis and adhesion. *Journal of immunology.* 2003;170(6):3233-42. Epub 2003/03/11. doi: 10.4049/jimmunol.170.6.3233. PubMed PMID: 12626582.

94. Tsai SY, Segovia JA, Chang TH, Morris IR, Berton MT, Tessier PA, Tardif MR, Cesaro A, Bose S. DAMP molecule S100A9 acts as a molecular pattern to enhance inflammation during influenza A virus infection: role of DDX21-TRIF-TLR4-MyD88 pathway. *PLoS Pathog.* 2014;10(1):e1003848. Epub 2014/01/07. doi: 10.1371/journal.ppat.1003848. PubMed PMID: 24391503; PMCID: PMC3879357.

95. Mumolo MG, Bertani L, Ceccarelli L, Laino G, Di Fluri G, Albano E, Tapete G, Costa F. From bench to bedside: Fecal calprotectin in inflammatory bowel diseases clinical setting. *World J Gastroenterol.* 2018;24(33):3681-94. Epub 2018/09/11. doi: 10.3748/wjg.v24.i33.3681. PubMed PMID: 30197475; PMCID: PMC6127662.

96. Walsham NE, Sherwood RA. Fecal calprotectin in inflammatory bowel disease. *Clin Exp Gastroenterol.* 2016;9:21-9. Epub 2016/02/13. doi: 10.2147/CEG.S51902. PubMed PMID: 26869808; PMCID: PMC4734737.

97. Vogl T, Leukert N, Barczyk K, Strupat K, Roth J. Biophysical characterization of S100A8 and S100A9 in the absence and presence of bivalent cations. *Biochim Biophys Acta.* 2006;1763(11):1298-306. Epub 2006/10/20. doi: 10.1016/j.bbamcr.2006.08.028. PubMed PMID: 17050004.

98. Markowitz J, Carson WE, 3rd. Review of S100A9 biology and its role in cancer. *Biochim Biophys Acta.* 2013;1835(1):100-9. Epub 2012/11/06. doi: 10.1016/j.bbcan.2012.10.003. PubMed PMID: 23123827; PMCID: PMC3670606.

99. Xia C, Braunstein Z, Toomey AC, Zhong J, Rao X. S100 Proteins As an Important Regulator of Macrophage Inflammation. *Front Immunol.* 2017;8:1908. Epub 2018/01/31. doi: 10.3389/fimmu.2017.01908. PubMed PMID: 29379499; PMCID: PMC5770888.
100. Hermani A, Hess J, De Servi B, Medunjanin S, Grobholz R, Trojan L, Angel P, Mayer D. Calcium-binding proteins S100A8 and S100A9 as novel diagnostic markers in human prostate cancer. *Clin Cancer Res.* 2005;11(14):5146-52. Epub 2005/07/22. doi: 10.1158/1078-0432.CCR-05-0352. PubMed PMID: 16033829.
101. Broome AM, Ryan D, Eckert RL. S100 protein subcellular localization during epidermal differentiation and psoriasis. *The journal of histochemistry and cytochemistry : official journal of the Histochemistry Society.* 2003;51(5):675-85. Epub 2003/04/22. doi: 10.1177/002215540305100513. PubMed PMID: 12704215; PMCID: PMC3785113.
102. Donato R, Cannon BR, Sorci G, Riuzzi F, Hsu K, Weber DJ, Geczy CL. Functions of S100 proteins. *Curr Mol Med.* 2013;13(1):24-57. Epub 2012/07/28. PubMed PMID: 22834835; PMCID: PMC3707951.
103. Riva M, Kallberg E, Bjork P, Hancz D, Vogl T, Roth J, Ivars F, Leanderson T. Induction of nuclear factor-kappaB responses by the S100A9 protein is Toll-like receptor-4-dependent. *Immunology.* 2012;137(2):172-82. Epub 2012/07/19. doi: 10.1111/j.1365-2567.2012.03619.x. PubMed PMID: 22804476; PMCID: PMC3461398.
104. Nemeth J, Stein I, Haag D, Riehl A, Longerich T, Horwitz E, Breuhahn K, Gebhardt C, Schirmacher P, Hahn M, Ben-Neriah Y, Pikarsky E, Angel P, Hess J. S100A8 and S100A9 are novel nuclear factor kappa B target genes during malignant progression of murine and human liver carcinogenesis. *Hepatology.* 2009;50(4):1251-62. Epub 2009/08/12. doi: 10.1002/hep.23099. PubMed PMID: 19670424.
105. Wang S, Song R, Wang Z, Jing Z, Wang S, Ma J. S100A8/A9 in Inflammation. *Front Immunol.* 2018;9:1298. Epub 2018/06/27. doi: 10.3389/fimmu.2018.01298. PubMed PMID: 29942307; PMCID: PMC6004386.
106. Gao H, Zhang X, Zheng Y, Peng L, Hou J, Meng H. S100A9-induced release of interleukin (IL)-6 and IL-8 through toll-like receptor 4 (TLR4) in human periodontal ligament cells. *Mol Immunol.* 2015;67(2 Pt B):223-32. Epub 2015/06/04. doi: 10.1016/j.molimm.2015.05.014. PubMed PMID: 26038301.
107. Simard JC, Cesaro A, Chapeton-Montes J, Tardif M, Antoine F, Girard D, Tessier PA. S100A8 and S100A9 induce cytokine expression and regulate the NLRP3 inflammasome via ROS-dependent activation of NF-kappaB(1.). *PloS one.* 2013;8(8):e72138. doi: 10.1371/journal.pone.0072138. PubMed PMID: 23977231; PMCID: 3747084.
108. Alkhateeb T, Kumbhare A, Bah I, Youssef D, Yao ZQ, McCall CE, El Gazzar M. S100A9 maintains myeloid-derived suppressor cells in chronic sepsis by inducing miR-21 and miR-181b. *Mol Immunol.* 2019;112:72-81. Epub 2019/05/12. doi: 10.1016/j.molimm.2019.04.019. PubMed PMID: 31078118; PMCID: PMC6646085.
109. Dai J, Kumbhare A, Youssef D, McCall CE, El Gazzar M. Intracellular S100A9 Promotes Myeloid-Derived Suppressor Cells during Late Sepsis. *Front Immunol.* 2017;8:1565. Epub 2017/12/06. doi: 10.3389/fimmu.2017.01565. PubMed PMID: 29204146; PMCID: PMC5698275.
110. Zhao F, Hoechst B, Duffy A, Gamrekashvili J, Fioravanti S, Manns MP, Greten TF, Korangy F. S100A9 a new marker for monocytic human myeloid-derived suppressor cells. *Immunology.*

- 2012;136(2):176-83. Epub 2012/02/07. doi: 10.1111/j.1365-2567.2012.03566.x. PubMed PMID: 22304731; PMCID: PMC3403264.
111. Cheng P, Eksioglu EA, Chen X, Kandell W, Le Trinh T, Cen L, Qi J, Sallman DA, Zhang Y, Tu N, Adams WA, Zhang C, Liu J, Cleveland JL, List AF, Wei S. S100A9-induced overexpression of PD-1/PD-L1 contributes to ineffective hematopoiesis in myelodysplastic syndromes. *Leukemia*. 2019;33(8):2034-46. Epub 2019/02/10. doi: 10.1038/s41375-019-0397-9. PubMed PMID: 30737486; PMCID: PMC6687540.
112. Gabrilovich DI. Myeloid-Derived Suppressor Cells. *Cancer immunology research*. 2017;5(1):3-8. Epub 2017/01/06. doi: 10.1158/2326-6066.CIR-16-0297. PubMed PMID: 28052991; PMCID: PMC5426480.
113. Gabrilovich DI, Nagaraj S. Myeloid-derived suppressor cells as regulators of the immune system. *Nat Rev Immunol*. 2009;9(3):162-74. Epub 2009/02/07. doi: nri2506 [pii] 10.1038/nri2506. PubMed PMID: 19197294; PMCID: 2828349.
114. Simon S, Labarriere N. PD-1 expression on tumor-specific T cells: Friend or foe for immunotherapy? *Oncoimmunology*. 2017;7(1):e1364828. Epub 2018/01/04. doi: 10.1080/2162402X.2017.1364828. PubMed PMID: 29296515; PMCID: PMC5739549.
115. Ahn E, Araki K, Hashimoto M, Li W, Riley JL, Cheung J, Sharpe AH, Freeman GJ, Irving BA, Ahmed R. Role of PD-1 during effector CD8 T cell differentiation. *Proceedings of the National Academy of Sciences of the United States of America*. 2018;115(18):4749-54. Epub 2018/04/15. doi: 10.1073/pnas.1718217115. PubMed PMID: 29654146; PMCID: PMC5939075.
116. Saeidi A, Zandi K, Cheok YY, Saeidi H, Wong WF, Lee CYQ, Cheong HC, Yong YK, Larsson M, Shankar EM. T-Cell Exhaustion in Chronic Infections: Reversing the State of Exhaustion and Reinvigorating Optimal Protective Immune Responses. *Front Immunol*. 2018;9:2569. Epub 2018/11/27. doi: 10.3389/fimmu.2018.02569. PubMed PMID: 30473697; PMCID: PMC6237934.
117. Thommen DS, Schumacher TN. T Cell Dysfunction in Cancer. *Cancer cell*. 2018;33(4):547-62. Epub 2018/04/11. doi: 10.1016/j.ccell.2018.03.012. PubMed PMID: 29634943.
118. Kumar BV, Connors TJ, Farber DL. Human T Cell Development, Localization, and Function throughout Life. *Immunity*. 2018;48(2):202-13. Epub 2018/02/22. doi: 10.1016/j.immuni.2018.01.007. PubMed PMID: 29466753; PMCID: PMC5826622.
119. Xing Y, Hogquist KA. T-cell tolerance: central and peripheral. *Cold Spring Harb Perspect Biol*. 2012;4(6). Epub 2012/06/05. doi: 10.1101/cshperspect.a006957. PubMed PMID: 22661634; PMCID: PMC3367546.
120. Golubovskaya V, Wu L. Different Subsets of T Cells, Memory, Effector Functions, and CAR-T Immunotherapy. *Cancers (Basel)*. 2016;8(3). Epub 2016/03/22. doi: 10.3390/cancers8030036. PubMed PMID: 26999211; PMCID: PMC4810120.
121. Takeuchi A, Saito T. CD4 CTL, a Cytotoxic Subset of CD4(+) T Cells, Their Differentiation and Function. *Front Immunol*. 2017;8:194. Epub 2017/03/11. doi: 10.3389/fimmu.2017.00194. PubMed PMID: 28280496; PMCID: PMC5321676.
122. McBride JA, Striker R. Imbalance in the game of T cells: What can the CD4/CD8 T-cell ratio tell us about HIV and health? *PLoS Pathog*. 2017;13(11):e1006624. Epub 2017/11/03. doi: 10.1371/journal.ppat.1006624. PubMed PMID: 29095912; PMCID: PMC5667733.
123. Mitogawa T, Nishiya K, Ota Z. Frequency of gamma delta T cells in peripheral blood, synovial fluid, synovial membrane and lungs from patients with rheumatoid arthritis. *Acta Med*

- Okayama. 1992;46(5):371-9. Epub 1992/10/01. doi: 10.18926/AMO/32664. PubMed PMID: 1442157.
124. Nielsen MM, Witherden DA, Havran WL. gammadelta T cells in homeostasis and host defence of epithelial barrier tissues. *Nat Rev Immunol.* 2017;17(12):733-45. Epub 2017/09/19. doi: 10.1038/nri.2017.101. PubMed PMID: 28920588; PMCID: PMC5771804.
125. Zarin P, Chen EL, In TS, Anderson MK, Zuniga-Pflucker JC. Gamma delta T-cell differentiation and effector function programming, TCR signal strength, when and how much? *Cell Immunol.* 2015;296(1):70-5. Epub 2015/04/14. doi: 10.1016/j.cellimm.2015.03.007. PubMed PMID: 25866401.
126. Pereira P, Boucontet L, Cumano A. Temporal predisposition to alphabeta and gammadelta T cell fates in the thymus. *Journal of immunology.* 2012;188(4):1600-8. Epub 2012/01/13. doi: 10.4049/jimmunol.1102531. PubMed PMID: 22238456.
127. Smith-Garvin JE, Koretzky GA, Jordan MS. T cell activation. *Annu Rev Immunol.* 2009;27:591-619. Epub 2009/01/10. doi: 10.1146/annurev.immunol.021908.132706. PubMed PMID: 19132916; PMCID: PMC2740335.
128. Green DR, Droin N, Pinkoski M. Activation-induced cell death in T cells. *Immunol Rev.* 2003;193:70-81. Epub 2003/05/20. doi: 10.1034/j.1600-065x.2003.00051.x. PubMed PMID: 12752672.
129. Chen L, Flies DB. Molecular mechanisms of T cell co-stimulation and co-inhibition. *Nat Rev Immunol.* 2013;13(4):227-42. Epub 2013/03/09. doi: 10.1038/nri3405. PubMed PMID: 23470321; PMCID: PMC3786574.
130. Magee CN, Boenisch O, Najafian N. The role of costimulatory molecules in directing the functional differentiation of alloreactive T helper cells. *Am J Transplant.* 2012;12(10):2588-600. Epub 2012/07/05. doi: 10.1111/j.1600-6143.2012.04180.x. PubMed PMID: 22759274; PMCID: PMC3459149.
131. Raeber ME, Zurbuchen Y, Impellizzieri D, Boyman O. The role of cytokines in T-cell memory in health and disease. *Immunol Rev.* 2018;283(1):176-93. Epub 2018/04/18. doi: 10.1111/imr.12644. PubMed PMID: 29664568.
132. Arens R, Schoenberger SP. Plasticity in programming of effector and memory CD8 T-cell formation. *Immunol Rev.* 2010;235(1):190-205. Epub 2010/06/12. doi: 10.1111/j.0105-2896.2010.00899.x. PubMed PMID: 20536564; PMCID: PMC2937176.
133. Blair DA, Turner DL, Bose TO, Pham QM, Bouchard KR, Williams KJ, McAleer JP, Cauley LS, Vella AT, Lefrancois L. Duration of antigen availability influences the expansion and memory differentiation of T cells. *Journal of immunology.* 2011;187(5):2310-21. Epub 2011/07/22. doi: 10.4049/jimmunol.1100363. PubMed PMID: 21775679; PMCID: PMC3159832.
134. Jameson SC, Masopust D. Understanding Subset Diversity in T Cell Memory. *Immunity.* 2018;48(2):214-26. Epub 2018/02/22. doi: 10.1016/j.immuni.2018.02.010. PubMed PMID: 29466754; PMCID: PMC5863745.
135. Topham DJ, Reilly EC. Tissue-Resident Memory CD8(+) T Cells: From Phenotype to Function. *Front Immunol.* 2018;9:515. Epub 2018/04/11. doi: 10.3389/fimmu.2018.00515. PubMed PMID: 29632527; PMCID: PMC5879098.
136. Willinger T, Freeman T, Hasegawa H, McMichael AJ, Callan MF. Molecular signatures distinguish human central memory from effector memory CD8 T cell subsets. *Journal of*

- immunology. 2005;175(9):5895-903. Epub 2005/10/21. doi: 10.4049/jimmunol.175.9.5895. PubMed PMID: 16237082.
137. Abdou NL, Alavi JB, Abdou NI. Human bone marrow lymphocytes: B and T cell precursors and subpopulations. *Blood*. 1976;47(3):423-30. Epub 1976/03/01. PubMed PMID: 1082782.
138. Zhao E, Xu H, Wang L, Kryczek I, Wu K, Hu Y, Wang G, Zou W. Bone marrow and the control of immunity. *Cell Mol Immunol*. 2012;9(1):11-9. Epub 2011/10/25. doi: 10.1038/cmi.2011.47. PubMed PMID: 22020068; PMCID: PMC3251706.
139. Yanes RE, Gustafson CE, Weyand CM, Goronzy JJ. Lymphocyte generation and population homeostasis throughout life. *Semin Hematol*. 2017;54(1):33-8. Epub 2017/01/17. doi: 10.1053/j.seminhematol.2016.10.003. PubMed PMID: 28088985; PMCID: PMC5260809.
140. Aoki M, Aoki H, Ramanathan R, Hait NC, Takabe K. Sphingosine-1-Phosphate Signaling in Immune Cells and Inflammation: Roles and Therapeutic Potential. *Mediators Inflamm*. 2016;2016:8606878. Epub 2016/03/12. doi: 10.1155/2016/8606878. PubMed PMID: 26966342; PMCID: PMC4761394.
141. Chongsathidkiet P, Jackson C, Koyama S, Loebel F, Cui X, Farber SH, Woroniecka K, Elsamadicy AA, Dechant CA, Kemeny HR, Sanchez-Perez L, Cheema TA, Souders NC, Herndon JE, Coumans JV, Everitt JI, Nahed BV, Sampson JH, Gunn MD, Martuza RL, Dranoff G, Curry WT, Fecci PE. Sequestration of T cells in bone marrow in the setting of glioblastoma and other intracranial tumors. *Nat Med*. 2018;24(9):1459-68. Epub 2018/08/15. doi: 10.1038/s41591-018-0135-2. PubMed PMID: 30104766; PMCID: PMC6129206.
142. Mackay LK, Braun A, Macleod BL, Collins N, Tebartz C, Bedoui S, Carbone FR, Gebhardt T. Cutting edge: CD69 interference with sphingosine-1-phosphate receptor function regulates peripheral T cell retention. *Journal of immunology*. 2015;194(5):2059-63. Epub 2015/01/28. doi: 10.4049/jimmunol.1402256. PubMed PMID: 25624457.
143. Bankovich AJ, Shioh LR, Cyster JG. CD69 suppresses sphingosine 1-phosphate receptor-1 (S1P1) function through interaction with membrane helix 4. *J Biol Chem*. 2010;285(29):22328-37. Epub 2010/05/14. doi: 10.1074/jbc.M110.123299. PubMed PMID: 20463015; PMCID: PMC2903414.
144. Becker TC, Coley SM, Wherry EJ, Ahmed R. Bone marrow is a preferred site for homeostatic proliferation of memory CD8 T cells. *Journal of immunology*. 2005;174(3):1269-73. Epub 2005/01/22. doi: 10.4049/jimmunol.174.3.1269. PubMed PMID: 15661882.
145. Vercauteren SM, Starczynowski DT, Sung S, McNeil K, Salski C, Jensen CL, Bruyere H, Lam WL, Karsan A. T cells of patients with myelodysplastic syndrome are frequently derived from the malignant clone. *British journal of haematology*. 2012;156(3):409-12. Epub 2012/02/01. doi: 10.1111/j.1365-2141.2011.08872.x. PubMed PMID: 25289412; PMCID: PMC4191868.
146. Zou JX, Rollison DE, Boulware D, Chen DT, Sloand EM, Pfannes LV, Goronzy JJ, Bai F, Painter JS, Wei S, Cosgrove D, List AF, Epling-Burnette PK. Altered naive and memory CD4+ T-cell homeostasis and immunosenescence characterize younger patients with myelodysplastic syndrome. *Leukemia*. 2009;23(7):1288-96. Epub 2009/03/14. doi: 10.1038/leu.2009.14. PubMed PMID: 19282834; PMCID: PMC3252820.
147. Kook H, Zeng W, Guibin C, Kirby M, Young NS, Maciejewski JP. Increased cytotoxic T cells with effector phenotype in aplastic anemia and myelodysplasia. *Exp Hematol*. 2001;29(11):1270-7. Epub 2001/11/08. doi: 10.1016/s0301-472x(01)00736-6. PubMed PMID: 11698122.



148. Epling-Burnette PK, Painter JS, Rollison DE, Ku E, Vendron D, Widen R, Boulware D, Zou JX, Bai F, List AF. Prevalence and clinical association of clonal T-cell expansions in Myelodysplastic Syndrome. *Leukemia*. 2007;21(4):659-67. Epub 2007/02/16. doi: 10.1038/sj.leu.2404590. PubMed PMID: 17301813.
149. Amarante-Mendes GP, Adjemian S, Branco LM, Zanetti LC, Weinlich R, Bortoluci KR. Pattern Recognition Receptors and the Host Cell Death Molecular Machinery. *Front Immunol*. 2018;9:2379. Epub 2018/11/22. doi: 10.3389/fimmu.2018.02379. PubMed PMID: 30459758; PMCID: PMC6232773.
150. Takeuchi O, Akira S. Pattern recognition receptors and inflammation. *Cell*. 2010;140(6):805-20. Epub 2010/03/23. doi: 10.1016/j.cell.2010.01.022. PubMed PMID: 20303872.
151. Jang JH, Shin HW, Lee JM, Lee HW, Kim EC, Park SH. An Overview of Pathogen Recognition Receptors for Innate Immunity in Dental Pulp. *Mediators Inflamm*. 2015;2015:794143. Epub 2015/11/18. doi: 10.1155/2015/794143. PubMed PMID: 26576076; PMCID: PMC4630409.
152. Padovan E, Landmann RM, De Libero G. How pattern recognition receptor triggering influences T cell responses: a new look into the system. *Trends Immunol*. 2007;28(7):308-14. Epub 2007/06/01. doi: 10.1016/j.it.2007.05.002. PubMed PMID: 17537673.
153. Vaure C, Liu Y. A comparative review of toll-like receptor 4 expression and functionality in different animal species. *Front Immunol*. 2014;5:316. Epub 2014/07/30. doi: 10.3389/fimmu.2014.00316. PubMed PMID: 25071777; PMCID: PMC4090903.
154. Reynolds JM, Martinez GJ, Chung Y, Dong C. Toll-like receptor 4 signaling in T cells promotes autoimmune inflammation. *Proceedings of the National Academy of Sciences of the United States of America*. 2012;109(32):13064-9. Epub 2012/07/25. doi: 10.1073/pnas.1120585109. PubMed PMID: 22826216; PMCID: PMC3420161.
155. Gonzalez-Navajas JM, Fine S, Law J, Datta SK, Nguyen KP, Yu M, Corr M, Katakura K, Eckman L, Lee J, Raz E. TLR4 signaling in effector CD4+ T cells regulates TCR activation and experimental colitis in mice. *The Journal of clinical investigation*. 2010;120(2):570-81. Epub 2010/01/07. doi: 10.1172/JCI40055. PubMed PMID: 20051628; PMCID: PMC2810084.
156. Zanin-Zhorov A, Cohen IR. Signaling via TLR2 and TLR4 Directly Down-Regulates T Cell Effector Functions: The Regulatory Face of Danger Signals. *Front Immunol*. 2013;4:211. Epub 2013/07/31. doi: 10.3389/fimmu.2013.00211. PubMed PMID: 23898332; PMCID: PMC3722573.
157. Akirav EM, Preston-Hurlburt P, Garyu J, Henegariu O, Clynes R, Schmidt AM, Herold KC. RAGE expression in human T cells: a link between environmental factors and adaptive immune responses. *PloS one*. 2012;7(4):e34698. Epub 2012/04/18. doi: 10.1371/journal.pone.0034698. PubMed PMID: 22509345; PMCID: PMC3324532.
158. Chen Y, Akirav EM, Chen W, Henegariu O, Moser B, Desai D, Shen JM, Webster JC, Andrews RC, Mjalli AM, Rothlein R, Schmidt AM, Clynes R, Herold KC. RAGE ligation affects T cell activation and controls T cell differentiation. *Journal of immunology*. 2008;181(6):4272-8. Epub 2008/09/05. doi: 10.4049/jimmunol.181.6.4272. PubMed PMID: 18768885; PMCID: PMC2643976.
159. Durning SP, Preston-Hurlburt P, Clark PR, Xu D, Herold KC, Type 1 Diabetes TrialNet Study G. The Receptor for Advanced Glycation Endproducts Drives T Cell Survival and Inflammation in

- Type 1 Diabetes Mellitus. *Journal of immunology*. 2016;197(8):3076-85. Epub 2016/09/23. doi: 10.4049/jimmunol.1600197. PubMed PMID: 27655844; PMCID: PMC5101164.
160. Moser B, Desai DD, Downie MP, Chen Y, Yan SF, Herold K, Schmidt AM, Clynes R. Receptor for advanced glycation end products expression on T cells contributes to antigen-specific cellular expansion in vivo. *Journal of immunology*. 2007;179(12):8051-8. Epub 2007/12/07. doi: 10.4049/jimmunol.179.12.8051. PubMed PMID: 18056345.
161. Logsdon CD, Fuentes MK, Huang EH, Arumugam T. RAGE and RAGE ligands in cancer. *Curr Mol Med*. 2007;7(8):777-89. Epub 2008/03/12. doi: 10.2174/156652407783220697. PubMed PMID: 18331236.
162. Fritz G. RAGE: a single receptor fits multiple ligands. *Trends Biochem Sci*. 2011;36(12):625-32. Epub 2011/10/25. doi: 10.1016/j.tibs.2011.08.008. PubMed PMID: 22019011.
163. Kierdorf K, Fritz G. RAGE regulation and signaling in inflammation and beyond. *J Leukoc Biol*. 2013;94(1):55-68. Epub 2013/04/02. doi: 10.1189/jlb.1012519. PubMed PMID: 23543766.
164. Senatus LM, Schmidt AM. The AGE-RAGE Axis: Implications for Age-Associated Arterial Diseases. *Front Genet*. 2017;8:187. Epub 2017/12/21. doi: 10.3389/fgene.2017.00187. PubMed PMID: 29259621; PMCID: PMC5723304.
165. Son M, Chung WJ, Oh S, Ahn H, Choi CH, Hong S, Park KY, Son KH, Byun K. Age dependent accumulation patterns of advanced glycation end product receptor (RAGE) ligands and binding intensities between RAGE and its ligands differ in the liver, kidney, and skeletal muscle. *Immun Ageing*. 2017;14:12. Epub 2017/06/09. doi: 10.1186/s12979-017-0095-2. PubMed PMID: 28592983; PMCID: PMC5460364.
166. Bongarzone S, Savickas V, Luzi F, Gee AD. Targeting the Receptor for Advanced Glycation Endproducts (RAGE): A Medicinal Chemistry Perspective. *J Med Chem*. 2017;60(17):7213-32. Epub 2017/05/10. doi: 10.1021/acs.jmedchem.7b00058. PubMed PMID: 28482155; PMCID: PMC5601361.
167. Ramasamy R, Yan SF, Herold K, Clynes R, Schmidt AM. Receptor for advanced glycation end products: fundamental roles in the inflammatory response: winding the way to the pathogenesis of endothelial dysfunction and atherosclerosis. *Ann N Y Acad Sci*. 2008;1126:7-13. Epub 2008/05/02. doi: 10.1196/annals.1433.056. PubMed PMID: 18448789; PMCID: PMC3049155.
168. Derk J, MacLean M, Juranek J, Schmidt AM. The Receptor for Advanced Glycation Endproducts (RAGE) and Mediation of Inflammatory Neurodegeneration. *J Alzheimers Dis Parkinsonism*. 2018;8(1). Epub 2018/12/19. doi: 10.4172/2161-0460.1000421. PubMed PMID: 30560011; PMCID: PMC6293973.
169. Trinh TL, Kandell WM, Donatelli SS, Tu N, Tejera MM, Gilvary DL, Eksioglu EA, Burnette A, Adams WA, Liu J, Teer JK, Djeu JY, Coppola D, Wei S. Immune evasion by TGFbeta-induced miR-183 repression of MICA/B expression in human lung tumor cells. *Oncoimmunology*. 2019;8(4):e1557372. Epub 2019/03/25. doi: 10.1080/2162402X.2018.1557372. PubMed PMID: 30906652; PMCID: PMC6422376.
170. Torre LA, Siegel RL, Jemal A. Lung Cancer Statistics. *Advances in experimental medicine and biology*. 2016;893:1-19. doi: 10.1007/978-3-319-24223-1\_1. PubMed PMID: 26667336.
171. Hanahan D, Weinberg RA. Hallmarks of cancer: the next generation. *Cell*. 2011;144(5):646-74. doi: 10.1016/j.cell.2011.02.013. PubMed PMID: 21376230.

172. Ambros V. The functions of animal microRNAs. *Nature*. 2004;431(7006):350-5. doi: 10.1038/nature02871. PubMed PMID: 15372042.
173. Zhu W, Liu X, He J, Chen D, Hunag Y, Zhang YK. Overexpression of members of the microRNA-183 family is a risk factor for lung cancer: a case control study. *BMC cancer*. 2011;11:393. doi: 10.1186/1471-2407-11-393. PubMed PMID: 21920043; PMCID: 3183044.
174. Zhu W, Zhou K, Zha Y, Chen D, He J, Ma H, Liu X, Le H, Zhang Y. Diagnostic Value of Serum miR-182, miR-183, miR-210, and miR-126 Levels in Patients with Early-Stage Non-Small Cell Lung Cancer. *PloS one*. 2016;11(4):e0153046. doi: 10.1371/journal.pone.0153046. PubMed PMID: 27093275; PMCID: 4836744.
175. Li P, Sheng C, Huang L, Zhang H, Huang L, Cheng Z, Zhu Q. MiR-183/-96/-182 cluster is up-regulated in most breast cancers and increases cell proliferation and migration. *Breast cancer research : BCR*. 2014;16(6):473. doi: 10.1186/s13058-014-0473-z. PubMed PMID: 25394902; PMCID: 4303194.
176. Sarver AL, French AJ, Borralho PM, Thayanithy V, Oberg AL, Silverstein KA, Morlan BW, Riska SM, Boardman LA, Cunningham JM, Subramanian S, Wang L, Smyrk TC, Rodrigues CM, Thibodeau SN, Steer CJ. Human colon cancer profiles show differential microRNA expression depending on mismatch repair status and are characteristic of undifferentiated proliferative states. *BMC cancer*. 2009;9:401. doi: 10.1186/1471-2407-9-401. PubMed PMID: 19922656; PMCID: 2787532.
177. Zhou T, Zhang GJ, Zhou H, Xiao HX, Li Y. Overexpression of microRNA-183 in human colorectal cancer and its clinical significance. *European journal of gastroenterology & hepatology*. 2014;26(2):229-33. doi: 10.1097/MEG.0000000000000002. PubMed PMID: 24150523.
178. Li J, Fu H, Xu C, Tie Y, Xing R, Zhu J, Qin Y, Sun Z, Zheng X. miR-183 inhibits TGF-beta1-induced apoptosis by downregulation of PDCD4 expression in human hepatocellular carcinoma cells. *BMC cancer*. 2010;10:354. doi: 10.1186/1471-2407-10-354. PubMed PMID: 20602797; PMCID: 2909210.
179. Ren LH, Chen WX, Li S, He XY, Zhang ZM, Li M, Cao RS, Hao B, Zhang HJ, Qiu HQ, Shi RH. MicroRNA-183 promotes proliferation and invasion in oesophageal squamous cell carcinoma by targeting programmed cell death 4. *British journal of cancer*. 2014;111(10):2003-13. doi: 10.1038/bjc.2014.485. PubMed PMID: 25211657; PMCID: 4229630.
180. Mihelich BL, Khramtsova EA, Arva N, Vaishnav A, Johnson DN, Giangreco AA, Martens-Uzunova E, Bagasra O, Kajdacsy-Balla A, Nonn L. miR-183-96-182 cluster is overexpressed in prostate tissue and regulates zinc homeostasis in prostate cells. *J Biol Chem*. 2011;286(52):44503-11. doi: 10.1074/jbc.M111.262915. PubMed PMID: 22045813; PMCID: 3247959.
181. Yu J, Li A, Hong SM, Hruban RH, Goggins M. MicroRNA alterations of pancreatic intraepithelial neoplasias. *Clin Cancer Res*. 2012;18(4):981-92. doi: 10.1158/1078-0432.CCR-11-2347. PubMed PMID: 22114139; PMCID: 3288338.
182. Tang X, Zheng D, Hu P, Zeng Z, Li M, Tucker L, Monahan R, Resnick MB, Liu M, Ramratnam B. Glycogen synthase kinase 3 beta inhibits microRNA-183-96-182 cluster via the beta-Catenin/TCF/LEF-1 pathway in gastric cancer cells. *Nucleic acids research*. 2014;42(5):2988-98. doi: 10.1093/nar/gkt1275. PubMed PMID: 24335145; PMCID: 3950676.

183. Polakis P. The many ways of Wnt in cancer. *Current opinion in genetics & development*. 2007;17(1):45-51. doi: 10.1016/j.gde.2006.12.007. PubMed PMID: 17208432.
184. Liu WH, Chang LS. Suppression of Akt/Foxp3-mediated miR-183 expression blocks Sp1-mediated ADAM17 expression and TNFalpha-mediated NFkappaB activation in piceatannol-treated human leukemia U937 cells. *Biochemical pharmacology*. 2012;84(5):670-80. doi: 10.1016/j.bcp.2012.06.007. PubMed PMID: 22705645.
185. Tanaka H, Sasayama T, Tanaka K, Nakamizo S, Nishihara M, Mizukawa K, Kohta M, Koyama J, Miyake S, Taniguchi M, Hosoda K, Kohmura E. MicroRNA-183 upregulates HIF-1alpha by targeting isocitrate dehydrogenase 2 (IDH2) in glioma cells. *Journal of neuro-oncology*. 2013;111(3):273-83. doi: 10.1007/s11060-012-1027-9. PubMed PMID: 23263745.
186. Qiu M, Liu L, Chen L, Tan G, Liang Z, Wang K, Liu J, Chen H. microRNA-183 plays as oncogenes by increasing cell proliferation, migration and invasion via targeting protein phosphatase 2A in renal cancer cells. *Biochemical and biophysical research communications*. 2014;452(1):163-9. doi: 10.1016/j.bbrc.2014.08.067. PubMed PMID: 25152390.
187. Sarver AL, Li L, Subramanian S. MicroRNA miR-183 functions as an oncogene by targeting the transcription factor EGR1 and promoting tumor cell migration. *Cancer Res*. 2010;70(23):9570-80. doi: 10.1158/0008-5472.CAN-10-2074. PubMed PMID: 21118966.
188. Zhang L, Quan H, Wang S, Li X, Che X. MiR-183 promotes growth of non-small cell lung cancer cells through FoxO1 inhibition. *Tumour biology : the journal of the International Society for Oncodevelopmental Biology and Medicine*. 2015;36(10):8121-6. doi: 10.1007/s13277-015-3550-8. PubMed PMID: 25983004.
189. Djeu JY, Jiang K, Wei S. A view to a kill: signals triggering cytotoxicity. *Clin Cancer Res*. 2002;8(3):636-40. PubMed PMID: 11895890.
190. Morvan MG, Lanier LL. NK cells and cancer: you can teach innate cells new tricks. *Nature reviews Cancer*. 2016;16(1):7-19. doi: 10.1038/nrc.2015.5. PubMed PMID: 26694935.
191. Bauer S, Groh V, Wu J, Steinle A, Phillips JH, Lanier LL, Spies T. Activation of NK cells and T cells by NKG2D, a receptor for stress-inducible MICA. *Science*. 1999;285(5428):727-9. PubMed PMID: 10426993.
192. Wu J, Song Y, Bakker AB, Bauer S, Spies T, Lanier LL, Phillips JH. An activating immunoreceptor complex formed by NKG2D and DAP10. *Science*. 1999;285(5428):730-2. PubMed PMID: 10426994.
193. Groh V, Rhinehart R, Secrist H, Bauer S, Grabstein KH, Spies T. Broad tumor-associated expression and recognition by tumor-derived gamma delta T cells of MICA and MICB. *Proceedings of the National Academy of Sciences of the United States of America*. 1999;96(12):6879-84. PubMed PMID: 10359807; PMCID: 22010.
194. Sutherland CL, Rabinovich B, Chalupny NJ, Brawand P, Miller R, Cosman D. ULBPs, human ligands of the NKG2D receptor, stimulate tumor immunity with enhancement by IL-15. *Blood*. 2006;108(4):1313-9. doi: 10.1182/blood-2005-11-011320. PubMed PMID: 16621962.
195. Raulet DH, Gasser S, Gowen BG, Deng W, Jung H. Regulation of ligands for the NKG2D activating receptor. *Annu Rev Immunol*. 2013;31:413-41. doi: 10.1146/annurev-immunol-032712-095951. PubMed PMID: 23298206; PMCID: 4244079.
196. Carayannopoulos LN, Naidenko OV, Kinder J, Ho EL, Fremont DH, Yokoyama W. Ligands for murine NKG2D display heterogeneous binding behavior. *Eur J Immunol*. 2002;32(3):597-605.

- doi: 10.1002/1521-4141(200203)32:3<597::AID-IMMU597>3.0.CO;2-E. PubMed PMID: 11857333.
197. Diefenbach A, Jamieson AM, Liu SD, Shastri N, Raulet DH. Ligands for the murine NKG2D receptor: expression by tumor cells and activation of NK cells and macrophages. *Nat Immunol.* 2000;1(2):119-26. doi: 10.1038/77793. PubMed PMID: 11248803.
198. Lanier LL. NKG2D Receptor and Its Ligands in Host Defense. *Cancer immunology research.* 2015;3(6):575-82. doi: 10.1158/2326-6066.CIR-15-0098. PubMed PMID: 26041808; PMCID: 4457299.
199. Fujita H, Hatanaka Y, Sutoh Y, Suzuki Y, Oba K, Hatanaka KC, Mitsuhashi T, Otsuka N, Fugo K, Kasahara M, Matsuno Y. Immunohistochemical validation and expression profiling of NKG2D ligands in a wide spectrum of human epithelial neoplasms. *The journal of histochemistry and cytochemistry : official journal of the Histochemistry Society.* 2015;63(3):217-27. doi: 10.1369/0022155414563800. PubMed PMID: 25473094; PMCID: 4340732.
200. Okita R, Yukawa T, Nojima Y, Maeda A, Saisho S, Shimizu K, Nakata M. MHC class I chain-related molecule A and B expression is upregulated by cisplatin and associated with good prognosis in patients with non-small cell lung cancer. *Cancer Immunol Immunother.* 2016;65(5):499-509. doi: 10.1007/s00262-016-1814-9. PubMed PMID: 26940474.
201. Deng W, Gowen BG, Zhang L, Wang L, Lau S, Iannello A, Xu J, Rovis TL, Xiong N, Raulet DH. Antitumor immunity. A shed NKG2D ligand that promotes natural killer cell activation and tumor rejection. *Science.* 2015;348(6230):136-9. doi: 10.1126/science.1258867. PubMed PMID: 25745066; PMCID: 4856222.
202. Groh V, Wu J, Yee C, Spies T. Tumour-derived soluble MIC ligands impair expression of NKG2D and T-cell activation. *Nature.* 2002;419(6908):734-8. doi: 10.1038/nature01112. PubMed PMID: 12384702.
203. Salih HR, Rammensee HG, Steinle A. Cutting edge: down-regulation of MICA on human tumors by proteolytic shedding. *Journal of immunology.* 2002;169(8):4098-102. PubMed PMID: 12370336.
204. Eisele G, Wischhusen J, Mittelbronn M, Meyermann R, Waldhauer I, Steinle A, Weller M, Friese MA. TGF-beta and metalloproteinases differentially suppress NKG2D ligand surface expression on malignant glioma cells. *Brain : a journal of neurology.* 2006;129(Pt 9):2416-25. doi: 10.1093/brain/awl205. PubMed PMID: 16891318.
205. Castro D, Moreira M, Gouveia AM, Pozza DH, De Mello RA. MicroRNAs in lung cancer. *Oncotarget.* 2017;8(46):81679-85. doi: 10.18632/oncotarget.20955. PubMed PMID: 29113423; PMCID: PMC5655318.
206. Takamizawa J, Konishi H, Yanagisawa K, Tomida S, Osada H, Endoh H, Harano T, Yatabe Y, Nagino M, Nimura Y, Mitsudomi T, Takahashi T. Reduced expression of the let-7 microRNAs in human lung cancers in association with shortened postoperative survival. *Cancer Res.* 2004;64(11):3753-6. doi: 10.1158/0008-5472.CAN-04-0637. PubMed PMID: 15172979.
207. Allred DC, Harvey JM, Berardo M, Clark GM. Prognostic and predictive factors in breast cancer by immunohistochemical analysis. *Modern pathology : an official journal of the United States and Canadian Academy of Pathology, Inc.* 1998;11(2):155-68. PubMed PMID: 9504686.
208. Landi MT, Dracheva T, Rotunno M, Figueroa JD, Liu H, Dasgupta A, Mann FE, Fukuoka J, Hames M, Bergen AW, Murphy SE, Yang P, Pesatori AC, Consonni D, Bertazzi PA, Wacholder S,

- Shih JH, Caporaso NE, Jen J. Gene expression signature of cigarette smoking and its role in lung adenocarcinoma development and survival. *PloS one*. 2008;3(2):e1651. doi: 10.1371/journal.pone.0001651. PubMed PMID: 18297132; PMCID: 2249927.
209. Brown BD, Sitia G, Annoni A, Hauben E, Sergi LS, Zingale A, Roncarolo MG, Guidotti LG, Naldini L. In vivo administration of lentiviral vectors triggers a type I interferon response that restricts hepatocyte gene transfer and promotes vector clearance. *Blood*. 2007;109(7):2797-805. doi: 10.1182/blood-2006-10-049312. PubMed PMID: 17170119.
210. Korkolopoulou P, Kaklamanis L, Pezzella F, Harris AL, Gatter KC. Loss of antigen-presenting molecules (MHC class I and TAP-1) in lung cancer. *British journal of cancer*. 1996;73(2):148-53. Epub 1996/01/01. doi: 10.1038/bjc.1996.28. PubMed PMID: 8546899; PMCID: PMC2074307.
211. Ljunggren HG, Karre K. In search of the 'missing self': MHC molecules and NK cell recognition. *Immunol Today*. 1990;11(7):237-44. Epub 1990/07/01. doi: 10.1016/0167-5699(90)90097-s. PubMed PMID: 2201309.
212. Lanier LL, Corliss BC, Wu J, Leong C, Phillips JH. Immunoreceptor DAP12 bearing a tyrosine-based activation motif is involved in activating NK cells. *Nature*. 1998;391(6668):703-7. Epub 1998/03/07. doi: 10.1038/35642. PubMed PMID: 9490415.
213. Cantoni C, Bottino C, Vitale M, Pessino A, Augugliaro R, Malaspina A, Parolini S, Moretta L, Moretta A, Biassoni R. NKp44, a triggering receptor involved in tumor cell lysis by activated human natural killer cells, is a novel member of the immunoglobulin superfamily. *J Exp Med*. 1999;189(5):787-96. PubMed PMID: 10049942; PMCID: 2192947.
214. Lanier LL, Corliss B, Wu J, Phillips JH. Association of DAP12 with activating CD94/NKG2C NK cell receptors. *Immunity*. 1998;8(6):693-701. PubMed PMID: 9655483.
215. Orbelyan GA, Tang F, Sally B, Solus J, Meresse B, Ciszewski C, Grenier JC, Barreiro LB, Lanier LL, Jabri B. Human NKG2E is expressed and forms an intracytoplasmic complex with CD94 and DAP12. *Journal of immunology*. 2014;193(2):610-6. doi: 10.4049/jimmunol.1400556. PubMed PMID: 24935923; PMCID: 4091631.
216. Marrack P, Rubtsova K, Scott-Browne J, Kappler JW. T cell receptor specificity for major histocompatibility complex proteins. *Curr Opin Immunol*. 2008;20(2):203-7. doi: 10.1016/j.coi.2008.03.008. PubMed PMID: 18456484; PMCID: PMC3151152.
217. Stern-Ginossar N, Gur C, Biton M, Horwitz E, Elboim M, Stanietsky N, Mandelboim M, Mandelboim O. Human microRNAs regulate stress-induced immune responses mediated by the receptor NKG2D. *Nat Immunol*. 2008;9(9):1065-73. doi: 10.1038/ni.1642. PubMed PMID: 18677316.
218. Kishikawa T, Otsuka M, Yoshikawa T, Ohno M, Takata A, Shibata C, Kondo Y, Akanuma M, Yoshida H, Koike K. Regulation of the expression of the liver cancer susceptibility gene MICA by microRNAs. *Scientific reports*. 2013;3:2739. doi: 10.1038/srep02739. PubMed PMID: 24061441; PMCID: 3781398.
219. Yadav D, Ngolab J, Lim RS, Krishnamurthy S, Bui JD. Cutting edge: down-regulation of MHC class I-related chain A on tumor cells by IFN-gamma-induced microRNA. *Journal of immunology*. 2009;182(1):39-43. PubMed PMID: 19109132; PMCID: 2714222.
220. Moretta L, Pietra G, Vacca P, Pende D, Moretta F, Bertaina A, Mingari MC, Locatelli F, Moretta A. Human NK cells: From surface receptors to clinical applications. *Immunol Lett*. 2016;178:15-9. doi: 10.1016/j.imlet.2016.05.007. PubMed PMID: 27185471.

221. Llano M, Lee N, Navarro F, Garcia P, Albar JP, Geraghty DE, Lopez-Botet M. HLA-E-bound peptides influence recognition by inhibitory and triggering CD94/NKG2 receptors: preferential response to an HLA-G-derived nonamer. *Eur J Immunol.* 1998;28(9):2854-63. doi: 10.1002/(SICI)1521-4141(199809)28:09<2854::AID-IMMU2854>3.0.CO;2-W. PubMed PMID: 9754572.
222. Wieten L, Mahaweni NM, Voorter CE, Bos GM, Tilanus MG. Clinical and immunological significance of HLA-E in stem cell transplantation and cancer. *Tissue antigens.* 2014;84(6):523-35. doi: 10.1111/tan.12478. PubMed PMID: 25413103.
223. Ho JW, Hershkovitz O, Peiris M, Zilka A, Bar-Ilan A, Nal B, Chu K, Kudelko M, Kam YW, Achdout H, Mandelboim M, Altmeyer R, Mandelboim O, Bruzzone R, Porgador A. H5-type influenza virus hemagglutinin is functionally recognized by the natural killer-activating receptor NKp44. *Journal of virology.* 2008;82(4):2028-32. doi: 10.1128/JVI.02065-07. PubMed PMID: 18077718; PMCID: 2258730.
224. Brusilovsky M, Radinsky O, Cohen L, Yossef R, Shemesh A, Braiman A, Mandelboim O, Campbell KS, Porgador A. Regulation of natural cytotoxicity receptors by heparan sulfate proteoglycans in -cis: A lesson from NKp44. *Eur J Immunol.* 2015;45(4):1180-91. doi: 10.1002/eji.201445177. PubMed PMID: 25546090; PMCID: 4415513.
225. Silva-Santos B, Serre K, Norell H.  $\gamma\delta$  T cells in cancer. *Nat Rev Immunol.* 2015;15(11):683-91. doi: 10.1038/nri3904. PubMed PMID: 26449179.
226. Kandell WM, Donatelli SS, Trinh TL, Calescibetta AR, So T, Tu N, Gilvary DL, Chen X, Cheng P, Adams WA, Chen YK, Liu J, Djeu JY, Wei S, Eksioglu EA. MicroRNA-155 governs SHIP-1 expression and localization in NK cells and regulates subsequent infiltration into murine AT3 mammary carcinoma. *PloS one.* 2020;15(2):e0225820. Epub 2020/02/11. doi: 10.1371/journal.pone.0225820. PubMed PMID: 32040476; PMCID: PMC7010306.
227. Lanier LL. Up on the tightrope: natural killer cell activation and inhibition. *Nat Immunol.* 2008;9(5):495-502. Epub 2008/04/22. doi: ni1581 [pii] 10.1038/ni1581. PubMed PMID: 18425106; PMCID: 2669298.
228. Miller JS, Soignier Y, Panoskaltsis-Mortari A, McNearney SA, Yun GH, Fautsch SK, McKenna D, Le C, Defor TE, Burns LJ, Orchard PJ, Blazar BR, Wagner JE, Slungaard A, Weisdorf DJ, Okazaki IJ, McGlave PB. Successful adoptive transfer and in vivo expansion of human haploidentical NK cells in patients with cancer. *Blood.* 2005;105(8):3051-7. Epub 2005/01/06. doi: 2004-07-2974 [pii] 10.1182/blood-2004-07-2974. PubMed PMID: 15632206.
229. Waldhauer I, Steinle A. NK cells and cancer immunosurveillance. *Oncogene.* 2008;27(45):5932-43. Epub 2008/10/07. doi: onc2008267 [pii] 10.1038/onc.2008.267. PubMed PMID: 18836474.
230. Kim S, Iizuka K, Aguila HL, Weissman IL, Yokoyama WM. In vivo natural killer cell activities revealed by natural killer cell-deficient mice. *Proceedings of the National Academy of Sciences of the United States of America.* 2000;97(6):2731-6. Epub 2000/03/01. doi: 10.1073/pnas.050588297 050588297 [pii]. PubMed PMID: 10694580; PMCID: 15998.

231. Diefenbach A, Jensen ER, Jamieson AM, Raulet DH. Rae1 and H60 ligands of the NKG2D receptor stimulate tumour immunity. *Nature*. 2001;413(6852):165-71. Epub 2001/09/15. doi: 10.1038/35093109  
35093109 [pii]. PubMed PMID: 11557981.
232. Allavena P, Bianchi G, Giardina P, Polentarutti N, Zhou D, Introna M, Sozzani S, Mantovani A. Migratory Response of Human NK Cells to Monocyte-Chemotactic Proteins. *Methods*. 1996;10(1):145-9. Epub 1996/08/01. doi: S1046202396900882 [pii]. PubMed PMID: 8812655.
233. Ben-Baruch A. The multifaceted roles of chemokines in malignancy. *Cancer Metastasis Rev*. 2006;25(3):357-71. Epub 2006/10/04. doi: 10.1007/s10555-006-9003-5. PubMed PMID: 17016763.
234. Melgarejo E, Medina MA, Sanchez-Jimenez F, Urdiales JL. Monocyte chemoattractant protein-1: a key mediator in inflammatory processes. *Int J Biochem Cell Biol*. 2009;41(5):998-1001. Epub 2008/09/02. doi: S1357-2725(08)00310-5 [pii]  
10.1016/j.biocel.2008.07.018. PubMed PMID: 18761421.
235. Morrison BE, Park SJ, Mooney JM, Mehrad B. Chemokine-mediated recruitment of NK cells is a critical host defense mechanism in invasive aspergillosis. *The Journal of clinical investigation*. 2003;112(12):1862-70. Epub 2003/12/18. doi: 10.1172/JCI18125  
112/12/1862 [pii]. PubMed PMID: 14679181; PMCID: 296992.
236. Coca S, Perez-Piqueras J, Martinez D, Colmenarejo A, Saez MA, Vallejo C, Martos JA, Moreno M. The prognostic significance of intratumoral natural killer cells in patients with colorectal carcinoma. *Cancer*. 1997;79(12):2320-8. Epub 1997/06/15. PubMed PMID: 9191519.
237. Bartel DP. MicroRNAs: genomics, biogenesis, mechanism, and function. *Cell*. 2004;116(2):281-97. Epub 2004/01/28. doi: S0092867404000455 [pii]. PubMed PMID: 14744438.
238. Bezman NA, Cedars E, Steiner DF, Brelloch R, Hesslein DG, Lanier LL. Distinct requirements of microRNAs in NK cell activation, survival, and function. *Journal of immunology*. 2010;185(7):3835-46. Epub 2010/09/02. doi: jimmunol.1000980 [pii]  
10.4049/jimmunol.1000980. PubMed PMID: 20805417; PMCID: 2943981.
239. O'Connell RM, Rao DS, Chaudhuri AA, Baltimore D. Physiological and pathological roles for microRNAs in the immune system. *Nat Rev Immunol*. 2010;10(2):111-22. Epub 2010/01/26. doi: nri2708 [pii]  
10.1038/nri2708. PubMed PMID: 20098459.
240. Tili E, Michaille JJ, Wernicke D, Alder H, Costinean S, Volinia S, Croce CM. Mutator activity induced by microRNA-155 (miR-155) links inflammation and cancer. *Proceedings of the National Academy of Sciences of the United States of America*. 2011;108(12):4908-13. Epub 2011/03/09. doi: 1101795108 [pii]  
10.1073/pnas.1101795108. PubMed PMID: 21383199; PMCID: 3064319.
241. O'Connell RM, Taganov KD, Boldin MP, Cheng G, Baltimore D. MicroRNA-155 is induced during the macrophage inflammatory response. *Proceedings of the National Academy of Sciences of the United States of America*. 2007;104(5):1604-9. Epub 2007/01/24. doi: 0610731104 [pii]  
10.1073/pnas.0610731104. PubMed PMID: 17242365; PMCID: 1780072.



242. Trotta R, Chen L, Ciarlariello D, Josyula S, Mao C, Costinean S, Yu L, Butchar JP, Tridandapani S, Croce CM, Caligiuri MA. miR-155 regulates IFN-gamma production in natural killer cells. *Blood*. 2012;119(15):3478-85. Epub 2012/03/02. doi: blood-2011-12-398099 [pii] 10.1182/blood-2011-12-398099. PubMed PMID: 22378844; PMCID: 3325038.
243. Parihar R, Trotta R, Roda JM, Ferketich AK, Tridandapani S, Caligiuri MA, Carson WE, 3rd. Src homology 2-containing inositol 5'-phosphatase 1 negatively regulates IFN-gamma production by natural killer cells stimulated with antibody-coated tumor cells and interleukin-12. *Cancer Res*. 2005;65(19):9099-107. Epub 2005/10/06. doi: 65/19/9099 [pii] 10.1158/0008-5472.CAN-04-4424. PubMed PMID: 16204085.
244. Lesourne R, Fridman WH, Deroon M. Dynamic interactions of Fc gamma receptor IIB with filamin-bound SHIP1 amplify filamentous actin-dependent negative regulation of Fc epsilon receptor I signaling. *Journal of immunology*. 2005;174(3):1365-73. Epub 2005/01/22. doi: 174/3/1365 [pii]. PubMed PMID: 15661894.
245. Vadlamudi RK, Li F, Adam L, Nguyen D, Ohta Y, Stossel TP, Kumar R. Filamin is essential in actin cytoskeletal assembly mediated by p21-activated kinase 1. *Nat Cell Biol*. 2002;4(9):681-90. Epub 2002/08/29. doi: 10.1038/ncb838 ncb838 [pii]. PubMed PMID: 12198493.
246. Dyson JM, O'Malley CJ, Becanovic J, Munday AD, Berndt MC, Coghill ID, Nandurkar HH, Ooms LM, Mitchell CA. The SH2-containing inositol polyphosphate 5-phosphatase, SHIP-2, binds filamin and regulates submembraneous actin. *J Cell Biol*. 2001;155(6):1065-79. Epub 2001/12/12. doi: 10.1083/jcb.200104005 jcb.200104005 [pii]. PubMed PMID: 11739414; PMCID: 2150887.
247. Nishio M, Watanabe K, Sasaki J, Taya C, Takasuga S, Iizuka R, Balla T, Yamazaki M, Watanabe H, Itoh R, Kuroda S, Horie Y, Forster I, Mak TW, Yonekawa H, Penninger JM, Kanaho Y, Suzuki A, Sasaki T. Control of cell polarity and motility by the PtdIns(3,4,5)P3 phosphatase SHIP1. *Nat Cell Biol*. 2007;9(1):36-44. Epub 2006/12/19. doi: ncb1515 [pii] 10.1038/ncb1515. PubMed PMID: 17173042.
248. Valenzuela DM, Murphy AJ, Frendewey D, Gale NW, Economides AN, Auerbach W, Poueymirou WT, Adams NC, Rojas J, Yasenchak J, Chernomorsky R, Boucher M, Elsasser AL, Esau L, Zheng J, Griffiths JA, Wang X, Su H, Xue Y, Dominguez MG, Noguera I, Torres R, Macdonald LE, Stewart AF, DeChiara TM, Yancopoulos GD. High-throughput engineering of the mouse genome coupled with high-resolution expression analysis. *Nat Biotechnol*. 2003;21(6):652-9. Epub 2003/05/06. doi: 10.1038/nbt822 nbt822 [pii]. PubMed PMID: 12730667.
249. Wu Y, Tian Z, Wei H. Developmental and Functional Control of Natural Killer Cells by Cytokines. *Front Immunol*. 2017;8:930. Epub 2017/08/22. doi: 10.3389/fimmu.2017.00930. PubMed PMID: 28824650; PMCID: PMC5543290.
250. Conde C, Gloire G, Piette J. Enzymatic and non-enzymatic activities of SHIP-1 in signal transduction and cancer. *Biochemical pharmacology*. 2011;82(10):1320-34. Epub 2011/06/16. doi: S0006-2952(11)00364-9 [pii] 10.1016/j.bcp.2011.05.031. PubMed PMID: 21672530.
251. Gumbleton M, Vivier E, Kerr WG. SHIP1 intrinsically regulates NK cell signaling and education, resulting in tolerance of an MHC class I-mismatched bone marrow graft in mice.

- Journal of immunology. 2015;194(6):2847-54. Epub 2015/02/18. doi: 10.4049/jimmunol.1402930. PubMed PMID: 25687756; PMCID: PMC4355317.
252. Lebel-Haziv Y, Meshel T, Soria G, Yeheskel A, Mamon E, Ben-Baruch A. Breast cancer: coordinated regulation of CCL2 secretion by intracellular glycosaminoglycans and chemokine motifs. *Neoplasia*. 2014;16(9):723-40. Epub 2014/09/24. doi: 10.1016/j.neo.2014.08.004. PubMed PMID: 25246273; PMCID: PMC4234876.
253. Lehmann MH, Torres-Dominguez LE, Price PJ, Brandmuller C, Kirschning CJ, Sutter G. CCL2 expression is mediated by type I IFN receptor and recruits NK and T cells to the lung during MVA infection. *J Leukoc Biol*. 2016;99(6):1057-64. Epub 2016/03/20. doi: 10.1189/jlb.4MA0815-376RR. PubMed PMID: 26992431.
254. Brooks R, Fuhler GM, Iyer S, Smith MJ, Park MY, Paraiso KH, Engelman RW, Kerr WG. SHIP1 inhibition increases immunoregulatory capacity and triggers apoptosis of hematopoietic cancer cells. *Journal of immunology*. 184(7):3582-9. Epub 2010/03/05. doi: jimmunol.0902844 [pii] 10.4049/jimmunol.0902844. PubMed PMID: 20200281.
255. Li L, Zhang J, Diao W, Wang D, Wei Y, Zhang CY, Zen K. MicroRNA-155 and MicroRNA-21 promote the expansion of functional myeloid-derived suppressor cells. *Journal of immunology*. 2014;192(3):1034-43. Epub 2014/01/07. doi: 10.4049/jimmunol.1301309. PubMed PMID: 24391219.
256. Vigorito E, Perks KL, Abreu-Goodger C, Bunting S, Xiang Z, Kohlhaas S, Das PP, Miska EA, Rodriguez A, Bradley A, Smith KG, Rada C, Enright AJ, Toellner KM, Maclennan IC, Turner M. microRNA-155 regulates the generation of immunoglobulin class-switched plasma cells. *Immunity*. 2007;27(6):847-59. Epub 2007/12/07. doi: 10.1016/j.immuni.2007.10.009. PubMed PMID: 18055230; PMCID: PMC4135426.
257. Wang J, Yu F, Jia X, Iwanowycz S, Wang Y, Huang S, Ai W, Fan D. MicroRNA-155 deficiency enhances the recruitment and functions of myeloid-derived suppressor cells in tumor microenvironment and promotes solid tumor growth. *Int J Cancer*. 2015;136(6):E602-13. Epub 2014/08/22. doi: 10.1002/ijc.29151. PubMed PMID: 25143000; PMCID: PMC4289468.
258. Forster SC, Tate MD, Hertzog PJ. MicroRNA as Type I Interferon-Regulated Transcripts and Modulators of the Innate Immune Response. *Front Immunol*. 2015;6:334. Epub 2015/07/29. doi: 10.3389/fimmu.2015.00334. PubMed PMID: 26217335; PMCID: PMC4495342.
259. Banerjee A, Schambach F, DeJong CS, Hammond SM, Reiner SL. Micro-RNA-155 inhibits IFN-gamma signaling in CD4+ T cells. *Eur J Immunol*. 2010;40(1):225-31. Epub 2009/10/31. doi: 10.1002/eji.200939381. PubMed PMID: 19877012; PMCID: PMC2807623.
260. Hope JL, Stairiker CJ, Spantidea PI, Gracias DT, Carey AJ, Fike AJ, van Meurs M, Brouwers-Haspels I, Rijsbergen LC, Fraietta JA, Mueller YM, Klop RC, Stelekati E, Wherry EJ, Erkeland SJ, Katsikis PD. The Transcription Factor T-Bet Is Regulated by MicroRNA-155 in Murine Anti-Viral CD8(+) T Cells via SHIP-1. *Front Immunol*. 2017;8:1696. Epub 2018/01/24. doi: 10.3389/fimmu.2017.01696. PubMed PMID: 29358931; PMCID: PMC5765282.
261. Yang L, Pang Y, Moses HL. TGF-beta and immune cells: an important regulatory axis in the tumor microenvironment and progression. *Trends Immunol*. 2010;31(6):220-7. Epub 2010/06/12. doi: 10.1016/j.it.2010.04.002. PubMed PMID: 20538542; PMCID: PMC2891151.

262. Liu JH, Wei S, Blanchard DK, Djeu JY. Restoration of lytic function in a human natural killer cell line by gene transfection. *Cell Immunol.* 1994;156(1):24-35. Epub 1994/06/01. doi: S0008-8749(84)71150-6 [pii] 10.1006/cimm.1994.1150. PubMed PMID: 7911075.
263. Wei S, Gamero AM, Liu JH, Daulton AA, Valkov NI, Trapani JA, Larner AC, Weber MJ, Djeu JY. Control of lytic function by mitogen-activated protein kinase/extracellular regulatory kinase 2 (ERK2) in a human natural killer cell line: identification of perforin and granzyme B mobilization by functional ERK2. *J Exp Med.* 1998;187(11):1753-65. PubMed PMID: 9607917.
264. Ma L, Sun P, Zhang JC, Zhang Q, Yao SL. Proinflammatory effects of S100A8/A9 via TLR4 and RAGE signaling pathways in BV-2 microglial cells. *Int J Mol Med.* 2017;40(1):31-8. Epub 2017/05/13. doi: 10.3892/ijmm.2017.2987. PubMed PMID: 28498464; PMCID: PMC5466387.
265. McCoy CE, Sheedy FJ, Qualls JE, Doyle SL, Quinn SR, Murray PJ, O'Neill LA. IL-10 inhibits miR-155 induction by toll-like receptors. *J Biol Chem.* 2010;285(27):20492-8. Epub 2010/05/04. doi: 10.1074/jbc.M110.102111. PubMed PMID: 20435894; PMCID: PMC2898307.
266. Cheung ST, So EY, Chang D, Ming-Lum A, Mui AL. Interleukin-10 inhibits lipopolysaccharide induced miR-155 precursor stability and maturation. *PLoS one.* 2013;8(8):e71336. Epub 2013/08/21. doi: 10.1371/journal.pone.0071336. PubMed PMID: 23951138; PMCID: PMC3741136.
267. Mashima R. Physiological roles of miR-155. *Immunology.* 2015;145(3):323-33. Epub 2015/04/02. doi: 10.1111/imm.12468. PubMed PMID: 25829072; PMCID: PMC4479532.
268. Pauls SD, Marshall AJ. Regulation of immune cell signaling by SHIP1: A phosphatase, scaffold protein, and potential therapeutic target. *Eur J Immunol.* 2017;47(6):932-45. Epub 2017/05/10. doi: 10.1002/eji.201646795. PubMed PMID: 28480512.
269. Fernandes S, Brooks R, Gumbleton M, Park MY, Russo CM, Howard KT, Chisholm JD, Kerr WG. SHIPi Enhances Autologous and Allogeneic Hematolymphoid Stem Cell Transplantation. *EBioMedicine.* 2015;2(3):205-13. Epub 2015/06/09. doi: 10.1016/j.ebiom.2015.02.004. PubMed PMID: 26052545; PMCID: PMC4452032.
270. de Gramont A, Faivre S, Raymond E. Novel TGF-beta inhibitors ready for prime time in onco-immunology. *Oncoimmunology.* 2017;6(1):e1257453. Epub 2017/02/16. doi: 10.1080/2162402X.2016.1257453. PubMed PMID: 28197376; PMCID: PMC5283641.
271. Walker D, Lue LF, Paul G, Patel A, Sabbagh MN. Receptor for advanced glycation endproduct modulators: a new therapeutic target in Alzheimer's disease. *Expert Opin Investig Drugs.* 2015;24(3):393-9. Epub 2015/01/15. doi: 10.1517/13543784.2015.1001490. PubMed PMID: 25586103; PMCID: PMC5502774.
272. Galasko D, Bell J, Mancuso JY, Kupiec JW, Sabbagh MN, van Dyck C, Thomas RG, Aisen PS, Alzheimer's Disease Cooperative S. Clinical trial of an inhibitor of RAGE-Abeta interactions in Alzheimer disease. *Neurology.* 2014;82(17):1536-42. Epub 2014/04/04. doi: 10.1212/WNL.0000000000000364. PubMed PMID: 24696507; PMCID: PMC4011464.

## Appendix A: Copyright Permissions of Previously Published Material

**Citation:** Kandell WM, Donatelli SS, Trinh TL, Calescibetta AR, So T, Tu N, et al. (2020) MicroRNA-155 governs SHIP-1 expression and localization in NK cells and regulates subsequent infiltration into murine AT3 mammary carcinoma. PLoS ONE 15(2): e0225820. <https://doi.org/10.1371/journal.pone.0225820>

**Editor:** Fabrizio Mattei, Istituto Superiore di Sanità, ITALY

**Received:** January 28, 2019; **Accepted:** November 13, 2019; **Published:** February 10, 2020

**Copyright:** © 2020 Kandell et al. This is an open access article distributed under the terms of the [Creative Commons Attribution License](https://creativecommons.org/licenses/by/4.0/), which permits unrestricted use, distribution, and reproduction in any medium, provided the original author and source are credited.

**Data Availability:** All relevant data are within the manuscript and its Supporting Information files.

**Funding:** This work was funded by the Manuel and Adeline Garcia Endowed Chair to J.Y.D.; DOD LC140277 to J.Y.D., <https://www.grants.gov/learn-grants/grant-making-agencies/department-of-defense.html>; DOD LC140270 to T.L.T., <https://www.grants.gov/learn-grants/grant-making-agencies/department-of-defense.html>;

Original Research

Open access

### Immune evasion by TGF $\beta$ -induced miR-183 repression of MICA/B expression in human lung tumor cells

Thu Le Trinh, Wendy M. Kandell, Sarah S. Donatelli, Nhan Tu, Melba M. Tejera, Danielle L. Gilvary,

...show all

Article: e1557372 | Received 02 Apr 2018, Accepted 01 Dec 2018, Published online: 17 Jan 2019

Download citation <https://doi.org/10.1080/2162402X.2018.1557372> Check for updates

Full Article Figures & data References Supplemental Citations Metrics Licensing Reprints & Permissions PDF

© 2019 Taylor & Francis Group, LLC

This is an Open Access article distributed under the terms of the Creative Commons Attribution-NonCommercial-NoDerivatives License (<http://creativecommons.org/licenses/by-nc-nd/4.0/>), which permits non-commercial re-use, distribution, and reproduction in any medium, provided the original work is properly cited, and is not altered, transformed, or built upon in any way.

#### People also read

Article  
Prognostic significance of circulating PD-1, PD-L1, pan-BTN3As, BTN3A1 and BTLA in

## Appendix B: Institutional Animal Care and Use Committee Approval




RESEARCH INTEGRITY AND COMPLIANCE  
INSTITUTIONAL ANIMAL CARE & USE COMMITTEE

---

### MEMORANDUM

TO: Sheng Wei,

FROM:   
Farah Moulvi, MSPH, IACUC Coordinator  
Institutional Animal Care & Use Committee  
Research Integrity & Compliance

DATE: 5/14/2019

PROJECT TITLE: Nanoparticle-based targeting of miR183 for immunotherapy of lung cancer

FUNDING SOURCE: Florida Department of Health  
James and Esther King Biomedical Research Program

IACUC PROTOCOL #: R IS00005998

PROTOCOL STATUS: **Amendment APPROVED**

---

The Institutional Animal Care and Use Committee (IACUC) received your Modification concerning the above referenced IACUC protocol.

On **5/14/2019** the IACUC reviewed and approved your Modification for the following:

**Modification: Amendment Request for IACUC Study 2.1.1**

**Added: Additional strain of approved species**

**Modification: Additional Strains 2.5.1**

**B6.Cg-Mir155tm1Rsky/J (<https://www.jax.org/strain/007745>)**

**We are in the process of peer review for one of our publications and the reviewers require that we use splenocytes for two experiments similar to what we have carried out in the past and currently under this protocol. The mice will not be experimented on but immediately euthanized and used for tissues.**

---

RESEARCH & INNOVATION • RESEARCH INTEGRITY AND COMPLIANCE  
INSTITUTIONAL ANIMAL CARE AND USE COMMITTEE  
PHS No. A4100-01, AAALAC No. 000434, USDA No. 58-R-0015  
University of South Florida • 12901 Bruce B. Downs Blvd., MDC35 • Tampa, FL 33612-4799  
(813) 974-7106 • FAX (813) 974-7091

## Appendix C: Institutional Review Board Approval



### PROTOCOL APPROVAL

<b>DATE:</b>	20 May 2019
<b>TO:</b>	Sheng Wei, MD
<b>PROTOCOL:</b>	Moffitt Cancer Center - MCC 20090, Novel strategies specifically targeting the MDS malignant clone (Pro00034203)
<b>APPROVAL DATE:</b>	20 May 2019 - Via Expedited Review, IRB# 00000971
<b>EXPIRATION DATE:</b>	20 May 2020

### IRB APPROVED DOCUMENTATION:

- Protocol Version:**
- Protocol (Version Date: 4/26/19)

The IRB approved the above referenced protocol and your site on 20 May 2019.

**The IRB determined above referenced study met the criteria for a Waiver of Consent per 45 CFR 46.116(d) and a Waiver of HIPAA Authorization per 45 CFR 164.512(i)(2). The IRB granted the Waiver of Consent and Waiver of HIPAA Authorization.**

If the study is expected to last beyond the approval period, you must request and receive re-approval prior to the expiration date noted above. A report to the Board on the status of this study is due prior to the expiration date or at the time the study closes, whichever is earlier. It is recommended that you submit status reports at least 4 weeks prior to your expiration date to avoid any additional fees or lapses in approval.

Approved investigators and sites are required to submit to Advarra for review, and await a response prior to implementing, any amendments or changes in the protocol; informed consents; advertisements or recruitment materials ("study-related materials"); investigators; or sites (primary and additional).

Approved investigators and sites are required to notify Advarra of the following reportable events, including, but not limited to: unanticipated problems involving risks to subjects or others; unanticipated adverse device effects; protocol violations that may affect the subjects' rights, safety, or well-being and/or the completeness, accuracy and reliability of the study data; subject death; suspension of enrollment; or termination of the study.

Please review the IRB Handbook located in the "Reference Materials" section of Advarra CIRBI™ Platform ([www.cirbi.net](http://www.cirbi.net)). A copy of the most recent IRB roster is also available.

Thank you for selecting Advarra IRB to provide oversight for your research project.